Genetic and Phenotypic Characterization of Tomato Mutants Exhibiting Upward Curly Leaf (curl), Isolated from Micro-Tom Mutant Collections

Genetic and Phenotypic Characterization of Tomato Mutants Exhibiting Upward Curly Leaf (*curl*), Isolated from Micro-Tom Mutant Collections

September 2017

Sri Imriani Pulungan

Genetic and Phenotypic Characterization of Tomato Mutants Exhibiting Upward Curly Leaf (*curl*), Isolated from Micro-Tom Mutant Collections

A Dissertation Submitted to

the Graduate School of Life and Environmental Sciences,

the University of Tsukuba

in Partial Fulfillment of the Requirements

for the Degree of Doctor of Philosophy in Agricultural Science

(Doctoral Program in Biosphere Resource Science and Technology)

Sri Imriani Pulungan

Table of contents

Abbreviation

a.a.	: amino acid
AC	: Ailsa Craig
bp	: base pair
CAPS	: cleaved amplified polymorphic sequences
cDNA	: complementary DNA
ch	: chromosome
cM	: centi-morgan
curl	: curly leaf
DAS	: day after sowing
dCAPS	: derived cleaved amplified polymorphic sequences
EDTA	: ethylene diamine tetraacetic acid
EMS	: ethyl methanesulfonate
EtBr	: ethidium bromide
FAA	: formalin acetic acid
IAA	: indole-3-acetic acid
LAX	: like AUX1
MT	: Micro-Tom
NBRP	: National BioResource Project
NGS	: next generation sequencing
PM	: plasma membrane
qRT-PCR	: quantitative reverse transcription-PCR
SEM	: scanning electron microscope
SGN	: Solanum Genomics Network
SNP	: single nucleotide polymorphism
TAE	: Tris-acetate-EDTA
TILLING	: Targeting Induced Local Lesions IN Genome
TFs	: transcription factors
WAS	: week after sowing
WES	: whole exome sequence
WGS	: whole-genome sequence
WT	: wild-type

Chapter 1

General Introduction

1.1 Introduction

Leaves are the major plant organs whose primary function involves photosynthesis. Leaves play a major role in sensing the quality, quantity and duration of light, all of which are crucial for complete plant growth and development. Understanding leaf initiation and development are important subjects in plant biology. Many aspects of leaf development have been well documented due to their importance and intriguing characteristics (Kalve at al., 2014).

Formation and development of a normal leaf is a complex process that involves several stages including the initiation and differentiation of leaf primordia, the specification of leaf identity and polarity, the balanced cell division and expansion, as well as vascular formation and spesification (Yu et al., 2005; Liu et al., 2011). These processes are influenced by a combination of several factors, such as hormones, transcriptional and post-transcriptional regulators and the morphological properties of the tissue (Bar and Ori, 2014). Leaf initiation and development are also sensitive to genetic and environmental factors. In most dicotyledonous plants, leaf primordia are formed from proliferative and undifferentiated cells in the shoot apical meristem (SAM) (Blein at al., 2013; Floyd and Bowman, 2010). The rates of cell division and elongation at each stage are known to govern the final shape of the plant and throughout the leaf developmental process. Following leaf initiation, three axes are established, proximo-distal, medio-lateral, and dorso-ventral (reviewed by Bar and Ori, 2014).

Most leaves are dorsoventrally (upper to bottom) flattened and develop distinct upper (adaxial) and lower (abaxial) surfaces. Balanced coordination of polarity, auxin response, and cell division is essential for formation of normal and flat leaves development. Any imbalance of these coordination results in altered leaf shapes such as curly, crinkly, twisted, rolled, radial, or shrunken leaves (Yu et al., 2005; Liu et al., 2010; Liu et al., 2011; Serrano-Cartagene et al., 2000). The formation of flat leaves enables the optimum capture of sunlight during photosynthesis.

In recent decades, extensive studies have been carried out in several model species to dissect the complex mechanism of leaf initiation, growth, and development. Several genes and transcription factors (TFs) controlling leaf adaxial and abaxial fates have been characterized. Adaxial and abaxial fates are specified and regulated by the antagonistic interaction of several transcription factors. Six families of TFs have been reported to control adaxial-abaxial polarity in the model plant *Arabidopsis thaliana*; class III homeodomain-leucine zipper (HD-ZIP), ASYMMETRIC LEAVES (AS), KANADI (KAN), AUXIN RESPONSE FACTOR (ARF), FILAMENTOUS FLOWER (FIL), and YABBY3 (YAB3) (reviewed in Nakata and Okada, 2013). Adaxial and abaxial fates are specified and regulated by the antagonistic interaction of these TFs. In addition to these TFs, micro RNAs (miRNAs) are also known to regulate abaxial-adaxial leaf polarity through post-transcriptional gene expression (Han et al., 2004).

Another important factor in controlling leaf morphogenesis is the phytohormone auxin. indole-3-acetic acid (IAA) is the natural form of auxin that controls various aspects plant growth and development, including cell division, expansion and differentiation, leaf initiation, and morphogenesis. One of the unique and intriguing features of auxin is its transport (Paciorek et al., 2005; Tromas and Perrot-Rechenmann, 2010). It is known that auxin is synthesized in young leaves and in the shoot apex and is transported basipetally to all plant organs (reviewed in Bennet et al., 1998; Tromas and Perrot-Rechenmann, 2010). Auxin transport involves two patterns: long-distance transport through phloem and short-distance or cell-to-cell transport called polar auxin transport (PAT). At the cellular level, IAA is distributed through a combination of membrane diffusion (passive uptake), carrier-mediated uptake or proton-driven distribution (Delbarre et al., 1996). PAT contributes to 85% of short-distance auxin transport. It is well established that polar auxin localization controls the direction of auxin movement in whole-plant organs.

Several auxin carriers have been identified, including AUX1/LAX (LAX: like AUX1), PIN

and PGP/MDR-like proteins. AUX1/LAX is reported to be an auxin influx carrier that facilitates auxin movement from outside the cell to inside the cell, while PIN is an efflux carrier that pumps auxin from the cell into the intercellular space. PGP/MDR-like proteins are reported to have the ability to be either influx or efflux carriers (Yang and Murphy, 2009), but the contribution of these proteins is considerably small compared to that of the AUX1/LAX and PIN families (Kramer and Bennet, 2006; reviewed in Swarup and Peret, 2012).

There are numerous studies highlighting the effects of mutations in *AUX/LAX* gene family in the model plant *Arabidopsis*. However, most studies have focused on root phenotypes. For instance, the AUX1/LAX family has been reported to promote lateral root emergence and formation (Marchant et al., 2002; Swarup et al., 2008; reviewed in Peret et al., 2009), root gravitropism (Bennet et al., 1996; Marchant et al., 1999), and root-pathogen interactions (Lee et al., 2011). Recently, *AUX1* function in the aerial parts of plants has received interest, but studies are still considerably scarce. In *Arabidopsis*, *AUX1* has been reported to control phyllotaxis patterning (Bainbridge et al., 2008), vascular patterning, xylem differentiation (Fabregas et al., 2015), and leaf serration (Kasprzewska et al., 2015). Additionally, although PAT is governed and maintained by the coordinated action of AUX1/LAX and PIN carrier proteins, among auxin carriers, PIN1 is the most studied. The role of the PIN protein family in leaf morphogenesis is well documented, yet the role of AUX1/LAX remains neglected or is underestimated. Furthermore, almost all studies have been carried out in the model plant *Arabidopsis*, while the role of auxin influx carriers in other model plants such as tomato is poorly understood.

Our research group has developed a mutant tomato population of the 'Micro-Tom' cultivar generated by γ-ray irradiation and ethyl methanesulfonate (EMS) treatment (Saito et al., 2011). We isolated six lines of *curly leaf* (*curl*) mutants from the 'Micro-Tom' mutant population as previously described (Saito et al., 2011; Shikata et al., 2016). The *curl* mutants showed

dorsoventrally impaired leaf flatness, which exhibited severe upward bending on the transverse axis. Forward genetics is an approach of determining the responsible gene for a phenotype. Several forward genetics strategies based on WGS have been reported in the model plant species *Arabidopsis* and rice (reviewed in Schneeberger et al., 2009). Next-generation mapping and MutMap methods (Austin et al., 2011; Abe et al., 2012) used similar approach (reviewed in Garcia et al., 2016).

To date, several publicly available DNA marker databases have led to map-based cloning strategies using PCR-based markers combined with next-generation sequencing (NGS) technology, dramatically reducing the time and cost of causal gene identification in mutants as well as improving the efficiency of the identification process (Ariizumi et al., 2014; Garcia et al., 2016). NGS has emerged as a powerful tool to detect numerous sequence variant within shorter time. In tomato, several years ago, a high-quality genome sequence has been publicly available for the cultivar 'Heinz 1706' (Tomato Genome Consortium, 2012). More recently, the miniature cultivar 'Micro-Tom' has also been sequenced (Kobayashi et al., 2014). This effort has made utilizing NGS approach to investigate responsible gene largely possible. Exome sequence is a NGS method that target only small region in genome, which only target in the protein coding. The amount of data produced by whole-exome sequence (WES) much more manageable compared to WGS (reviewed in Warr et al., 2015). Recently, NGS strategy using WES has been proven to accelerate forward genetics in several plant species (Mascher et al., 2014; King et al., 2015; reviewed by Hashmi et al., 2015). In addition, the use of exome sequences has also been proven to be a significant tool for accelerating breeding programs. These advantages have made WES a promising approach for investigating the genes responsible for controlling mutant phenotypes. Therefore, in this study, I used the WES to investigate the responsible gene for the loss-of-function of mutant that preceded by map-based cloning approach.

By contrast, reverse genetics is the approach that starts from known a protein or DNA and then works backward to make a mutant gene, ending up with a mutant phenotype. Targeting-Induced Local Lesions IN Genomes (TILLING) has been established as a reverse genetic approach for mutant screening generated by point mutation like EMS. This method was initially reported in *Arabidopsis* (McCallum et al., 2000a, 000b), as a high- throughput reverse genetics tool for screening mutants. The TILLING technology has several advantages over other reverse genetic strategies. For example, with allelic series screening of mutants with known gene of interest, we could find unbiased by phenotype selection, in the loss-of-function and partial loss-of-function of mutants. And it is possible to screen novel function of alleles that often provide more valuable information (reviewed in Stemple et al., 2004). Our research group has successfully developed TILLING platform in tomato 'Micro-Tom' cultivar (Okabe et al., 2011), and the same author has also reported that the TILLING platform provides an opportunity to isolate novel mutant alleles for functional genomic studies and breeding (Okabe et al., 2012). Therefore, in this study, beside applying forward genetics approach to investigate the responsible gene for the curly leaf mutant phenotype, I applied TILLING as a reverse genetics approach to screen another nonsense mutation and to validate the phenotype consistency.

In this study, through map-based cloning combined with WES, I characterized several alleles of the curly leaf mutants, which have nonsense mutation in the *SlLAX1* gene. I reported that the *SlLAX1* gene, potential as an auxin influx carrier, controls leaf flatness in tomato. This feature has never been characterized in any plant species. The characterization of several alleles of single *curl* mutants in this study sheds light on the pivotal role of *SlLAX1* in controlling leaf flatness mediated by normal adaxial-abaxial cell expansion. I also combined forward and reverse genetic approaches to validate the candidate gene. Using TILLING technology, I screened another nonsense mutant allele that consistently shows an indistinguishable curly leaf

phenotype with that of the *curl* mutants obtained by a forward genetic approach.

1.2 Objective of this study

The objectives of this study are (1) to investigate the responsible gene controlling the curly leaf (*curl*) mutant phenotype (2) to characterize the morphology and genetic features of the *curl* mutants (3) to characterize the role of the responsible gene in leaf morphogenesis.

Chapter 2

Genetic Analysis and Determining the Responsible Gene of the *Curly Leaf* Mutants

2.1. Introduction

Tomato (*Solanum lycopersicum* L.) is an economically important crop in both tropical and in temperate regions. It is widely cultivated in almost all countries and it is used for both as fresh consumption and as raw material for processing industries. Tomato belongs to Solanaceae family that contains a large number of important crops consumed by human beings. It is considered as one of the main sources of nutrition to support our health. In fact, tomatoes contain a lot of nutrition, minerals and vitamins, recognized as important functional compounds such as lycopene, one of the bright red carotenoids, serving as antioxidant agent that contribute to human diet (Passam et al., 2007). Besides that, tomatoes are also known as a good source of folic acid, potassium, vitamin A and C (Davies and Hobson, 1981). Due to its potential health benefit, tomato has received much interest in recent years.

Furthermore, tomato has been selected as an excellent model plant for genomic studies in the Solanaceae family, particularly as the most important model system for fleshy fruit development, vegetative development as well as a model for climacteric fruit (Giovannoni, 2004). Additionally, in 2012, the tomato genome sequence has also been published (Tomato Genome Consortium, 2012). This effort can be valued as a significant achievement for accelerating tomato research both in basic and in applied researches as well as for breeding program. Among tomato cultivars, 'Micro-Tom' is widely used as research material due to its excellent characteristics such as rapid life cycle, suitable for indoor cultivation, and easy to transform (Meissner et al., 1997; Emmanuel and Levy, 2002; Marti et al., 2006). In recent decades, various aspects in tomato researches including physiology, biotic and abiotic stress response, genetic and molecular biology have been established.

One of important factor in biological research to know gene function is mutagenesis. Physical and chemical mutagens are often used to induce genetic variation in genome. For instance, using EMS and fast-neutron mutagenesis, Menda et al., (2004) had developed tomato

mutant population which were generated from ‘M82’ cultivar background. And more recently, using EMS treatment Gady et al., 2009 and Minoia et al., 2010 had developed new mutant population derived from cv. Red Setter and cv. TPAADASU background. In ‘Micro-Tom’ background, several mutant collections generated from various either physical or chemical mutagen sources have also been reported (Meissner et al., 1997; Meissner et al., 2000; Mathews et al., 2003).

Our research group has developed a mutant tomato population of the ‘Micro-Tom’ cultivar generated by γ-ray irradiation and EMS treatment (Saito et al., 2011). I isolated six lines of *curly leaf* (*curl*) mutants from the ‘Micro-Tom’ mutant population as previously described (Saito et al., 2011; Shikata et al., 2016). The *curl* mutants showed dorsoventrally impaired leaf flatness, which exhibited severe upward bending on the transverse axis/ hyponastic leaf. Forward genetic approach through the isolation of gain-of-function or loss-of-function mutants has accelerated our understanding of some biological processes and facilitated both investigations of genes responsible for phenotypes of interest and investigations of gene function. To date, several publicly available DNA marker databases have led to map-based cloning strategies using PCR-based markers combined with NGS technology, dramatically reducing the time and cost of causal gene identification in mutants as well as improving the efficiency of the identification process (Ariizumi et al., 2014; Garcia et al., 2016). Recently, NGS strategy using whole-exome sequence WES has been proven to accelerate forward genetics in several plant species (Mascher et al., 2014; King et al., 2015; reviewed by Hashmi et al., 2015). In addition, the use of exome sequences has also been proven to be a significant tool for accelerating breeding programs. Moreover, the use of exome sequences is also more affordable compared to the use of whole-genome sequences. These advantages have made WES a promising approach for investigating the genes responsible for controlling mutant phenotypes.

In this chapter, I conducted map-based cloning combined with the WES to investigate the responsible gene controlling the *curl* mutant phenotype. Then, the mutation was also confirmed by direct sequencing method. Furthermore, to check the phenotype consistency, using TILLING technology as a reverse genetic approach, I screened a new mutant allele which carried a nonsense mutation in the *SlLAX1* gene. This new mutant allele was then grown and the sequence was checked by direct sequencing.

2.2 Material and Methods

2.2.1 Plant Materials

Tomato (*Solanum lycopersicum* cv. Micro-Tom) curly leaf (*curl*) mutants were generated by EMS (ethyl methanesulfonate) and γ-ray irradiation. The mutants were obtained from the National BioResources (NBRP) Project at the University of Tsukuba (Saito et al., 2011; Shikata et al., 2016). The NBRP accession numbers are listed in the Table 2.1. From the M_3 mutagenized population, I isolated six lines of the curly leaf phenotype mutants, herein referred to as '*curl*' mutants. The mutant screening was carried out visually using mature plants showing severe curly leaf phenotypes. Five mutant alleles, *curl 1-5*, were generated by γ-ray irradiation, and one mutant allele, *curl-6*, was generated by EMS mutagenesis. Furthermore, using TILLING methodology, I screened another EMS mutant, *curl-7*. These mutants were registered in the TOMATOMA mutant database (Saito et al., 2011, http://tomatoma.nbrp.jp/). Unless otherwise stated, further analyses of the *curl* mutants were conducted after two backcrosses to the WT 'Micro-Tom' to remove any possible background mutation following the mutagenesis treatment.

2.2.2 Growth Condition

Plants were grown both in a cultivation room and a greenhouse facility of Gene Research Center, University of Tsukuba. In the cultivation room, light was supplied for 16 h. Air temperature was set at 25 ºC. The plants were watered once a day with commercial nutrient solution (Otsuka number 1 and 2, Otsuka Chemical Co. Ltd., Osaka, Japan). For seed germination, seeds of WT 'Micro-Tom' and the *curl* mutants were sown on wet filter paper to stimulate germination. Approximately seven days after sowing, seedlings were transplanted into a rock wool (5 cm^3) pot. The rock wool pots were covered by aluminum foil to prevent fungal attack.

2.2.3 Segregation analysis and allelism test

To perform the segregation analysis, each mutant line was backcrossed to the wild-type (WT) 'Micro-Tom,' and the F_1 hybrids were self-pollinated to obtain an F_2 population. Then, the ratio between mutant and WT phenotype was recorded. The mutants were also crossed to another tomato cultivar 'Ailsa Craig'.

The allelism test was carried out by crossing all possible pairs of mutants to check for the presence of the curly leaf phenotype in the F_1 generation. Reciprocal crossings were also performed.

2.2.4 Genomic DNA Extraction

Genomic DNA was extracted from 2-month-old plants. A maximum of 300 mg of fresh leaf sample was frozen in liquid nitrogen and immediately ground using a TissueLyser (Qiagen, Germany). Genomic DNA was extracted using a Maxwell 16 Tissue DNA Purification Kit (Promega, Madison, USA). DNA concentration was measured by a spectrophotometer (NanoDrop 2000c, Thermo Scientific).

2.2.5 Construction of mapping population, DNA marker using SNP, CAPS and dCAPS.

To perform rough mapping using DNA markers, *curl-2* was crossed to another tomato cultivar, 'Ailsa Craig', to obtain a mapping population. From approximately 100 plants of the F_2 mapping population, 19 plants exhibiting the curly mutant phenotype were isolated, and genomic DNA was extracted from the leaves of the individual plants. These plants were subjected to rough mapping experiments. The PCR mix solution and PCR program are described in the table 2.2, 2.3, 2.4, and 2.5, respectively. All SNP, CAPS and dCAPS DNA markers were designed according to the AMF_2 (F_2: *S. lycopersicum* 'Ailsa Craig' x *S. lycopersicum* 'Micro-Tom') linkage map information that publicly available from the Kazusa DNA Research Institute (KDRI) webpage (http://marker.kazusa.or.jp/Tomato/, Shirasawa et al., 2010). The primers used for PCR are described in Table 2.6.

Thermal cycling to amplify CAPS and SNP DNA markers was conducted using a 3-step cycle as follows: pre-denaturation at 95 °C for 2 min, denaturation at 95 °C for 25 sec, annealing at 55-58 °C for 45 sec, 30-35 extension cycles at 72 °C for 30 sec, and final extension at 72 °C for 5 min. After PCR amplification, 7.5 µl of PCR product, 2 µl of buffer, and 0.15 µl of restriction enzyme (New England Biolabs: Toyobo; Nippon Gene or Takara, Japan) were used for the enzymatic reaction. This reaction was incubated at 37 °C or 60 °C for at least six hours. The primers and enzymes used are described in Table 2.6. After performing the enzymatic reaction, a 3-5 µl solution was used for electrophoresis. Electrophoresis was performed using 1x TAE buffer at 100 V for 20-30 min. Electrophoresis was conducted using 2-3% agarose gel and 1 µl of SYBR Safe DNA Gel Stain (Invitrogen, USA) per 100 ml of TAE buffer. Subsequently, after conducting electrophoresis, the agarose gel was placed in an ethidium bromide (EtBr) solution for 10-15 min, after which the banding pattern was checked using a UV transilluminator.

2.2.6 Exome sequence and variant identification

WES was performed to narrow down the candidate genes. Four alleles, *curl-1*, *curl-2*, *curl-3*, and *curl*-6, of the *curl* mutants of the F_2 mutant population that was backcrossed to the WT were used. The mutants and WT phenotypes were selected in the F_2 population based on the presence or absence of curly leaves among approximately 100 F_2 plants for each line, after which their DNA samples were bulked based on phenotype. Exome sequence analysis was then performed based on the Roche exome sequence SeqCap® EZ SR protocol (http://sequencing.roche.com/). Briefly, genomic DNA was treated with a Covaris® S220 Ultrasonicator (Covaris, Massachusetts, USA) to achieve an average length of 200 bp. Then, a multiplex NGS library was constructed using a KAPA® Library Preparation Kit and SeqCap® adapter kit (Roche, Basel, Switzerland). After constructing the NGS library, exome capture was conducted using a custom probe set that was designed based on the tomato genome reference

version SL2.40 (supporting dataset, Sol Genomics Network, https://solgenomics.net). This probe set was designed to capture 49.5 Mb of exonic DNA regions (supplementary data S1). The resultant exome library was amplified by 14 cycles of post-capture ligation-mediated PCR with KAPA HiFi HostStart ReadyMix (Roche) and then subjected to Illumina HiSeq-2000 sequencing set to the 100-bp paired-end mode. Paired-end short read data were subjected to quality filtering using FASTXToolkit with the parameters of –Q 20 –P 90. Then, short reads were aligned to the tomato genome reference version SL2.50 using bowtie2 software with the following parameters: L,0,-0.16 --mp 2,2 --np 1 --rdg 1,1 --rfg 1,1. On average, 98.8 ± 0.03% of the target exonic regions was covered by short reads. The average read depth was 18 ± 1.5. Genome-wide DNA polymorphisms and mutations were identified based on the alignment results by the HaplotypeCaller function of the Genome Analysis Toolkit (GATK) with the following parameters: -mmq 5 -forceActive -stand_call_conf 10 -stand_emit_conf 10. The resultant DNA variant information was further combined into one genomic VCF dataset with the GenotypeGVCFs function of the GATK. Three wild-type WES datasets (accession No. DRR097500 to DRR097502, DNA Data Bank of Japan (DDBJ)), two wild-type whole-genome NGS datasets (DDBJ accession No. DRR097503 and DRR097504), and one publicly available wild-type whole-genome NGS dataset (Kobayashi et al., 2014) were used as controls to remove intra-cultivar variations that are present between wild-type 'Micro-Tom' lines. DNA variants were further removed if their allele frequencies exceeded >90% in wild-type F_2 bulked segregants because they were also expected to be intra-cultivar variations. Those variants with < 20% allele frequency or with a read depth < 6 were also removed because they were likely to be false-positives. WES datasets for *curl* mutants are available in DDBJ (accession No. DRR097492 to DRR097502).

2.2.7 RNA extraction

Maximum 100 mg of leaf was placed in 1.5 ml sterile tube and immediately frozen in liquid nitrogen and then grinded using pestle until completely become fine powder. RNA was extracted using a commercial kit, RNeasy Plant Mini Kit (Qiagen, Germany), according to manufacturer's protocol. This step was combined with removing any contamination of genomic DNA using 'on column DNA digestion step' (RNase-Free DNase, Qiagen, Germany). RNA concentration was measured by a spectrophotometer (NANODROP, Thermo Scientific, 2000c). Then, the extracted RNA was immediately stored in a -80 ºC refrigerator.

Subsequently, to avoid any contamination of genomic DNA, another step of genomic DNA removing procedure was conducted using RNA Clean & Concentrator™-5 (Zymo research, USA). Maximum 10 µg of RNA was used for this reaction according to manufacturer's protocol. In the final step, RNA was diluted using 10-15 µl of nuclease free water and RNA concentration was measured.

2.2.8 cDNA synthesis

A 2000 ng RNA was used for the cDNA synthesis. cDNA was synthesis using a SuperScript III First-Strand Synthesis (Invitrogen, ThermoFisher Scientific, USA) in 20 µl reaction volume using oligo$(dT)_{12-18}$ primer. Oligo$(dT)_{12-18}$ primer was used because we expected to obtain full-length cDNA. During this process, 1µL of RNaseOUT was also applied. The final concentration of cDNA was 100 ng/ µL. This cDNA was used as stock for qRT-PCR gene expression as well as sequencing analysis. The synthesized cDNA was stored in a -30 ºC refrigerator.

2.2.9 qRT-PCR analysis

mRNA expression was quantified using qRT-PCR. A 10 ng/µl cDNA template of three biological replicates was used for *SlLAX1* gene expression analysis. The *SlActin* gene was used as an internal control (Lovdal and Lillo. 2009). qRT-PCR was carried out using a CFX96 Real-

Time System (Bio-Rad) with SYBR Premix ExTaq II (Ili RNase H Plus; TaKaRa Bio, Japan). The primers used for qRT-PCR are listed in Table 2.7. Relative gene expression was quantified using the $\Delta\Delta C_T$ method (Pfaffl, 2001). The primers for qRT-PCR were designed using the Primer3Plus website (http://primer3plus.com/), using joining two exons in either forward or reverse primer to exclude any potential contamination of genomic DNA. qRT-PCR mix reaction and thermal cycle condition is described in the Table 2.8 and Table 2.9 respectively. For the confirmation of the primers specificity, melting curve of amplified products was analyzed using a regular method, according to the manufacturer's instructions.

2.2.10 Cloning and sequencing of full-length coding sequence the *SlLAX1* gene

Sequencing analysis was performed to confirm the mutation site of the *curl* mutants according to exome sequence result. The full-length coding sequence (1236 bp) of the *SlLAX1* gene from three independent plants was amplified by PCR using KOD plus neo enzyme. Primer sequences are listed in the Table 2.7. PCR mix reaction and condition are described in Table 2.10 and 2.11, respectively. Subsequently, PCR products were loaded onto a 0.8–1.5% agarose gel, which was then electrophoresed for 45-60 min. Next, the band was visualized under 70% UV and then cut either with a gel cutter or blade. Any visible desired product band was individually cut, removed, and subsequently subjected to purification using a Wizard® SV Gel and PCR Clean-Up System (Promega, Madison, USA). DNA purification by centrifugation was applied. The purified PCR product was then cloned into the entry vector pCR8/GW/TOPO (Invitrogen, http://www.lifetechnologies.com/) using an In-Fusion® HD Cloning Kit (Takara Bio USA, Inc.) according to manufacturer's protocol. Then, plasmids from clones were purified using a FastGene Plasmid Mini Kit (Nippon Genetics, Japan). The plasmid fragment was sequenced using M13 primer (Table 2.7). In the sequencing mix reaction, 450-900 ng of plasmid cDNA and 1 µl of primer (10 pmol) were used, after which distilled water was added to reach a total volume of 21 µl.

Sequencing analysis was performed using a 96-capillary Applied Biosystems/ABI 3730xl DNA Analyzer (Thermo Fisher Scientific). The sequencing data were viewed using SnapGene Viewer software. The alignment of nucleotide and amino acid sequences was analyzed using a parallel editor of GENETYX Ver. 11 software.

2.2.11 Screening new *SlLAX1* mutant allele by TILLING

To obtain new *SlLAX1* mutant alleles and to validate the leaf phenotype consistency, I screened our EMS mutant population using TILLING technology. The TILLING population was previously described by Okabe et al. (2013), and the TILLING experiments were performed as described by Okabe et al. (2011). I attempted to screen for mutations in the coding region of the *SlLAX1* gene. The primer pair was designed to span exon 6. Given that exon 6 is the longest exon, I also identified an EMS mutant line, *curl-6*, that carries a nonsense mutation in exon 6 of *SlLAX1*. The primer pairs used in the TILLING experiment were forward 5'-TGGTACATGGGAACTAGCTAAGCC-3' and reverse 5'-ACCTGACGAGCGGATGATTTTC-3,' which amplified 865 bp of genomic DNA template; the 5' end of each primer was labeled with DY-681 or DY-781, which are equivalent of IRDye 700 or IRDye 800 (https://www.biomers.net/), respectively.

2.2.12 Statistical analyses

Unless otherwise stated, the data are presented as the mean ± SE (standard error). Student's *t*-test (at the 95 and 99% significance levels) was used to analyze the significant level between two values with equal variance. Chi-square (χ^2) tests were performed using MS Excel 2016 to examine the goodness of fit between the expected and observed Mendelian ratio in the segregating F_2 population of mutants backcrossed to WT 'Micro-Tom', and the degrees of freedom and expected Mendelian ratio used for monogenic traits were 1 and 3:1 (WT: mutant phenotype), respectively.

2.3 Result

2.3.1 Isolation of the *curl* mutants from the mutant population

Our research group previously developed a large mutant population of 'Micro-Tom', a model tomato cultivar, using γ-ray irradiation and EMS mutagenesis (Saito et al., 2011; Shikata et al., 2016). From the M_3 generation of this mutant population, I isolated six mutant lines exhibiting a severe curly leaf phenotype (Fig. 2.1 A and B). To investigate the gene responsible for controlling the mutant phenotype, I then characterized these mutants. The newly developed young leaves of the *curl* mutants were flat and indistinguishable from those of wild-type (WT) (Fig. 2.1, C and D), suggesting that the impairment of leaf curvature was not detectable at the early vegetative stage. The leaves became curly at the later stage and were continuously curly until the end of growing period. The initiation of curly leaves was not related to the transition from the vegetative to the reproductive stage, and the leaf phenotype could not be restored at any stage once the curly leaves had formed. Growing the *curl* mutants in a high-humidity environment in *in vitro* culture could not rescue the curly phenotype (Fig. 2.1 E). Additionally, curly leaves continuously appeared regardless of water availability in the soil medium (Fig. 2.1 F and G). The plant water potential of the mutants and WT were also comparable (Table 2.12). These data suggested that the curly leaf mutant phenotype is persistent, irrespective of relative humidity or water availability.

2.3.2 All The *curl* mutant alleles exhibited monogenic recessive inheritance pattern

To examine the inheritance pattern of *curl* mutants, I crossed the mutants with WT and another tomato cultivar, 'Ailsa Craig', and observed the segregation ratio in the F_2 population. Phenotypic observation was carried out visually according to the presence or absence of the curly leaf phenotype in the F_2 generation. The mutant phenotype appeared in the F_2 generation only, as a recessive genetic trait (Table 2.13). The ratio of WT and mutant phenotypes fit a Mendelian segregation ratio for monogenic traits (3:1), indicating a monogenic recessive

inheritance of all *curl* mutants. Similarly, in the 'Ailsa Craig' background, the inheritance of the *curl* mutants was also recessive (Table 2.14).

2.3.3 Mutation occurred in the same allele

Allelism test was performed to observe complementation effects among mutant alleles and to examine whether mutations occurred because of the same causal gene. Complementation effect was tested in the F_1 generation. All crosses between each pair of mutants showed curly leaf phenotypes (Table 2.15), indicating that they are allelic (a mutation occurred in the same allele). The *curl-6* mutant generated from EMS treatment (see Plant Material) was also allelic with the other mutants which were generated from γ-ray irradiation. After confirming that all *curl* mutants were allelic, for further analyses, I only used three mutant alleles, namely, *curl-1*, *curl-2*, and *curl-6*.

2.3.4 Map position of the *curl* locus

To identify the candidate gene controlling the curly leaf phenotype, I performed a map-based cloning approach using PCR-based DNA markers including CAPS and SNPs (Shirasawa et al., 2010; Chusreeaeom et al., 2014; Ariizumi et al., 2014; Hao et al., 2017). Tomato has 12 chromosomes, and I used DNA markers that covered all chromosomes (Table 2.16). I used publicly available linkage map information from the Kazusa DNA Research Institute (KDRI) webpage, http://marker.kazusa.or.jp/Tomato/, for AMF_2 (F_2: *S. lycopersicum* 'Ailsa Craig' x *S. lycopersicum* 'Micro-Tom'). I developed a mapping population from *curl-2* crossed with 'Ailsa Craig' (see Materials and Methods) and performed rough mapping. I found that the mutation likely occurred in the short arm of chromosome 9 (Table 2.16). The highest 'Micro-Tom' allele frequency was observed in this chromosome region between markers tomInf5375 and 14109_151 and ranged from 0.68-0.89, suggesting that the responsible gene could be localized in the short arm of chromosome 9 close to marker 14109_151 (physical position SL2.40ch09: 2052389), Fig. 2.2, Table 2.16.

2.3.5 Exome sequence revealed that *SlLAX1* gene is commonly mutated in several *curl* mutant alleles

To narrow down the candidate region obtained by map-based cloning/rough mapping of chromosome, I performed WES. Four lines of the *curl* mutants, *curl-1,2,3* and *6* were used for the WES analysis. The F_2 progenies derived from the cross between mutant and wild-type 'Micro-Tom' were divided into flat leaf and curly phenotype based on presence or absence of curly leaf phenotype, and then flat leaf and mutant bulked segregants were subjected to exome sequencing. By bowtie2-GATK pipeline using the tomato genome reference version SL2.50 as a reference (see Materials and Methods), I identified 5,430, 5,110, 5,050, and 4,829 genome-wide mutations for *curl-1*, *curl-2*, *curl-3*, and *curl-6* mutant segregants, respectively. When allele frequencies were compared between these mutants, a strong association was found around the top region of chromosome 9 in all of the four mapping populations (Fig. 2.3). This result suggested that the causal gene for curly phenotype is located in this chromosome region, in agreement with the result of map-based cloning (Table 2.16; Fig. 2.2). Furthermore, I then searched for the gene in which mutation is commonly occurring in some of the *curl* mutants. I found that mutations are commonly occurring in *Solyc09g014380.2.1*, which is a homologue of *Arabidopsis AtAUX1* (AT2G38120; BLASTx E-value = 0.0, protein amino acid similarity = 93 %). The *SlLAX1* gene spans ~3.8 kb genomic region, while cDNA including UTR region spans 1.8 kb. The *SlLAX1* has seven exons, including UTR region in both 5' and 3' end (Fig. 2.3). The *curl*-2 and *curl*-6 had nucleotide substitution from G to A in the exon 6, physical position SL2.50ch09: 6010739 bp (Table 2.17). This SNP produced stop codon instead of tryptophan on the position 262 (W262X). Whereas, *curl-1* and *curl-3* had SNP from G to T in the splicing junction of intron 4, physical position SL2.50ch09: 6009292 bp.

2.3.6 Mutation validation by dideoxy sequencing: the *curl* mutants produced truncated amino acid and splicing variant

To validate the mutation detected by the WES analysis, I performed dideoxy sequencing of cDNA prepared from the mature curly leaf of four mutant lines used in the WES. I thoroughly cloned the full-length coding sequence of *SlLAX1* gene and used the vector primer, M13 (Table 2.7) for sequencing. The genomic, cDNA and amino acid sequences were obtained from the Sol Genomics Network (https://solgenomics.net/) website.

In the *curl-2* and the *curl*-6 *SlLAX1* cDNA, I found a single base pair substitution from G to A in the 786th bp within the exon 6 (Fig. 2.4A), in agreement with the WES analysis (Table 2.17). This mutation led conversion amino acid (a.a.) tryptophane to stop codon (Fig. 2.4B). Normal WT produced 411 a.a. fitted to *SlLAX1* a.a. reference sequence, whereas the *curl-2* and *curl-6* produced only 261 a.a., losing the last 150 a.a. (63.7% out of WT protein).

As described above, exome sequencing found that the *curl-1* and *curl*-3 had a mutation in the 1st nucleotide or splicing junction of intron 4 (Table 2.17). Interestingly, sequencing of *SlLAX1* cDNA in these alleles revealed that abnormal splicing is occurred around the intron 4, which led to deletion of five nucleotides within exon 4 (nucleic acid 433-437, Fig. 2.4C). Given that mutation in the *curl-1* and *curl-3* is G to T substitution in the first nucleotide of intron 4, presumably, there was an alteration in donor and recipient intron splicing. Splicing of intron 4 was occurred in the position of 435 bp from start codon in the tomato genome of the WT, whereas intron splicing is occurred in 5 bp upstream of the end of exon 4 (430 bp from start codon) in both the *curl-1* and the *curl-3* alleles. Then the next sequence from following exon 5 is GGTTGA; this TGA may produce premature stop codon, which is a position of 435 bp from the start codon (Fig. 2.4D). Thus, *curl-1* and *curl-3* alleles could produce a C-terminal truncated SlLAX1 protein that is only 145 a.a. length of protein (35% of WT protein, Fig. 2.4 E). Taken together, these dideoxy sequencing results confirmed the mutation revealed by WES

analysis in all alleles of the *curl* mutants.

2.3.7. Phenotype-genotype association of the *curl* mutants in F_2 generation

To confirm the exome sequence result whether *Solyc09g014380.2.1* is truly responsible gene for this mutant phenotype, I performed several validation methods including dideoxy sequencing, gene expression analysis and checking association phenotype-genotype using dCAPS DNA markers in the mutation site from F_2 mapping population in the WT 'Micro-Tom' background which were subjected to the WES.

In the F_2 generation of mutants which were back-crossed to the WT 'Micro-Tom', phenotypic of all individual was observed based on presence of absence of curly leaf phenotype among approximately 100 F_2 plant. Then, the phenotype-genotype association was confirmed using dCAPS markers that designed in the predicted mutation site according to exome sequence result. For this observation, only three mutant lines were used as representative, *curl-1*, *curl-3*, and *curl-6*. Because they are allelic, I considered that testing these three lines were enough to obtain an evidence. The result showed that all mutant phenotype from each line was perfectly consistent with genotype (Table 2.18, 2.19, and 2.20), indicating the correct predicted SNP or mutation present between the WT and the *curl* mutant alleles tested in *the curl-1, curl-3, and curl-6*.

2.3.8 Reduced gene expression of *SlLAX1* was observed in the *curl* mutants

Furthermore, I analyzed the transcript level of the *SlLAX1* by qRT-PCR using mature curly leaf cDNA. I designed primers that targeted downstream of the nonsense mutation in exon 6 by joining exon 6 and exon 7 in the forward primer to remove any potential contaminants from genomic DNA. The expression of the *SlLAX1* gene in the three curly leaf mutants was significantly reduced to only 35-40% of WT expression (Fig. 2.5), which indicates low abundance of this gene transcript in the mutants.

2.3.9 Screening a new allele of nonsense mutation of *SlLAX*1 by TILLING and validation the phenotype consistency

Because our research group had previously developed large mutant resources in the 'Micro-Tom' background and proved that TILLING is an efficient tool for isolating desired mutants from the mutant collection (Okabe et al., 2011), I utilized TILLING to search for other *SlLAX1* mutant alleles. Currently, we have 9,216 EMS mutant lines. Among them, I screened 4,608 lines in the M_2 and M_3 generations to obtain new *SlLAX1* mutant alleles. In addition, because I only had one EMS mutant screened by forward genetics (*curl-6*), I attempted to obtain other mutant alleles to confirm the phenotype consistency.

I designed a primer pair to amplify 865 bp along exon 6 of the *SlLAX1* gene for TILLING screening target and found five new mutant alleles that carried intron, missense, and nonsense mutations (Fig. 2.6, Table 2.21). The *curl-6*/TOMJPE8506, which was previously identified by forward genetics, was also confirmed by TILLING screening. Then, to validate the mutant phenotype, one line that carried a nonsense mutation, TOMJPW601-1, was renamed as '*curl-7*' and used for further analysis. TILLING screening showed that this line carries one base pair substitution from G to A in the 185th a.a. that led to the conversion of tryptophan to a premature stop codon that discarded the last 226 a.a. (Fig. 2.7A). I then grew the screened line and observed the presence of the curly leaf phenotype in the M_3 generation. The *curl-7* mutant exhibited curly leaf phenotype like as the other *curl* mutant alleles (Fig. 2.7B and C). This result supports the evidence that *SlLAX1* is the gene responsible for the curly leaf phenotype in tomato.

Furthermore, I performed dideoxy sequencing of the full-length coding sequence of the *SlLAX1* gene to validate the TILLING result. Consistent with the predicted result, *curl-7* carried a G to A nucleotide substitution in 554th bp (Fig. 2.8A) that produced a nonsense mutation in the 185th a.a. (Fig. 2.8B), suggesting that the *SlLAX1* mutation is associated with

the curly leaf phenotype. Taken together, using a forward genetic approach, I characterized multiple alleles showing that mutation in *SlLAX1* produces the curly leaf phenotype, and a reverse genetic approach validated this finding. The mutations in the same gene consistently resulted the same phenotype, strongly suggesting that *SlLAX1* functions in controlling tomato curly leaf phenotype.

2.4 Discussion

2.4.1 Mutation in the *curl* mutants is affected by *SlLAX1* gene

In this study, I characterized several alleles of tomato mutants exhibiting severe leaf upward-curling phenotypes at the mature leaf stage (Fig. 2.1). This mutant phenotype occurs irrespective of water content or relative humidity (Fig. 2.1E, G; Table 2.12). Six lines were isolated using a forward genetic approach by visually selecting curly leaf phenotypes in a previously generated tomato mutant population (Saito et al., 2011; Shikata et al., 2016).

Map-based cloning combined with WES revealed that the mutation occurred in the *SlLAX1* gene (Table. 2.16 and 2.17). Then, to validate the candidate gene by utilizing TILLING as a reverse genetic approach, I screened another nonsense mutation allelic line, *curl-7*, which was generated by EMS. The *curl-7* mutant leaves were indistinguishable from those of the other previously selected lines (Fig. 2.7B, C). Furthermore, I confirmed the full-length coding sequence of *SlLAX1* (Fig. 2.8A, B), which supported the evidence that *SlLAX1* is likely the gene responsible for the curly leaf mutant phenotype. Taken together, the characterization of multiple alleles in this study that consistently showed indistinguishable phenotypes is strong evidence for the role of *SlLAX1* in controlling the curly leaf phenotype.

SlLAX1 (*Solyc09g014380*) encodes a transmembrane amino acid transporter protein and belongs to the amino acid/auxin permease (AAAP) family. Conserved domain searches indicate that the *SlLAX1* amino acid sequence contains one conserved domain, *SLC5-6-like_sbd*, which is a member of the solute-binding domain superfamily. This superfamily includes the solute-binding domain of SLC5 proteins, SLC6 proteins, and nucleobase-cation-symport-1 (NCS1) transporters. SLC5s co-transports Na^+ with sugars, amino acids, inorganic ions and vitamins (https://www.ncbi.nlm.nih.gov/cdd, Marchler-Bauer A et al., 2015, 2017).

Homology searches indicated that the SlLAX1 protein sequence is homologous to *Arabidopsis thaliana AtAUX1* (*AT2G38120*). In *Arabidopsis*, AUX1 is one of four auxin influx

carriers belonging to AUX1/LAX family that controls several developmental processes including gravitropism responses, venation patterns, and lateral roots (Vieten et al., 2007; Bennet et al., 1996). Although recent findings have indicated that the AUX/LAX1 family also control aerial part development such as leaf serration (Kasprzewska et al., 2015), phyllotaxis patterning, vascular patterning, and xylem differentiation (Bainbridge et al., 2008; Fabregas et al., 2015), the role of AUX1/LAX gene family in leaf curling are poorly understood. In contrast, mutations in many auxin-related genes showed an impaired leaf flatness phenotype (Esteve-Bruna et al., 2013; Zgurski et al., 2005). In tomato, few studies have shown a relationship between auxin and leaf flatness; for instance, *SlARF4-RNAi* lines produce hyponastic leaves (Sagar et al., 2013) and *SlPIN4-RNAi* lines show leaf flatness defects as well as altered plant architecture (Pattison and Catala, 2012). However, the role of *SlLAX1* in controlling leaf curly phenotype has not been reported in tomato or other major crops.

2.4.2 *SlLAX1* is essential for controlling tomato leaf flatness

The tomato *AUX1/LAX* family consists of five genes (*SlLAX1-5*). They share high identity and similarity; the identity of *SlLAX2*, *SlLAX3*, *SlLAX4*, and *SlLAX5* with *SlLAX1* are 80.36%, 79.70%, 92.65%, and 80.87%, respectively (Sol Genomics Network). All *SlLAX* genes are expressed in the mature leave and root of tomato (Pattison and Catala, 2012). These authors reported that all *SlLAX* genes are expressed in the mature leaves of tomato. The single mutants depleting *SlLAX1* used in this study, *curl-1-7,* showed a severe phenotype effect in leaf flatness, suggesting that the importance of *SlLAX1* in controlling leaf flatness in mature leaves, and other *SlLAX* genes may not have strong function in this process. In agreement with this finding, a study of *Arabidopsis* roots revealed that among four auxin influx carriers conserved in the *Arabidopsis* genome, *AUX1* was the influx carrier that had the strongest affinity (Peret et al., 2012), although all *AUX1/LAX* family genes encode functional auxin influx carriers. This finding is also supported by a more recent study conducted by Rutschow et al., (2014), who

proposed that *AUX1* dominates auxin flux into *Arabidopsis* protoplasts. This reason presumably explains why the single mutant *curl1-7* produced a severe curly leaf phenotype.

Although the functional redundancy of the *AUX1/LAX* family, in addition to the function of *SlLAX1* itself, is poorly characterized in tomato, their function in *Arabidopsis* is well characterized especially in root development. Like tomato, *Arabidopsis* has several (four) *AUX1/LAX* genes that share high identity and similarity. Peret et al. (2012) reported that four *Arabidopsis* influx carrier family genes regulate the distinct auxin-dependent developmental program and that the coding sequences of *AUX1/LAX* genes have undergone subfunctionalization. *AUX1/LAX* genes exhibit nonredundant and complementary expression patterns in roots. Furthermore, these authors also reported evidence of the inability of LAX to rescue *aux1* mutant phenotypes with respect to root development. Additionally, the authors also reported that *Arabidopsis AUX1/LAX* genes perform distinct developmental function. However, these results vary among *Arabidopsis* tissues observed in the context of phyllotaxy, vascular patterning, and xylem differentiation; *AUX1/LAX* could play redundant function (Bainbridge et al., 2008; Fabregas et al., 2015). Non-redundancy in tomato has not been reported; nonetheless, this possibility has also to be taken into account. The functional redundancy of *SlLAXs* family in tomato leaf curling phenotype awaits further investigation.

2.4.3 Curly leaf phenotype of the *curl* mutants is induced by the loss-of-function of *SlLAX1*

AUX1 protein is located in the plasma membrane (PM). Swarup et al., (2004) first reported on the basis of experimental evidence that *AtAUX1* has 11 transmembrane domains. Then, by observing root gravitropism and resistance to 2,4-D as the most prominent and well-characterized traits of this mutant, they also characterized several allele series of *aux1* mutants ranging from null, partial loss-of-function, and missense mutations in order to understand the important functional domains and amino acids within the AUX1 polypeptide. The result

suggested that the central region of AUX1, between TM VI and VIII, proven to be particularly important for protein function. Using a publicly available server (http://www.cbs.dtu.dk/services/TMHMM/), I checked the prediction of transmembrane helices in the SlLAX1 protein. The *curl-2* and *curl-6* mutants carried a mutation in the W262X a.a., which located in transmembrane domain VII. Furthermore, independent research conducted by Peret et al., (2012) also revealed that the N-terminal half of AUX1 is essential for the correct localization of the AUX1 expression domain. I showed that both the *curl-1* and *curl-3* mutations are located in transmembrane helix IV, where the N-terminal half of SlLAX1 is located (http://www.cbs.dtu.dk/services/TMHMM/). Furthermore, the *curl-1/curl-3*, *curl-2/curl-6*, and *curl-7* mutations caused nonsense mutations that can produce only 35, 63, and 45% of the WT protein, respectively (Fig. 2.4B, D, and 2.8A). Additionally, the relative expression of the *curl* mutant alleles (*curl-1*, *curl-2,* and *curl-6*) was less than 40% compared to that of WT (Fig. 4F). These reasons presumably account for the loss-of-function mutations of the *SlLAX1* gene.

Tables and Figures

Table 2.1 Description of mutant lines in TOMATOMA mutant collection database and mutagen source

Mutant lines used in this study	Mutant line in TOMATOMA database	Mutagen source
curl-1	TOMJPG1056	γ-ray
curl-2	TOMJPG1450	γ-ray
curl-3	TOMJPG2156	γ-ray
curl-4	TOMJPG2484	γ-ray
curl-5	TOMJPG5605	γ-ray
curl-6	TOMJPT8506	EMS
curl-7	TOMJPW601-1	EMS

γ-ray: gamma-ray irradiation
EMS: ethyl methanesulphonate

Table 2.2 Reaction mix for PCR amplification of CAPS or dCAPS marker using Ex-Taq enzyme

Solution	Amount (µl)
Forward primer (10 µM)	0.4
Reverse primer (10 µM)	0.4
dNTP	1.6
10x buffer	2.0
SDW (sterilized distillate water)	15.1
Ex Taq enzyme	0.1
Genome DNA template	0.4
Total volume	20

Table 2.3 Thermal cycle condition for PCR amplification of CAPS or dCAPS marker using Ex Taq enzyme

3-step cycle		
Pre-denaturation	: 94 ºC 2 m	
Denaturation	: 94 ºC 1 m	35- 40 cycles
Annealing	: 55-58 ºC 1 m	
Extension	: 72 ºC 2 m	
Final extension	: 72 ºC 5 m	

Table 2.4 Reaction mix for PCR amplification of CAPS or dCAPS marker using Go Taq enzyme

Solution	Amount (µl)
Forward primer (10 µM)	0.4
Reverse primer (10 µM)	0.4
Go Taq 2x	7.5
SDW (sterilized distillate water)	5.2
Genome DNA template (10 ng/µl)	0.5 - 1
Total volume	15

Table 2.5 Thermal cycle condition for PCR amplification of CAPS or dCAPS marker using Ex Taq enzyme

3-step cycle		
Pre-denaturation	: 95 ºC 2 m	
Denaturation	: 95 ºC 25 s	35 cycles
Annealing	: 55-58 ºC 45 s	
Extension	: 72 ºC 30 s	
Final extension	: 72 ºC 5 m	

Table 2.6 Primer sequence and enzymes used on chromosome mapping experiment

Locus	Marker	Restriction enzyme	Ch	Arm	Position (cM)	Forward primer sequence 5' to 3'	Reverse primer sequence 5' to 3'
8181_419	CAPS	*Alu* I	1	S	27.874	AAATCATCATGCGAACACCA	CATACGTTCATGCCACGTTC
Tomlnf4286		*Hha* I	1	L		CCTAGGTTGAGCACGACGAT	GGCCTAAAGATCACAACCCA
10431_124		*Rsa* I	3	S	0	TCATTGGGGGAAAAGAAAAA	CTTGGCATTTCCCTTCAAAA
1622_2500		*Alu* I	3	L	117.167	ATTGATGGACCATACGGAGC	TGCTGAACCTGATTTACCCC
2325_361		*Xho* I	4	S	37.911	ACGACCCTTCACAGTGTTCC	ACTTCACATACCCTGCGGTC
5264_772		*Hha* I	4	L	126.237	CGAAACAAAAGAGCCAAGGA	CATCGACAAATTGGTTGTGC
5799_537	CAPS	*Mbo* I	5	L	44.081	GGCGACCTGAACTACTTTGAG	TCTGAAGTGCCATCAAATCG
8669_1517	CAPS	*Hha* I	7	S	9.84	AACGAGAGGAAGGAAGAGCC	TTTTCATGAGTTCTGCACGC
19921_317	CAPS	*Alu* I	7	L	113.074	TGGGAGGAATGGCTTATCTC	GGCCATATTAGTCTACCGAACAA
2404_427	CAPS	*Alu* I	8	S	2.144	GCGCATAAAACACAACGAAA	CCTACTGTTGCCTTGGGCTA
3194_739	CAPS	*Rsa* I	8	L	108.942	CTAATAGCACAAATCGCGCA	GTGGATTTGGAAGCTGCTGT
tomInf5375	SNP	*Rsa* I	9	S	224180	CGAGTAACCAAGGGACCAAA	AAAGTTGATGTGGGCAAAGG
tomInf2042	SNP	*Rsa* I	9	S	527639	TTCAAAGCTTGTCTACCGGC	TTTCAACAGGGTCAAAGCGT
7195_279	CAPS	*Rsa* I	9	S	636025	GCTGGTTCGGTGAGATTGAT	TCAGAAACTCCGCAAAATCC
6033_534	CAPS	*Mbo* I	9	S	1109483	CCATCCACCCCATGATATGT	GGTGTTCCGGAAAGCAGTAA
11485_183	CAPS	*Rsa* I	9	L	63818080	CTATGCTCAAATGGGGGCTA	CAGGTAAAACAAAAATAGAGAGTGC
12496_320	CAPS	*Hha* I	10	L	79.045	ACGAGCTACCACCGAAGCTA	TGGCAGTTGGTAACTGAACG
3033_96	CAPS	*Rsa* I	11	S	10.458	TAATTCTTGGGAACCAGCCA	GCAGACACCATCGTTTTCCT
5972_1026	CAPS	*Rsa* I	11	L	117.219	ATTAACAGCGACTGGGTTGG	TCTACGTGCCTTTCCTTGCT
15328_509	CAPS	*Hha* I	12	S	0	AATGTTTCAAAACCACCCCA	ATGCAAGCAGGAACGTTAGG
6139_385	CAPS	*Mbo* I	12	L	131.316	GTGCTGCCGTTACGTTTACA	CCTTGGATCATTTGCAGCTT

Ch: chromosome; S: short; L: long; cM: centi Morgan

[a] DNA markers locus according to AMF2 (F2: *S. lycopersicum* 'Ailsa Craig' x *S. lycopersicum* 'Micro-Tom) linkage map information that publicly available from the Kazusa DNA Research Institute (KDRI) homepage, http://marker.kazusa.or.jp/Tomato/

Table 2.7 Primer pair that used for qRT-PCR and gene cloning of *SlLAX1*

Primer name	Forward sequence 5'- to -3	Reverse sequence 5'- to -3'	Purpose	Remarks
SlLAX1_infusion	ATGGTATCAGGAATAGTACTACAAGTGTTCT	TTAGTGATGGATAGGCGCGGTAT	Cloning into a plasmid	
M13 vector	TGTAAAACGACGGCCAG	GTCATAGCTGTTTCCTG	Sequencing	
qRT-PCR-SlLAX1	TCATCCGCTCGTCAGAATGC	ATTGGTCATGCTAGCCCAAC	qRT-PCR	Span two exon junction in forward primer

Table 2.8 Reaction mix for qRT-PCR reaction of *SlLAX1* gene

Solution	Amount (µl)
Forward primer (10 µM)	0.8
Reverse primer (10 µM)	0.8
SYBR Premix Ex Taq II (2x)	10
RNase-free water	7.4
cDNA template (10 ng/µl)	1
Total volume	20

Table 2.9 Thermal cycle condition for for qRT-PCR reaction of *SlLAX1* gene

3-step cycle		
Pre-denaturation	: 95 ºC 30 s	
Denaturation	: 95 ºC 5 s	40 cycles
Annealing	: 60 ºC 30 s	
Extension	: 60 ºC 30 s	

Table 2.10 Reaction mix for PCR amplification of *SlLAX1* gene sequencing using KOD-Plus- Neo enzyme

Solution	Amount (µl)
Forward primer (10 µM)	1.5
Reverse primer (10 µM)	1.5
10x KOD-Plus-Neo buffer	5
2 mM dNTPs	5
25 mM $MgSO_4$	4
SDW (sterilized distillate water)	31
KOD Plus-Neo enzyme	1
cDNA template (10-25 ng/µl)	1
Total volume	50

Table 2.11 Thermal cycle condition for PCR amplification of *SlLAX1* gene sequencing using KOD-Plus-Neo enzyme

3-step cycle		
Pre-denaturation	: 94 ºC 3 m	
Denaturation	: 98 ºC 10 s	40 cycles
Annealing	: 55-58 ºC 30 s	
Extension	: 68 ºC 2 m	
Final extension	: 68 ºC 7 m	

Table 2.12 Leaf water potential of the *curl* mutants.

Line	Leaf water potential (Psi)
WT	-18.3±0.6
curl-1	-18.5±0.6
curl-6	-18.8±0.4

Values are means ± SE (*n*=6). Leaf water potential was measured at well-watered condition at the 1st leaflet. Leaf water potential of WT and the *curl* mutants was comparable.

Table 2.13 Segregation analysis of the *curl* mutants back-crossed to WT 'Micro-Tom'.

Mutant line[a]	F_1[b] WT: curly	F_2[b] WT: curly	χ^2 value[c]	χ^2 reference[d]	*P*-value	Inheritance pattern[e]
curl-1	4:0	105:25	2.30	3.84	0.13	monogenic recessive
curl-2	1:0	79:31	0.59	3.84	0.44	monogenic recessive
curl-3	5:0	70:25	0.08	3.84	0.76	monogenic recessive
curl-6	2:0	123:30	2.37	3.84	0.12	monogenic recessive

[a]The *curl* mutants were crossed to the WT 'Micro-Tom'.
[b]The number of progeny exhibiting normal (WT) and curly leaf phenotype is shown.
[c] χ^2 value was calculated based on progeny segregation at F_2 population.
[d] χ^2 distribution in the table reference value, with probability >0.05, and degree of freedom 1.
[e] Inheritance pattern of the curl mutants, estimated based on χ^2 value at 95% ($P<0.05$) significant level.

Table 2.14 Segregation analysis of the *curl* mutants back-crossed to cv 'Ailsa Craig'.

Mutant line[a]	F_1[b] WT: curly	F_2[b] WT: curly	χ^2 value[c]	χ^2 references[d]	*P*-value	Inheritance pattern[e]
curl-1	5:0	n.d	n.d	3.84	n.d	monogenic recessive
curl-2	5:0	100:19	1.92	3.84	0.16	monogenic recessive
curl-3	2:0	n.d.	n.d.	3.84	n.d	monogenic recessive
curl-6	2:0	409:120	1.51	3.84	0.21	monogenic recessive

[a]The *curl* mutants were crossed to the WT 'Micro-Tom'.
[b]The number of progeny exhibiting normal (WT) and curly leaf phenotype is shown.
[c] χ^2 value was calculated based on progeny segregation at F_2 population.
[d] χ^2 distribution in the table reference value, with probability >0.05, and degree of freedom 1.
[e] Inheritance pattern of the curl mutants, estimated based on χ^2 value at 95% ($P<0.05$) significant level.

Table 2.15 The result of allelism test among the *curl* mutants.

Mutant line ♀	Mutant line ♂					
	WT	*curl-1*	*curl-2*	*curl-3*	*curl-4*	*curl-6*
WT		normal	normal	normal	normal	normal
curl-1	normal		n.d.	n.d.	n.d.	curly
curl-2	normal	curly		n.d.	n.d.	curly
curl-3	normal	n.d.	curly		curly	curly
curl-4	normal	n.d.	curly	curly		curly
curl-6	normal	curly	curly	curly	curly	

The allelism test was carried out by crossing all possible pairs and observing the results at the F_1 generation.

The F_1 generation phenotype was evaluated visually by observing the presence of a curly leaf phenotype.

Normal represents the wild-type phenotype

Curly represents the curly leaf phenotype.

n.d. not determined.

♀, ♂: female recipient and male donor, respectively.

Table 2.16 Chromosome mapping using CAPS, dCAPS and SNP markers in the *curl-2*

Marker/locus	Ch.	arm	Indivdual DNA sample from *curl-2* x AC F2																		Allele frequency (%)	
			1	2	3	4	5	6	7	8	9	10	11	12	13	14	15	16	17	18	19	MT	AC
8181_419	1	S	A	H	M	H	H	A	A	H	H	H	H	H	A	H	H	H	A	H	M	0.42	0.58
tomInf4286	1	L	A	H	M	H	M	A	H	H	A	H	H	H	A	M	H	H	H	H	M	0.50	0.50
tomInf6860	2	S	A	H	H	A	M	H	H	H	M	A	A	H	A	A	A	H	A	M	A	0.34	0.66
tomInf2289	2	L	H	H	M	A	M	A	M	H	H	H	A	H	M	H	H	M	M	H	H	0.58	0.42
10431_124	3	S	H	A	A	A	A	H	H	A	H	M	H	A	M	H	H	H	M	H	M	0.45	0.55
1622_2500	3	L	H	H	H	A	M	M	H	H	M	H	H	H	A	H	A	H	H	A	A	0.45	0.55
2325_361	4	S	A	A	H	A	H	A	H	H	A	A	A	H	H	H	M	A	A	A	A	0.24	0.76
5264_772	4	L	H	M	M	H	H	H	H	A	H	H	H	M	H	M	H	H	A	A	M	0.55	0.45
solCAP_51607	5	S	M	H	M	M	H	H	H	A	H	H	H	H	H	H	M	A	M	H	H	0.58	0.42
5799_537	5	L	M	H	M	M	H	H	H	A	H	H	M	H	H	H	A	H	M	H	A	0.55	0.45
8669_1517	7	S	H	M	H	A	H	H	A	M	M	M	M	H	M	H	M	H	H	A	M	0.63	0.37
19921_317	7	L	A	H	H	A	M	H	A	M	H	H	M	M	M	A	A	A	H	A	H	0.45	0.55
2404_427	8	S	H	M	H	A	M	H	A	H	H	H	H	M	H	M	A	A	M	M	H	0.55	0.45
3194_739	8	L	H	H	H	H	M	A	A	H	H	H	M	M	A	A	H	M	A	A	H	0.45	0.55
tomInf5375	9	S	M	M	M	H	M	M	M	H	H	H	M		M	M	M	H	M	A		0.79	0.21
tomInf2042	9	S	M	A	A	H	M	M	M	H	H	H	M	M	M	M	M	A	M	H	H	0.68	0.32
7195_279	9	S	M	M	M	H	M	M	M	H	H	H	M	M	M	H	M	H	M	H	H	0.79	0.21
6033_534	9	S	M	M	M	H	M	M	M	H	H	M	M	M	M	M	M	H	M	H	M	0.87	0.13
14109_151	9	S	M	M	M	M	M	M	H	H	H	M	M	M	M	M	M	H	M	M	M	0.89	0.11
11485_183	9	L	H	H	M	H	A	A	M	H	M	H	H	H	H	H	H	M	A	M	H	0.55	0.45
tomInf3936	10	S	H	A	A	A	A	H	A	A		H	H	A	H	M	M	H	H	H	H	0.36	0.64
12496_320	10	L	M	H	H	H	A	A	H	H	M	A	A	H	H	H	H	H	A	A	M	0.42	0.58
3033_96	11	S	M	M	H	H	M	M	H	H		H	M	H	H	H	H	M	M	H	A	0.67	0.33
5972_1026	11	L	H	H	M	H	A	H	M	A	H	A	M	M	A	H	H	H	H	H	M	0.53	0.47
15328_509	12	S	M	H	H	H	H	H	H	H	H	A	H	H	H	H	M	A	M	H	H	0.53	0.47

Mutation in the *curl* mutants is likely located in short arm of chromosome 9, close to the marker 14109_151, physical position S.L2.40ch09: 2052389)

DNA markers locus according to AMF2 (F2: *S. lycopersicum* 'Ailsa Craig' x *S. lycopersicum* 'Micro-Tom) linkage map information that publicly available from the Kazusa DNA Research Institute (KDRI) homepage, http://marker.kazusa.or.jp/Tomato/.

Ch, chromosome; S, short arm; L, long arm; M, Micro-Tom, A, Ailsa Craig; H, Heterozygous; CAPS, cleaved amplified polymorphic sequences, SNP, single nucleotide polymorphism; dCAPS, derived CAPS.

Table 2.17 Predicted mutation position, amino acid substitution, and mutation type based on the whole exome sequence result.

Chromosome[a]	Position[b] (bp)	REF nuc[c]	ALT nuc[d]	Within[e]	Gene[f]	Strand	Amino acid substitution	Mutation type	Arabidopsis homolog	Arabidopsis homolog name	*curl* mutant allele
SL2.50ch09	6010739	G	A	Exon 6	*Solyc09g014380.2.1*	plus	W262*	nonsense	*AT2G38120.1*	*AtAUX1*	*curl-2, curl-6*
SL2.50ch09	6009292	G	T	Intron.4	*Solyc09g014380.2.1*	plus	-	intron	*AT2G38120.1*	*AtAUX1*	*curl-1, curl-3*

[a] The location in the chromosome in the tomato genome

[b] Position of nucleotide substitution according to tomato genome sequence database, version SL2.50 (Sol Genomics Network)

[c] Tomato genome sequence reference according to the position in column [b]

[d] Alternative nucleotide sequence/ nucleotide substitution according to the position in column [b]

[e] Location of nucleotide substitution of the gene in column [f]

[f] Gene mutated according to Sol Genomic Network database

* represents a stop codon

Table 2.18. Phenotype-genotype association of the *curl-1* in the 'Micro-Tom' background

Individual plant sample	phenotype	curly intensity	Genotype
1	curly	very strong	Mutant
2	curly	very strong	Mutant
3	curly	very strong	Mutant
4	curly	very strong	Mutant
5	curly	very strong	Mutant
6	curly	very strong	Mutant
7	curly	very strong	Mutant
8	curly	very strong	Mutant
9	curly	very strong	Mutant
10	curly	very strong	Mutant
11	curly	very strong	Mutant
12	curly	very strong	Mutant
13	curly	very strong	Mutant
14	curly	very strong	Mutant
15	normal		Heterozygous
16	normal		WT Micro-Tom
17	normal		Heterozygous
18	normal		WT Micro-Tom
19	normal		WT Micro-Tom
20	normal		Heterozygous
21	normal		WT Micro-Tom
22	normal		WT Micro-Tom
23	normal		WT Micro-Tom
24	normal		WT Micro-Tom
25	normal		Heterozygous
26	normal		WT Micro-Tom
27	normal		WT Micro-Tom
28	normal		WT Micro-Tom
29	normal		Heterozygous
30	normal		WT Micro-Tom
31	normal		Heterozygous
32	normal		WT Micro-Tom
33	normal		WT Micro-Tom
34	normal		WT Micro-Tom
35	normal		WT Micro-Tom
36	normal		WT Micro-Tom
37	normal		WT Micro-Tom
38	normal		WT Micro-Tom
39	normal		Heterozygous
40	normal		WT Micro-Tom
41	normal		WT Micro-Tom
42	normal		WT Micro-Tom
43	normal		WT Micro-Tom

44	normal		Heterozygous
45	normal		WT Micro-Tom
46	normal		Heterozygous
47	normal		WT Micro-Tom
48	normal		WT Micro-Tom
49	normal		WT Micro-Tom
50	normal		WT Micro-Tom
51	normal		Heterozygous
52	normal		WT Micro-Tom
53	normal		WT Micro-Tom
54	normal		Heterozygous
55	normal		WT Micro-Tom
56	normal		WT Micro-Tom
57	normal		WT Micro-Tom
58	normal		WT Micro-Tom
59	normal		WT Micro-Tom
60	normal		WT Micro-Tom
61	normal		WT Micro-Tom
62	normal		WT Micro-Tom
63	normal		WT Micro-Tom
64	normal		Heterozygous
65	normal		WT Micro-Tom
66	normal		WT Micro-Tom
67	normal		WT Micro-Tom
68	normal		Heterozygous
69	normal		WT Micro-Tom
70	normal		Heterozygous
71	normal		WT Micro-Tom
72	normal		Heterozygous
73	normal		WT Micro-Tom
74	normal		WT Micro-Tom
75	normal		WT Micro-Tom
76	normal		WT Micro-Tom
77	normal		WT Micro-Tom
78	normal		WT Micro-Tom
79	normal		WT Micro-Tom
80	normal		WT Micro-Tom
81	normal		WT Micro-Tom
82	normal		WT Micro-Tom
83	normal		WT Micro-Tom
84	normal		WT Micro-Tom
85	normal		WT Micro-Tom
86	normal		Heterozygous
87	normal		WT Micro-Tom
88	normal		Heterozygous
89	normal		WT Micro-Tom

90	normal	Heterozygous
91	normal	WT Micro-Tom
92	normal	WT Micro-Tom
93	normal	Heterozygous
94	normal	WT Micro-Tom
95	normal	WT Micro-Tom
96	normal	WT Micro-Tom
97	normal	Heterozygous
98	normal	Heterozygous
99	normal	Heterozygous
100	normal	WT Micro-Tom
101	normal	WT Micro-Tom
102	normal	Heterozygous
103	normal	Heterozygous

Phenotype-genotype association was tested in the F_2 generation using dCAPS marker designed in the predicted mutation site. In the *curl-1*, among 103 F_2 population, 14 plants showed curly leaf phenotype. Consistently, all plants showing mutant phenotype were also showed mutant genotype.

Table 2.19. Phenotype-genotype association of the *curl-3* in the 'Micro-Tom' background

Individual plant sample	phenotype	curly intensity	Genotype
1	curly	very strong	Mutant
2	curly	very strong	Mutant
3	curly	very strong	Mutant
4	curly	very strong	Mutant
5	curly	very strong	Mutant
6	curly	very strong	Mutant
7	curly	very strong	Mutant
8	curly	very strong	Mutant
9	curly	very strong	Mutant
10	curly	very strong	Mutant
11	curly	very strong	Mutant
12	curly	very strong	Mutant
13	curly	very strong	Mutant
14	curly	very strong	Mutant
15	curly	very strong	Mutant
16	curly	very strong	Mutant
17	curly	very strong	Mutant
18	curly	very strong	Mutant
19	curly	very strong	Mutant
20	curly	very strong	Mutant
21	curly	very strong	Mutant
22	curly	very strong	Mutant
23	curly	very strong	Mutant
24	curly	very strong	Mutant
25	curly	very strong	Mutant

26	normal	Heterozygous
27	normal	Heterozygous
28	normal	Heterozygous
29	normal	WT Micro-Tom
30	normal	WT Micro-Tom
31	normal	Heterozygous
32	normal	WT Micro-Tom
33	normal	WT Micro-Tom
34	normal	Heterozygous
35	normal	WT Micro-Tom
36	normal	WT Micro-Tom
37	normal	Heterozygous
38	normal	Heterozygous
39	normal	WT Micro-Tom
40	normal	Heterozygous
41	normal	Heterozygous
42	normal	Heterozygous
43	normal	Heterozygous
44	normal	Heterozygous
45	normal	Heterozygous
46	normal	Heterozygous
47	normal	Heterozygous
48	normal	WT Micro-Tom
49	normal	Heterozygous
50	normal	Heterozygous
51	normal	Heterozygous
52	normal	Heterozygous
53	normal	Heterozygous

54	normal	Heterozygous
55	normal	WT Micro-Tom
56	normal	Heterozygous
57	normal	Heterozygous
58	normal	Heterozygous
59	normal	WT Micro-Tom
60	normal	Heterozygous
61	normal	Heterozygous
62	normal	Heterozygous
63	normal	Heterozygous
64	normal	Heterozygous
65	normal	Heterozygous
66	normal	Heterozygous
67	normal	Heterozygous
68	normal	Heterozygous
69	normal	Heterozygous
70	normal	Heterozygous
71	normal	Heterozygous
72	normal	WT Micro-Tom
73	normal	Heterozygous
74	normal	Heterozygous
75	normal	Heterozygous
76	normal	Heterozygous
77	normal	Heterozygous
78	normal	WT Micro-Tom
79	normal	Heterozygous
80	normal	Heterozygous
81	normal	Heterozygous

82	normal	Heterozygous
83	normal	WT Micro-Tom
84	normal	Heterozygous
85	normal	Heterozygous
86	normal	Heterozygous
87	normal	WT Micro-Tom
88	normal	WT Micro-Tom
89	normal	Heterozygous
90	normal	Heterozygous
91	normal	Heterozygous
92	normal	Heterozygous
93	normal	Heterozygous
94	normal	Heterozygous
95	normal	WT Micro-Tom

Phenotype-genotype association was tested in the F_2 generation using dCAPS marker designed in the predicted mutation site. In the *curl-3*, among 95 plants in the F_2 population, 25 plants showed curly leaf phenotype. Consistently, all plants showing mutant phenotype were also showed mutant genotype.

Table 2.20. Phenotype-genotype association of the *curl-6* in the 'Micro-Tom' background

Individual plant sample	Phenotype	Curly intensity	Genotype
1	curly	very strong	Mutant
2	curly	very strong	Mutant
3	curly	very strong	Mutant
4	curly	very strong	Mutant
5	curly	very strong	Mutant
6	curly	very strong	Mutant
7	curly	very strong	Mutant
8	curly	very strong	Mutant
9	curly	very strong	Mutant
10	curly	very strong	Mutant
11	curly	very strong	Mutant
12	curly	very strong	Mutant
13	curly	very strong	Mutant
14	curly	very strong	Mutant
15	curly	very strong	Mutant
16	curly	very strong	Mutant
17	curly	very strong	Mutant
18	curly	very strong	Mutant
19	curly	very strong	Mutant
20	curly	very strong	Mutant
21	curly	very strong	Mutant
22	curly	very strong	Mutant
23	curly	very strong	Mutant
24	curly	very strong	Mutant
25	curly	very strong	Mutant

26	curly	very strong	Mutant
27	curly	very strong	Mutant
28	curly	very strong	Mutant
29	normal		Heterozygous
30	normal		Heterozygous
31	normal		Heterozygous
32	normal		Heterozygous
33	normal		Heterozygous
34	normal		WT Micro-Tom
35	normal		Heterozygous
36	normal		WT Micro-Tom
37	normal		WT Micro-Tom
38	normal		WT Micro-Tom
39	normal		WT Micro-Tom
40	normal		WT Micro-Tom
41	normal		WT Micro-Tom
42	normal		WT Micro-Tom
43	normal		Heterozygous
44	normal		WT Micro-Tom
45	normal		WT Micro-Tom
46	normal		Heterozygous
47	normal		Heterozygous
48	normal		Heterozygous
49	normal		Heterozygous
50	normal		Heterozygous
51	normal		Heterozygous
52	normal		WT Micro-Tom
53	normal		Heterozygous

54	normal	Heterozygous
55	normal	Heterozygous
56	normal	WT Micro-Tom
57	normal	WT Micro-Tom
58	normal	Heterozygous
59	normal	WT Micro-Tom
60	normal	Heterozygous
61	normal	Heterozygous
62	normal	WT Micro-Tom
63	normal	WT Micro-Tom
64	normal	Heterozygous
65	normal	Heterozygous
66	normal	Heterozygous
67	normal	WT Micro-Tom
68	normal	WT Micro-Tom
69	normal	WT Micro-Tom
70	normal	Heterozygous
71	normal	Heterozygous
72	normal	WT Micro-Tom
73	normal	Heterozygous
74	normal	WT Micro-Tom
75	normal	Heterozygous

Phenotype-genotype association was tested in the F_2 generation using dCAPS marker designed in the predicted mutation site. In the *curl-6*, among 75 plants in the F_2 population, 28 plants showed curly leaf phenotype. Consistently, all plants showing mutant phenotype were also showed mutant genotype.

Table 2.21 The new alleles of *SlLAX1* mutants screened by TILLING

Line	Position in Ch. 9[a] (bp)	Position from ATG start codon	REF nuc[b]	ALT nuc[c]	Within[d]	Strand	Amino acid substitution	Mutation type
TOMJPW4247	6010486	1820	G	A	Intron 5	plus	-	intron
TOMJPW4659	6010486	1820	G	A	Intron 5	plus	-	intron
TOMJPW601/*curl-7**	6010507	1841	G	A	Exon 6	plus	W185*	nonsense
TOMJPW1386	6010567	1901	C	A	Exon 6	plus	T205K	missense
TOMJPE8506/*curl-6***	6010739	2073	G	A	Exon 6	plus	W262*	nonsense
TOMJPW4310	6010768	2102	G	A	Exon 6	plus	R272K	missense

[a] position of nucleotide substitution according to tomato genome sequence database, version SL2.50 (Sol Genomics Network)
[b] Tomato genome sequence reference according to position in column [a]
[c] Alternative nucleotide sequence/ nucleotide substitution according to position in column [a]
[d] Location of nucleotide substitution of gene in the *SlLAX1* gene
* This line was further analyzed to confirm mutant phenotype as well as mutation by Sanger sequencing
** This line was previously found by forward genetic and mutation was also validated by TILLING
TILLING: Targeted Induced Local Lesion IN Genome

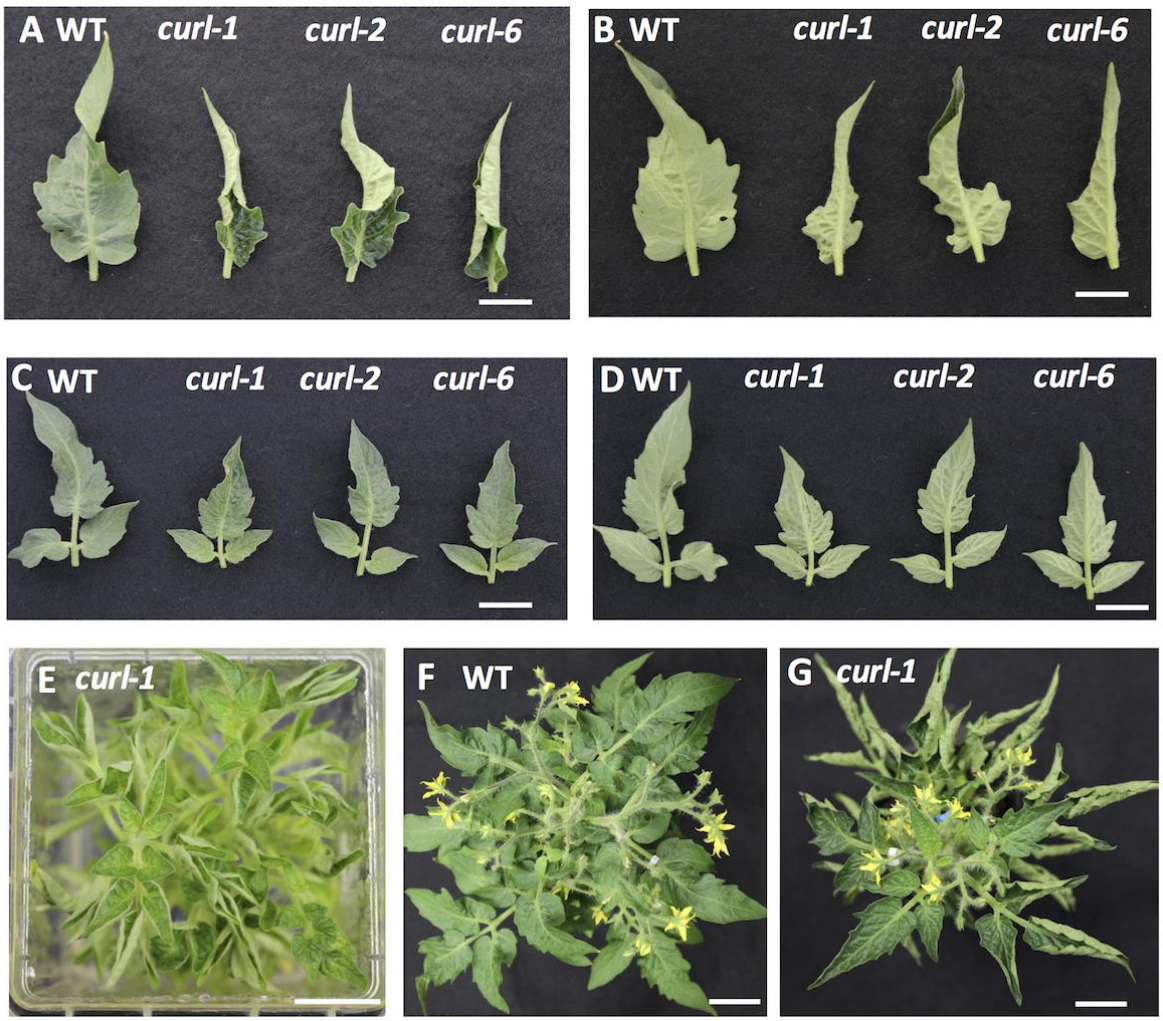

Fig. 2.1 Leaf morphology of the WT 'Micro-Tom' and three alleles of the *curl* mutants.

(A-B) Mature leaf morphology of mature *curl* mutants in (A) adaxial and (B) abaxial view. The leaf images were captured from 2-month-old plants from the 5th leaflet. Scale bar: 2 cm. (C-D) Young leaf appearance of *curl* mutants. (C) adaxial and (D) abaxial view. The newly developed young leaves of the *curl* mutants were flat and indistinguishable from those of WT. Scale bar: 1 cm) (E) Representative of the curl mutant (*curl-1*) when grown in *in vitro* culture. Scale bar: 2 cm. The curly phenotype was not restored (F-G) Wild-type (F) and representative *curl* mutant (G, *curl-1*) grown under well-watered conditions in the greenhouse. Plant images were captured from 2- month-old plant. Scale bar: 1.5 cm.

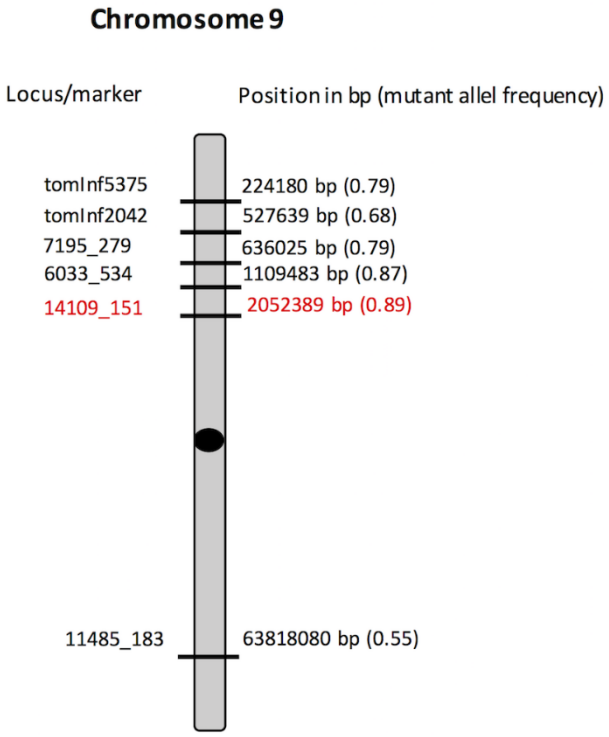

Fig. 2.2 Partial chromosome mapping result of the *curl* mutant locus.
The *curl* locus was found to associate with the marker 14109-151 on chromosome 9 in the F_2 mapping population derived from the cross between *S. lycopersicum* cv. 'Ailsa Craig' x *S. lycopersicum* cv. 'Micro-Tom'. The marker information was obtained from the Kazusa DNA Research Institute AMF_2 database (http://marker.kazusa.or.jp/). No such association was observed in other chromosomes (Table 2.16).

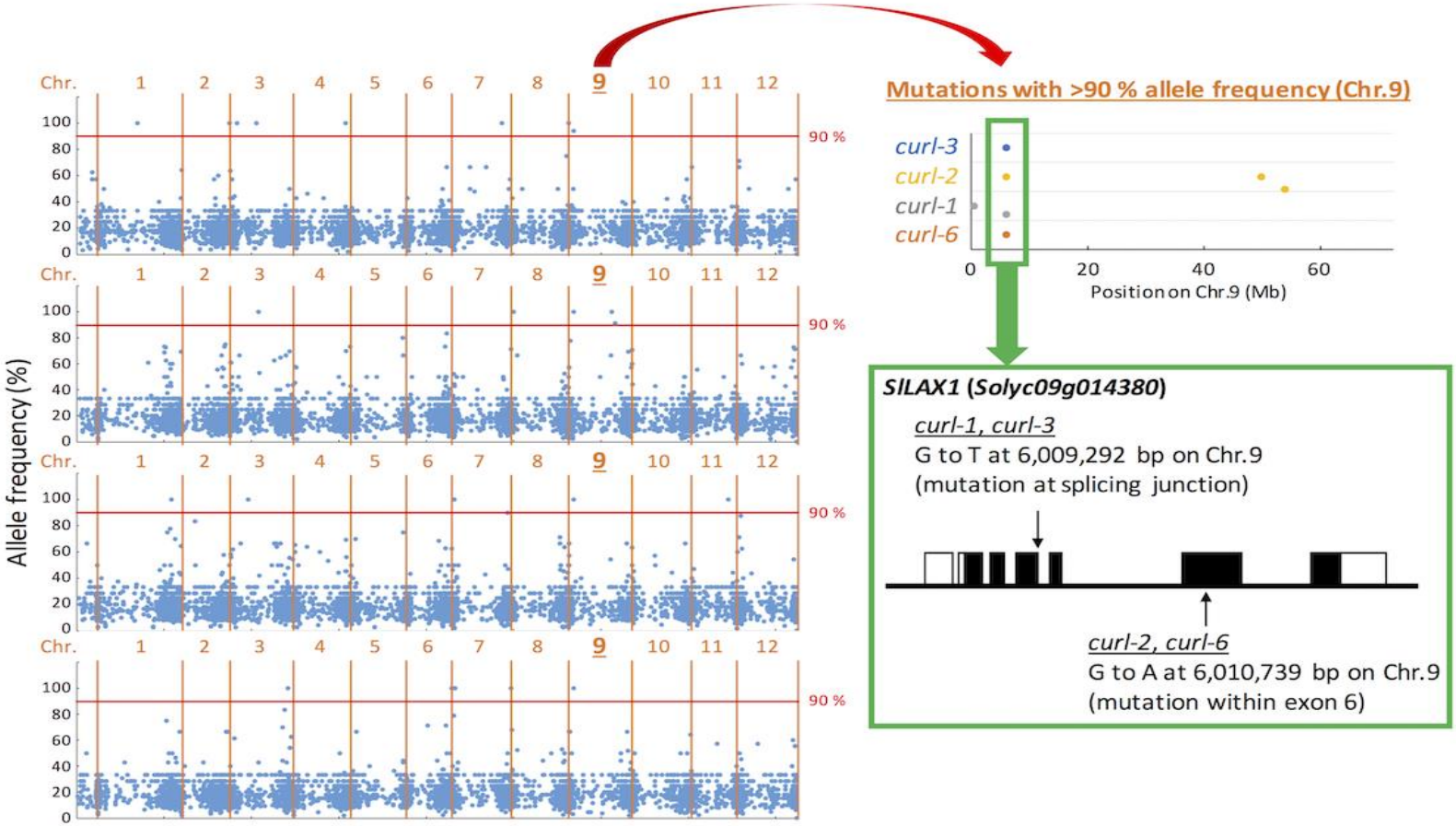

Fig. 2. 3 Identification of *SlLAX1* (*Solyc09g01480.2*) as the most plausible candidate gene responsible for the *curl* phenotype**.**
Genome-wide allele frequency data were obtained by exome sequencing of BCF_2 bulked segregants that show the *curl* mutant phenotype. To narrow down candidate efficiently, four mapping populations derived from independent *curl* alleles (*curl-1, 2, 3, 6*) were constructed and subjected to exome sequencing. In all four mapping populations, a strong association was commonly observed for mutations within the *SlLAX1* (*Solyc09g01480.2*) gene, which is a homolog of the Arabidopsis *AUXIN RESISTANT1* (*AUX1*) transporter gene. Black boxes indicate exons, transparent boxes indicate UTRs, and lines between boxes indicate introns.

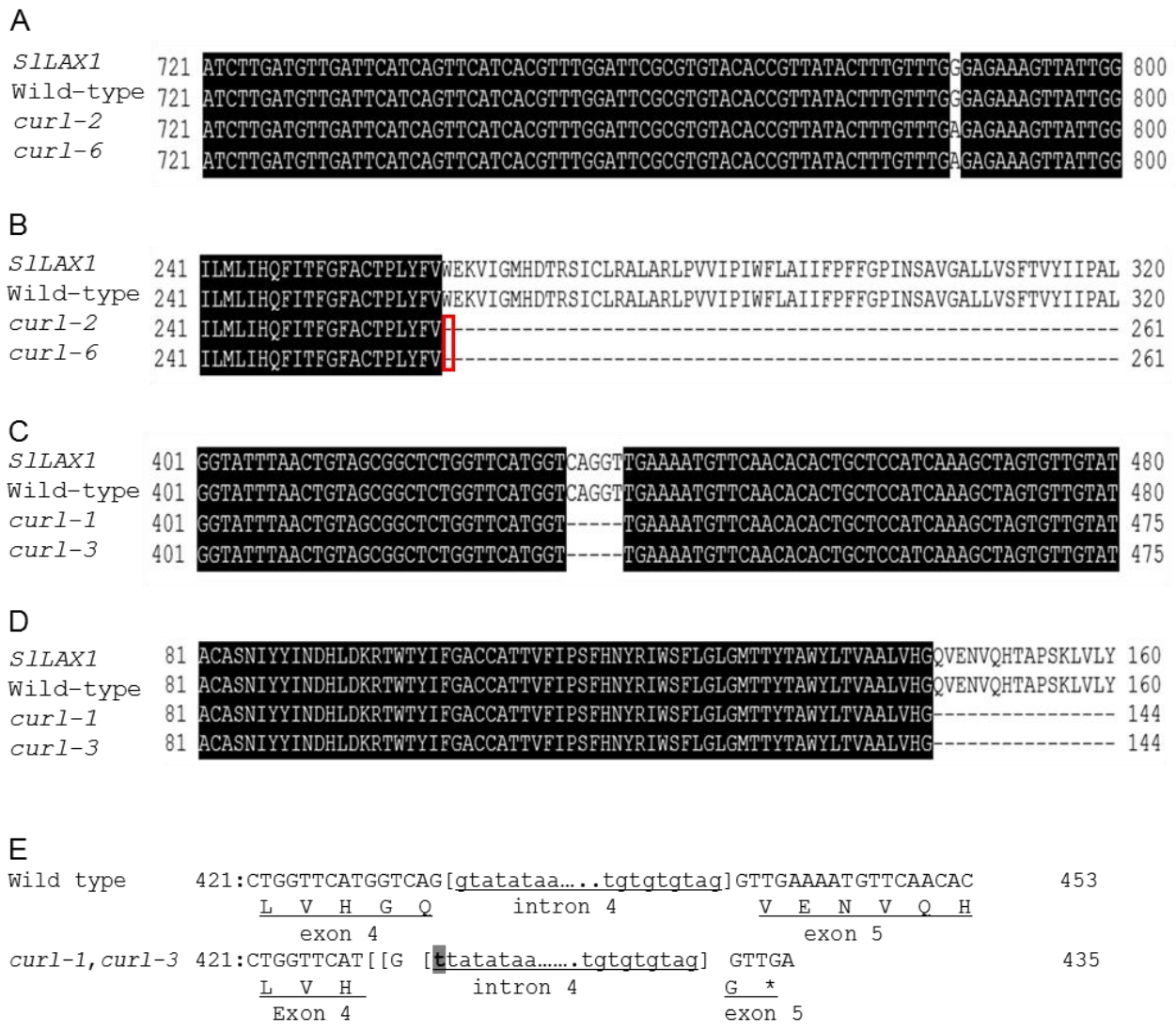

Fig. 2. 4 Changes in nucleotide and protein amino acid sequence of the *curl* mutants.

(A, B) A partial alignment of *SlLAX1* cDNA sequence (A) or deduced protein amino acid sequence (B) among the tomato reference (SL2.50), wild-type Micro-Tom, *curl-2*, and *curl-6*. The mutation in *curl-2* and *curl-6* causes a premature stop codon, as shown by the red box (W262X). (C, D) A partial alignment of *SlLAX1* cDNA sequence (C) or deduced protein amino acid sequence (D) among the tomato reference (SL2.50), wild-type Micro-Tom, *curl-1*, and *curl-3*. cDNA sequences were obtained by dideoxy sequencing (A, C). (E) Donor and acceptor splicing sites in intron 4 of the wild-type, *curl-1*, and *curl-3* mutants. Square brackets indicate splicing sites. Double square brackets indicate alternative splicing site in the *curl-1* and *curl-3* mutants. The one-letter code indicates an amino acid. Uppercase indicates an exon, whereas lowercase indicates an intron sequence. The bold letter indicates a mutated sequence in intron 4 of the *curl-1* and *curl-3* mutants.

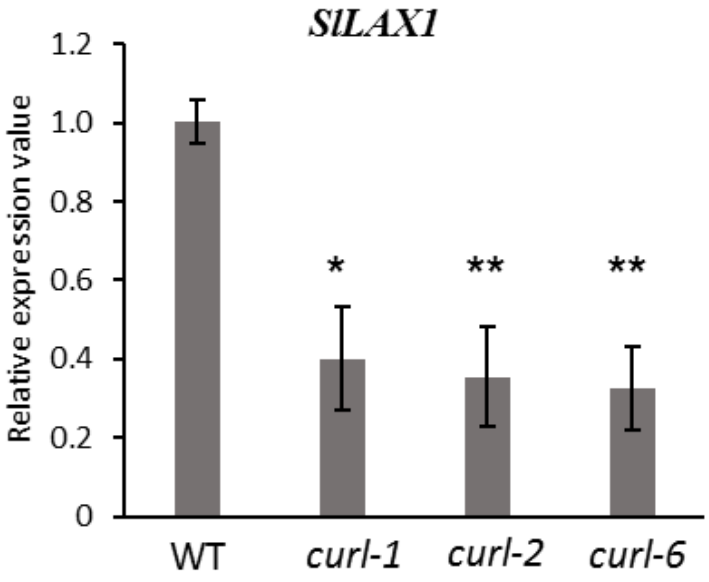

Fig. 2.5 Gene expression analysis of *SlLAX1* in the WT and the *curl* mutants.

Gene expression analysis was obtained by qRT-PCR. qRT-PCR primer was designed at downstream stop codon mutation in exon 6. The asterisks represent statistical significantly difference of means based on t-student test (* $P<0.05$, $^{**}P<0.01$).

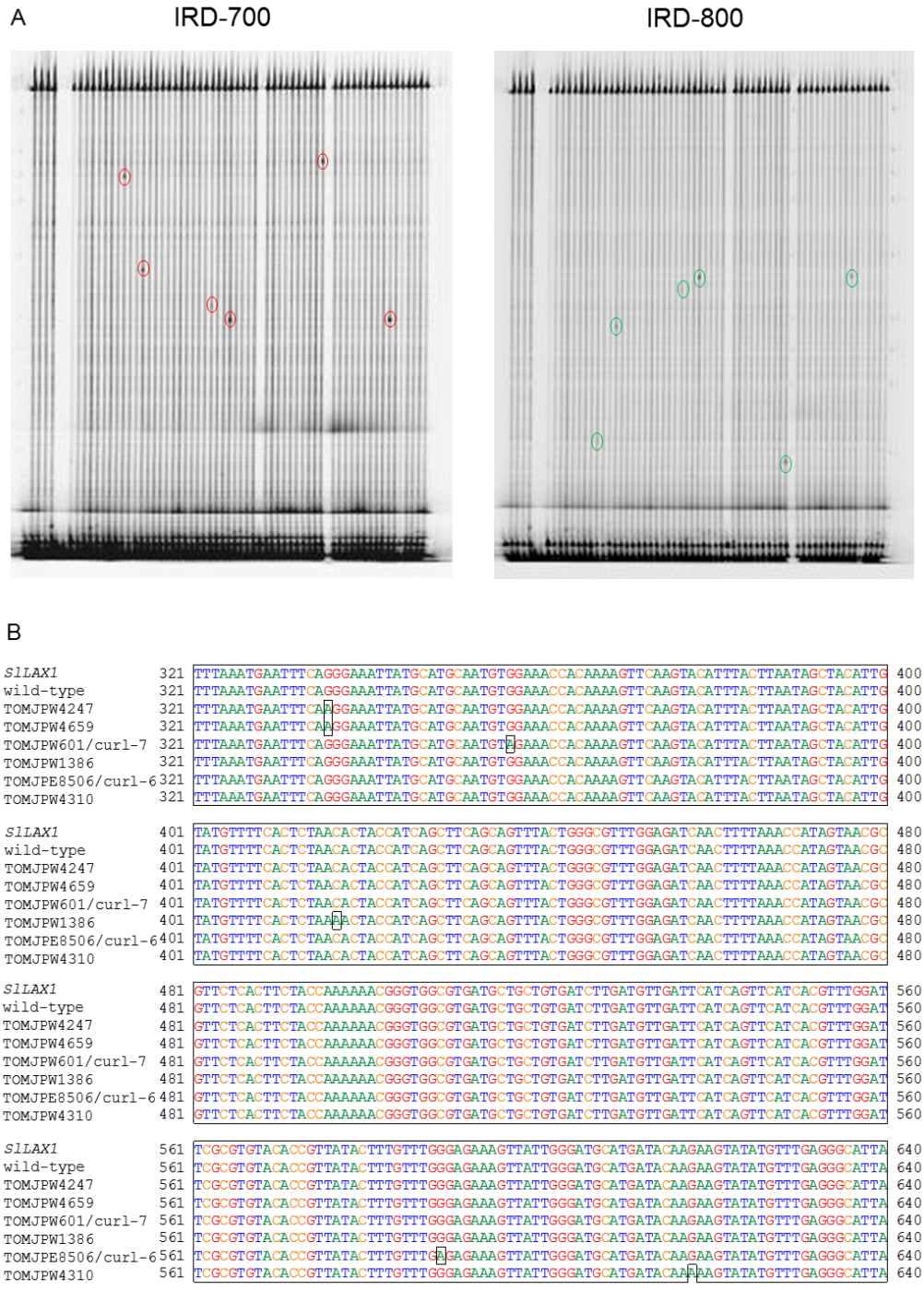

Fig. 2.6 *SlLAX1* TILLING second screening result and nucleotide sequence alignment at the screening target site.
(A) TILLING polyacrylamide gel image of the second screening. Mutations are shown as intense spots on the lanes both in IRD-700 (red circles) and IRD-800 (green circles). (B) Nucleotide sequence alignment at the targeted TILLING screening site. Point mutation are shown in each black transparent box.

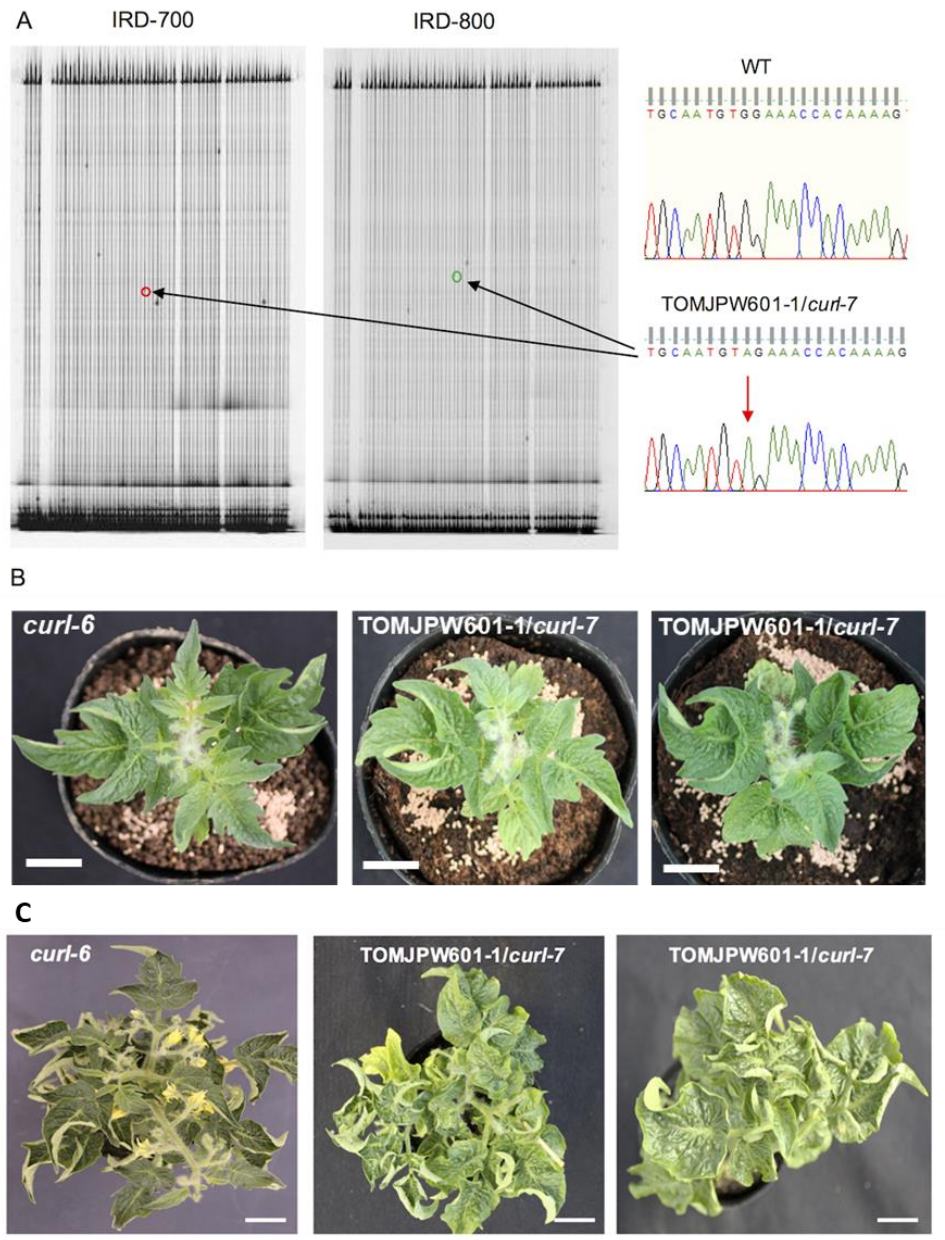

Fig. 2.7 TILLING screening result and confirmation of phenotype of the new mutant allele, TOMJPW601-1/*curl-7*.

(A) Polyacrylamide gel image of TILLING screening. The mutation in TOMJPW601-1/*curl*-7 is shown as an intense spot on the lanes both in IRD-700 (red circle) and IRD-800 (green circle). A single nucleotide change is shown on the sequence chromatogram (red arrowhead). (B-C) Whole-plant images of *curl-6* (left); a representative of the *curl* allele obtained using forward genetics; (middle and right) confirmation of the presence of curly leaves in the new selected allele, *curl-7*, in the M_3 generation. Plant images were captured from 1 month (B) when curly leaf was just formed and 3-month-old plants (C) when the curly leaf phenotype progressed. Scale bar: 2 cm.

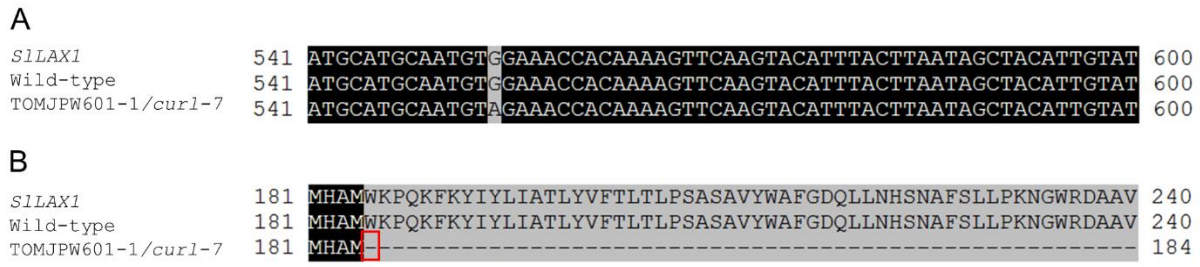

Fig. 2.8 cDNA and amino acid sequence of the new mutant allele, TOMJPW601-1/*curl-7*.

(A) A partial alignment of *SlLAX1* cDNA sequence among the tomato reference (SL2.50), wild-type Micro-Tom, and TOMJPW601-1/*curl-7.* Nucleic acid substitution in the *curl-7* mutant is shown by a gray highlight. (B) Partial protein amino acid sequence alignment of *SlLAX*1 (*Solyc09g01480.2*) among the tomato reference (SL2.50), wild-type Micro-Tom, and TOMJPW601-1/*curl-7*. Mutation in *curl-7* led to the conversion of tryptophan to a premature stop codon. The wild-type (WT) produced a 411-a.a. product, whereas *curl-7* produced only a 185-a.a. product. The premature stop codon is indicated by a red box.

Chapter 3

Phenotypic Characterization of the *curl* Mutants

3.1. Introduction

Auxin has been reported to play central role in diverse plant growth and development including embryogenesis, organogenesis, root initiation and lateral root development, leaf initiation and development, flower initiation, fruit formation, vascular tissue formation, tropic response, and dormancy (Steinmann et al., 1999; Swarup et al., 2001; Aloni et al., 2006; Sieburth and Deyholos, 2006; Bainbridge et al., 2008; Swarup et al., 2008; Péret et al., 2009; Vanneste and Friml, 2009; Wolters et al., 2011; Péret et al., 2012). Auxin controls almost all plant development aspects. Auxin also controls cell division, expansion, and differentiation.

Leaves are the major plant organs whose primary function involves photosynthesis. Leaves play a major role in sensing the quality, quantity and duration of light, all of which are crucial for complete plant growth and development. Formation and development of flat leaf enable to capture optimum amount of sunlight for photosynthesis. Leaf initiation and morphogenesis have been known to be controlled by auxin (Bar and Ori, 2014). Leaf initiation and development are also sensitive to genetic and environmental factors. In most dicotyledonous plants, leaf primordia are formed from proliferative and undifferentiated cells in the shoot apical meristem (SAM) (Blein at al., 2013; Floyd and Bowman, 2010). The rates of division and elongation of cells at each stage are known to govern the final shape of the plant and throughout the leaf developmental process. Following leaf initiation, three axes are established, proximo-distal, medio-lateral, and dorso-ventral (reviewed by Bar and Ori, 2014). Most leaves are dorsoventrally (upper to bottom) flattened and develop distinct upper (adaxial) and lower (abaxial) surfaces. Balanced coordination of polarity, auxin response, and cell division is essential for formation of normal and flat leaves development. Any imbalance of these coordination results in altered leaf shapes such as curly, crinkly, twisted, rolled, radial, or shrunken leaves (Yu et al., 2005; Liu et al., 2010; Liu et

al., 2011; Serrano-Cartagene et al., 2000).

The unique and intriguing features of auxin are its polar transport. Auxin is synthesized in young leaf and shoot apex and transport basipetally into root tip (reviewed in Bennet et al., 1998; Blakeslee et al., 2005; Tromas and Perrot-Rechenmann, 2010). PAT directs auxin movement into other plant organs. PAT is governed and maintained by the coordinated action of AUX1/LAX and PIN carrier proteins, as an auxin influx and efflux carriers, respectively. Although PAT is maintained by synergistic action of AUX1/LAX and PIN, among auxin carriers, PIN1 is the most studied. The role of the PIN protein family in leaf morphogenesis is well documented, yet the role of AUX1/LAX remains neglected or is underestimated. For instance, mutation in *PIN1* inhibits organ initiation in *Arabidopsis*, partially disrupt *pin1* vegetative meristem (Okada et al., 1991; Guenot et al., 2012). In *Cardamine hirasuta*, mutation in PIN1 change compound leaf into simple leaf (Barkoulas et al., 2008). Also, the role of *AUX1/ LAX* genes in root development is well documented, but the role of these genes in leaf morphogenesis remains unclear. For instance, the AUX1/LAX family has been reported to promote lateral root emergence and formation (Marchant et al., 2002; Swarup et al., 2008; reviewed in Peret et al., 2009), root gravitropism (Bennet et al., 1996; Marchant et al., 1999), and root-pathogen interactions (Lee et al., 2011). Recently, *AUX1* function in the aerial parts of plants has received interest, but studies are still considerably scarce. In *Arabidopsis*, *AUX1* has been reported to control phyllotaxis patterning (Bainbridge et al., 2008), vascular patterning, xylem differentiation (Fabregas et al., 2015), and leaf serration (Kasprzewska et al., 2015). Moreover, most studies have been conducted in the plant model, *Arabidopsis thaliana*, while studies in tomato are still scarce. Isolation and characterization of *curl* mutants which has nonsense mutation in *SlLAX1* in this study could help to investigate the pivotal role of this gene in normal leaf development.

In this chapter, I conducted some morphological experiments for detail characterization of the *curl* mutants in organ level. I checked root gravitropism of the mutant and lateral root formation as the most prominent trait of the *aux1* mutant in *Arabidopsis*, the presence of mutant phenotype in seedling stage, early vegetative development, and I also checked the curvature index for quantifying the severity of leaf curvature. Furthermore, I also checked the effect of mutation in whole plant growth.

3.2 Materials and Methods

3.2.1 Seedling stage

Both quantitative measurement and qualitative characterization of seedling stage were performed at seven days after germination using 12 biological replications. In quantitative measurement, primary leaf length and width were recorded. In qualitative measurement, hypocotyl color and its intensity, as well as hypocotyl pubescence were observed according to "descriptor for tomato, IPGRI (International Plant Genetic Resources Institute)".

3.2.2 Observation of the first curly leaf formed and the evolution of curly leaf

Time required for the first curly leaf formed was recorded right after the tip of leaf turned to curly. For quantification of the first curly leaf formed, eight plants from each line were recorded.

3.2.3 Plant height and stem diameter measurement

Plant height was measured from the basal stem to growth point of the main stem started from 4 weeks after sowing (WAS). Four WAS was at the stage when plant start initiation from vegetative to reproductive growth. Plant height was measured every 2 weeks until 10 WAS. Fifteen plants were used for this measurement.

Stem diameter was measured approximately 1 cm from the basal of stem, at the 3rd leaflet. It was measured at 4 and 6 WAS from 15 individual plants from each line.

3.2.4 Fresh, dry weight, and dry matter content of shoot and fruits of the *curl* mutants

Fresh, dry weight, and dry matter content were measured at the end of growing period (12 weeks after sowing). Fruits were detached and measured separately. Plant shoots and fruits were cut and weighed freshly. Then, they were incubated in oven 60 ^{o}C for several days until completely dry. Dry matter content was determined by comparing dry weight/ fresh weight x 100%. For this measurement, 15 plants were used.

3.2.5 Curvature Index (CI) of the mutant leaf

Curvature index (CI) of mutants was measured by a method introduced by Liu et al., 2010.

The formula used to measure leaf curvature index is:

CI= (ab-a'b')/ab

CI= curvature index

ab= the distance between points *a* and *b* on two margins of curvature before flattening of leaves

a'b' = the distance between *a* and *b* on two margins after flattening

Negative (-) CI represents upward curvature.

By applying this method, Liu et al., (2010) had successfully quantified the curvature index of 22 *Arabidopsis* mutants with has various degree of curvature. This method also allows us to characterize any subtle difference by numerical representation. In addition, this method is also applicable to know the global and local curvature, the direction, axis and the extent of curvature of phenotype of interest. Furthermore, because I have three mutant alleles that used for further characterization, comparing their phenotypic severity by quantification of CI was considerably valuable. In many cases, the mutants of several genes/ lines are similar in the phenotypes of curvature, and visual observation relies on the ability and skill of the observer and thus is not certain.

Furthermore, the CI of young and mature leaves were measured to investigate the progression of leaf curvature. For measurement of CI, 15 mature leaves from the 5^{th} leaflet were used. Young leaf CI was also measured. Young leaves were defined as newly formed leaves while progression of incurvature still slow, or slightly turned to curve in the tip and middle area, but the degree of curvature still very low.

For the curvature measurement, two points exactly in the middle of leaf was recorded. The leaf

curvature along transverse and longitudinal axis was also measured using this formula.

3.2.6 Petiole length, leaf width and length

For petiole length, leaf width and length measurement, a leaf from each plant at the 5th leaflet was used, 15 leaves were used for each parameter measured. Most leaves had turned to curly at the time of measurement, then the leaves were flattened. Leaf width was examined by measuring of two distances of each edge at the middle area of leaf. Leaf length was examined by measuring of distance from proximal to distal edge of the leaves.

Length and width ratio (LWR) was quantified by simply divided leaf length and width value of each measurement. Likewise, petiole length and leaf length ratio (PLR), petiole width to leaf width ratio (PWR) were quantified by comparing petiole length and leaf length and leaf width, respectively.

3.2.7 Leaf area and perimeter measurement

Leaf area and perimeter analysis were conducted at young and mature leaf stages, 15 leaves which harvested from the same position were used as the samples. Leaves photograph were captured using a digital camera, and the leaf area and perimeter were measured using CellSensStandard software (Olympus, Japan). The value of before and after flattening was compared to investigate percentage of the leaf area reduction as an effect of mutation, and the curly severity of young and mature leaves can also be clarified. Leaf perimeter and leaf area were measured by following the edge of leaf using a closed polygon measurement tool on the CellSensStandard software. Then, leaves were flattened and photograph after leaf flattening was taken. The reduction in leaf area and leaf perimeter (%) were measured by comparing the values before flattening and the values after flattening (multiplied by 100).

3.2.8 Fresh and dry weight measurement

Fresh weight was measure at the end of growing period (12 weeks after sowing). Fruits were

detached and measured separately. The plant's shoot was incubated in oven 60 ^{o}C for several days until completely dry. Dry matter content was determined by comparing dry weight/ fresh weight x 100%.

3.2.9 Statistical analyses

Unless otherwise stated, data are presented as means ± SE (standard error). Analysis of variant (ANOVA) was carried out using IBM SPSS Statistics ver. 22. Student's *t*-test (at 95 and 99% significant level) was used to analyze significant level between two values with the equal variant.

3.3 Result

3.3.1 The mutation did not affect leaf curvature in the seedling stage

To investigate the effect of mutation at seedling stage, quantitative and quantitative seedling parameters were measured at 7 days after germination. The *curl-2* mutant showed reduce primary leaf length, however there was no significant reducing of leaf length in the *curl-1* and *curl-6*. For the leaf width, the *curl-6* was significantly reduced, in the other mutants were comparable (Table 3.1). For the qualitative trait observation of the *curl* mutants at seedling stage, hypocotyl color and its intensity as well as hypocotyl pubescence were observed, they all were comparable between the WT and the mutants (Table 3.2, Fig 3.1). The curl lateral roots were less than of the WT, but the curl mutants had longer primary root (Fig. 3.1). Until 3 weeks after sowing, the mutant leaves were normal, incurvature could not be noticed (Fig 3.2). At 3 weeks after sowing, the *curl* mutant leaves slightly turned to curly at the lower part of stem at, however it was not so obvious. In this stage, the WT and mutant were slightly distinguishable (Fig.3.3). At 5 weeks after sowing the incurvature was clearly visible (Fig. 3.4). Furthermore, I investigated when the first curly leaf formed was initiated. In all mutant lines observed, the first curly leaf was visible at 34 days after sowing (Table 3.3). At 2 months after sowing, almost all leaves (exclude newly developed leaves) had turned to curly, and the curly leaf could not be restored once it was formed (Fig. 3.5).

3.3.2 The mutation affected overall plant growth

In order to understand the effect of mutation in plant growth, plant height and stem diameter were observed. Plant height was measured every two weeks from 4 to 10 weeks after sowing (WAS). The plant height of all mutant lines was significantly reduced at all measurements and more obvious in the *curl-1* (Table 3.4) suggested the inhibition of the stem elongation of the mutants. The stem diameter was measured at 4 and 6 WAS. Consistent with the plant height, stem

diameter of the *curl* mutants was also reduced (Table 3.5), and the reduction was more obvious in the *curl-1*.

Furthermore, to investigate the effect of mutation in the plant growth more detail, at the end of growing period, the weight of shoot and fruits were measured (Table 3.6 and Table 3.7), respectively. Either the fresh weight or the dry weight of mutants were markedly reduced compared to that of WT. Likewise, the fresh weight and dry weight of fruits of all mutant lines were also significantly reduced. Consistently, the dry matter content of the mutant shoot and fruit was lower compared to that of WT. Taken together, these data suggested that the mutation affected overall plant growth of the mutants from the early developmental stage and growth inhibition effect was continuous until the latest stage of growth development.

3.3.3 The mutation affected leaf flatness with high extent upward curvature

To investigate how and when the curly leaf is formed and its progression in the organ level, the curvature index (CI) was measured both for young and mature leaves using the method introduced by Liu et al., (2010). Measuring the CI allows us to quantitatively understand both the direction of curvature and the specific curvature location (transversal or longitudinal axis) as well as the extent of the leaf curvature. Negative curvature represents upward bending of the leaf. At the early stage of leaf initiation and development Negative curvature represents upward bending of the leaf. At the early stage of leaf initiation and development, mutants developed and maintained flat leaves; after several (4-7) days following leaf initiation, the leaves gradually became curly, and the curly leaf severity increased concomitant leaf maturity (Fig. 3.6). The leaf incurvature was initiated from young leaves along the transversal axis to a low extent, while the longitudinal axis remained flat in all mutant lines (Table 3.8). To understand the curly leaf progression, the curvature of mature leaves of all mutants was also measured (Table 3.9). Consistently, leaf incurvature was observed

along the transversal axis to a high extent, and the longitudinal axis remained flat until the later stage of leaf development. These data suggested that the mutation was only restricted to the adaxial-abaxial (upper to bottom) impairment of the leaf; medio-lateral (center to edge) and proximo-distal (basal to tip) leaf curvatures were not affected. Furthermore, these data also suggested that leaf incurvature was more severe as leaf maturity progressed.

In the young leaves, the tip and middle area were curly, while the basal area remained flat, which suggested that the leaf incurvature was initiated from the tip area followed by the middle area. In the mature leaves, the whole-leaf transversal axis had become curly (Fig. 3.7).

3.3.4 The *curl* mutants showed narrower leaf and shorter petiole

Furthermore, to investigate the effect of mutation on detail leaf features, petiole length, leaf length and width and their ratio were measured at young and mature leave stages. In the young leaves, the leaf length was affected by mutation, while the leaf length reduction was not so obvious (Table 3.10). The ratio of leaf length and width was comparable between the WT and all the *curl* mutants. In the mature leaves, the mutant leaves were shorter and slender as well as shorter petiole (Table 3.11, Fig. 3.8).

3.3.5 Leaf area was markedly reduced in the *curl* mutants

Leave is important plant organ that capture sunlight for photosynthesis. As a consequence of the curly leaf phenotype, the leaf surface that is exposed to sunlight could also be reduced. I also checked the percentage of reduced leaf area and perimeter both in young and mature leaves of mutants by flattening the *curl* mutant leaves. In the young leaves, leaf area was markedly reduced (41-56%, Table 3.12). The leaf perimeters of the WT and mutants were comparable. Consistently, in the mature leaves, the reduction in leaf area was more evident (55.8 – 64.0%) (Table 3.13), indicating a progression of severity that was concomitant with leaf maturity.

3.4 Discussion

Our understanding of auxin-dependent leaf morphogenesis has significantly improved by the characterization of several auxin mutants combined with molecular approaches. For instance, *axr-1* (*auxin-resistant 1*) shows leaf defects (Lincoln et al.,1990). Mutation in *incurvata13* (*icu13*), a recessive allele of *axr6*, causes leaf hyponasty (Esteve-Bruna et al., 2013), and mutations in *ARF3*, *ARF4*, *ASSYMETRIC LEAF 1* (*AS*) and *AS2* (Zgurski et al., 2005) in *Arabidopsis* show an impaired leaf flatness phenotype. In particular, it has been reported that mutation in the auxin efflux carrier PIN1 produces trumpet-like and rod-like leaves (Qi et al., 2014). Studies on the *AUX1/LAX* gene family in aerial parts of plants are scarce. In *Arabidopsis*, the *AUX1/LAX1* family has been reported to control leaf serration (Kasprzewska et al., 2015), phyllotaxis patterning, vascular patterning, and xylem differentiation (Bainbridge et al., 2008; Fabregas et al., 2015). In tomato, transgenic *SlARF4-RNAi* lines produce hyponastic leaves (Sagar et al., 2013). Tomato *SlPIN4-RNAi* lines show leaf flatness defects and altered plant architecture (Pattison et al., 2012). However, the role of *SlLAX1* has not been characterized.

The curly leaf phenotype was not observed at the early stage of leaf development and does not related to relative humidity and water availability. Thus, the curly leaf phenotype was not caused by impairment adaxial-abaxial polarity since adaxial-abaxial polarity is established at the very early stage of leaf development, that is, at the primordium stage. The regulation of leaf incurvature in the *curl* mutants is likely distinct from that of previously characterized adaxial-abaxial polarity *Arabidopsis* mutants, such as *kan1/kan2/kan3*, *rev/phb/phv*, *as1* and *as2*. In these mutants, adaxial-abaxial polarity defects were evidenced at very early stages; consequently, the mutant leaves became radial, needle like or trumpet shaped (Eshed et al., 2004; McConnell and Barton 1998; McConnell et al., 2001).

The progression of curly in the mature leaf or later development stage presumably related to auxin distribution and gradient through *SlLAX1*. Auxin is synthesized in young tissue. The main sites of auxin biosynthesis are young leaf and shoot apex. In this study, the curly leaf initiated from leaf tip/distal area (Fig. 3.6). Probably due to defective auxin transport mediated by *SlLAX1* mutation, auxin depletion is occurred firstly at the tip. This idea is supported by Reindhardt et al. (2003) work. By observing auxin accumulation using PIN: GFP, they concluded that leaf primordial tip is an auxin sink. In the same analogy, as *PIN1* and *AUX/LAX* act sinegically as auxin transport carriers, presumably the impairment of auxin influx in the *curl* mutants make depletion of auxin in the tip area. Also, Ljung et al. (2001) experiment data could explain this phenomenon. They reported that auxin content in the tobacco single leaf varied, the highest auxin content was in the petiole, and auxin gradient was gradually decrease in proximo-distal (basal to tip) direction, supporting the evident the initiation of the curly leaf was first observed in the leaf tip region, followed by middle and basal.

Also, the mutation in the *curl* mutants had effect in the whole plant growth (Table 3.4-3.7). The mutants leaf diameter and leaf area were also markedly narrower and reduced compared to that of WT (Table 3.12, 3.13 Fig. 3.8). It is also possible controlled by the mutation in *SlLAX1*. Alternatively, the severe curly leaf may also affect photosynthesis that led the reducing the overall growth of leaf. These two possibilities could not be distinguished in the current experimental data.

Tables and Figures

Table 3.1 Quantitative measurement of the *curl* seedling

Line	Primary leaf 1		Primary leaf 2	
	Length (cm)	Width (cm)	Length (cm)	Width (cm)
WT	2.2 ± 0.05	0.6 ± 0.01	2.1 ± 0.05	0.6 ± 0.01
curl-1	2.2 ± 0.05	0.6 ± 0.02	2.2 ± 0.05	0.6 ± 0.01
curl-2	1.8 ± 0.03**	0.6 ± 0.02	1.8 ± 0.03**	0.5 ± 0.02
curl-6	2.1 ± 0.06	0.5 ± 0.01**	2.1 ± 0.06	0.5 ± 0.01**

Seedling was measured at seven days after germination.
The *curl* mutants showed reduced primary leaf length in the *curl-2*.
Values are means ± SE (*n*=12). The asterisks represent statistical significantly difference of means based on t-student test (**P<0.01).

Table 3.2 Qualitative observation of the *curl* seedling

Line	Seedling qualitative traits**		
	Hypocotyl color	Hypocotyl color intensity	Hypocotyl pubescence
WT	purple	intermediate	present
curl-1	purple	intermediate	present
curl-2	purple	intermediate	present
curl-6	purple	intermediate	present

** according to descriptor for tomato, IPGRI (International Plant Genetic Resources Institute).

There was no different in seedling qualitative traits between WT and the *curl* mutants.

Table 3.3 The first *curly* leaf observed in each mutant allele

Mutant line	The first curly leaf observed (days)
curl-1	34.5
curl-2	34.4
curl-3	34.4
curl-4	34.3
curl-5	34.4
curl-6	34.5

Values are means, *n*=8. There was no different in the time of the first curly leaf formed, among all mutant alleles.

Table 3.4 The height of plants in 4, 6, 8 and 10 weeks after sowing (WAS)

	Plant height (cm)			
Line	4 WAS	6 WAS	8 WAS	10 WAS
WT	12.6 ± 0.24	17.9 ± 0.67	20.1 ± 0.77	21.7 ± 0.74
curl-1	8.4 ± 0.30**	12.3 ± 0.41**	13.2 ± 0.48**	14.0 ± 0.44**
curl-2	10.2 ± 0.21**	15.7 ± 0.24**	17.4 ± 0.43**	18.3 ± 0.54**
curl-6	9.8 ± 0.14*	14.5 ± 0.41**	16.1 ± 0.58**	17.0 ± 0.61**

Values are means ± SE (n=15). The asterisks represent statistical significantly difference of means based on t-student test ($^{*}P<0.05^{**}P<0.01$). Plant height was measured from the basal stem to growth point of the main stem. WAS: week after sowing

Table 3.5 Stem diameter of the *curl* mutants at 4 and 6 weeks after sowing (WAS)

	Stem diameter (mm)	
Line	4 WAS	6 WAS
WT	6.1 ± 0.06	6.59 ± 0.09
curl-1	4.6 ± 0.08**	5.07 ± 0.15**
curl-2	5.5 ± 0.10**	5.75 ± 0.09**
curl-6	4.9 ± 0.06**	5.30 ± 0.09**

Values are means ± SE (*n*=15). The asterisks represent statistical significantly difference of means based on t-student test (*P<0.05**P<0.01). Stem diameter was measured approximately 1 cm from the basal stem, at the 3rd leaflet. The *curl* mutation significantly reduced stem diameter at 4 and 6 WAS.

WAS: week after sowing

Table 3.6 Fresh, dry weight, and dry matter content of shoot of the *curl* mutants

Line	Fresh weight (g)	Dry weight (g)	Dry matter content (%)
WT	30.64 ± 1.32	2.89 ± 0.14	9 ± 0.00
curl-1	14.52 ± 0.73**	0.84 ± 0.08**	6 ± 0.00**
curl-2	22.52 ± 0.80**	1.79 ± 0.11**	8 ± 0.00
curl-6	16.18 ± 0.41**	1.21 ± 0.06**	7 ± 0.00

Values are means ± SE (*n*=15). The asterisks represent statistical significantly difference of means based on t-student test (**P<0.01). Fresh, dry weight and dry matter content of the *curl* mutants were significantly reduced in the curl mutants suggested reduced growth of mutants.

Table 3.7 Fresh, dry weight, and dry matter content of fruits of the *curl* mutants

Line	Fresh weight (g)	Dry weight (g)	Dry matter content (%)
WT	15.70 ± 1.11	1.18 ± 0.08	8 ± 0.00
curl-1	6.77 ± 1.21**	0.42 ± 0.09**	6 ± 0.01**
curl-2	6.25 ± 0.86**	0.46 ± 0.06**	7 ± 0.01**
curl-6	6.98 ± 0.84**	0.52 ± 0.06**	7 ± 0.00**

Values are means ± SE (*n*=15). The asterisks represent statistical significantly difference of means based on t-student test (**P<0.01). Fresh weight was measure at the end of growing period (12 weeks after sowing). Fruits were detached and measured. The fruits were incubated in oven 60° C for several days until completely dry. Dry matter content was determined by comparing dry weight/ fresh weight x 100%.

Table 3.8 The curvature of the young leave of the *curl* mutants

Line	Direction	Axis	Transverse CI	Longitudinal CI	Extent
WT	flat	-	0.0 ± 0.0	0.0 ± 0.0	
curl-1	upward	transverse	-0.3 ± 0.0**	0.0 ± 0.0	low
curl-2	upward	transverse	-0.2 ± 0.0**	0.0 ± 0.0	low
curl-6	upward	transverse	-0.3 ± 0.0**	0.0 ± 0.0	low

Values are means ± SE (*n*=15). Curvature index (CI) of mutants was measured by a method introduced by Liu et al. 2010.
CI= (ab-a'b')/ab
CI= curvature index
ab= the distance between points *a* and *b* on two margins of curvature before flattening of leaves
a'b' = the distance between *a* and *b* on two margins after flattening
Negative (-) CI represents upward curvature.
Values are means ± SE (*n*=15). The asterisks represents statistical significantly difference of means based on Student's *t*-test (**P<0.01).
The flatness of either young or mature leaf *curl* mutants was impaired along transverse axis, whereas longitudinal axis was normal.

Table 3.9 The curvature of mature leave of the *curl* mutants

Line	Direction	Axis	Transverse CI	Longitudinal CI	Extent
WT	flat	-	0.0 ± 0.0	0.00 ± 0.0	-
curl-1	upward	transverse	-0.7 ± 0.2**	-0.02 ± 0.0	high
curl-2	upward	transverse	-0.8 ± 0.2**	0.00 ± 0.0	high
curl-6	upward	transverse	-0.8 ± 0.2**	-0.01 ± 0.0	high

Values are means ± SE (*n*=15). Curvature index (CI) of mutants was measured by a method introduced by Liu et al. 2010.
CI= (ab-a'b')/ab
CI= curvature index
ab= the distance between points *a* and *b* on two margins of curvature before flattening of leaves
a'b' = the distance between *a* and *b* on two margins after flattening
Negative (-) CI represents upward curvature.
Values are means ± SE (*n*=15). The asterisks represents statistical significantly difference of means based on Student's *t*-test (**P<0.01).
The flatness of either young or mature leaf *curl* mutants was impaired along transverse axis, whereas longitudinal axis was normal.

Table 3.10 Young leaf quantitative measurement of the *curl* mutants

Line	Leaf length (cm)	Leaf width (cm)	LWR
WT	3.7 ± 0.1	1.4 ± 0.0	2.6 ± 0.1
curl-1	3.4 ± 0.1	1.3 ± 0.0	2.6 ± 0.1
curl-2	3.6 ± 0.1	1.3 ± 0.0	2.8 ± 0.1
curl-6	3.5 ± 0.1	1.3 ± 0.0	2.7 ± 0.1

LWR: length and width ratio

Values are means ± SE (n=15). The young leaf length and width of WT and the *curl* mutants was comparable.

Table 3.11 Mature leaf quantitative measurement of the *curl* mutants

Line	Leaf length (cm)	Leaf width (cm)	Petiole length (cm)	LWR	PLR	PWR
WT	5.15 ± 0.14	2.43 ± 0.07	0.50 ± 0.02	2.1 ± 0.06	0.10 ± 0.0	0.20 ± 0.01
curl-1	3.76 ± 0.09**	2.00 ± 0.08	0.38 ± 0.02*	1.9 ± 0.05	0.10 ± 0.01	0.19 ± 0.01
curl-2	4.13 ± 0.10*	2.01 ± 0.07	0.44 ± 0.03	2.1 ± 0.07	0.11 ± 0.01	0.22 ± 0.02
curl-6	3.86 ± 0.09**	2.07 ± 0.06**	0.38 ± 0.02**	1.9 ± 0.06**	0.10 ± 0.01	0.18 ± 0.01*

LWR: Length to width ratio
PLR: Petiole length and leaf length ratio
PWR: Petiole width to leaf width ratio
Values are means ± SE (n=15). The asterisks represent statistical significantly difference of means based on t-student test (*P<0.05, **P<0.01). The *curl* mutants showed shorter and narrower leaf as well as shorter petiole.

Table 3.12 Leaf area and leaf perimeter of young leaves of the *curl* mutants

	Leaf area			Leaf perimeter		
Line	Before flattening (mm^2)	After flattening (mm^2)	Reduction (%)	Before flattening (mm)	After flattening (mm)	Reduction (%)
WT	685.2 ± 47.7	662.0 ± 40.4	3.5	125.7 ± 5.6	124.6 ± 5.7	0.9
curl-1	397.1 ± 54.7**	694.3 ± 45.4	-42.8	119.3 ± 3.7	118.9 ± 3.9	0.3
curl-2	289.3 ± 54.3**	664.9 ± 24.1	-56.5	130.1 ± 3.1	129.4 ± 2.4	0.5
curl-6	316.6 ± 27.7**	649.7 ± 36.1	-51.3	121.1 ± 5.3	118.4 ± 3.5	2.3

Values are means ± SE (n=15). The asterisks represent statistical significantly difference of means based on Student's t-test (**P<0.01).

Table 3.13 Leaf area and leaf perimeter of mature leaves of the *curl* mutants

	Leaf area			Leaf perimeter		
Line	Before flattening (mm^2)	After flattening (mm^2)	Reduction (%)	Before flattening (mm)	After flattening (mm)	Reduction (%)
WT	1489.2 ± 63.2	1440.4 ± 57.3	3.4	188.1 ± 4.3	190.0 ± 5.8	-1.0
curl-1	530.4 ± 72.9**	1471.8 ± 77.1	-64.0	175.0 ± 7.9	191.3 ± 7.8	-8.6
curl-2	314.9 ± 70.4**	1362.1 ± 98.0	-76.9	180.6 ± 5.9	190.7 ± 7.2	-5.3
curl-6	697.2 ± 81.6**	1575.5 ± 122.7	-55.8	189.9 ± 9.2	214.7 ± 11.3	-11.6

Values are means ± SE (n=15). The asterisks represents statistical significantly difference of means based on Student's t-test (**P<0.01).

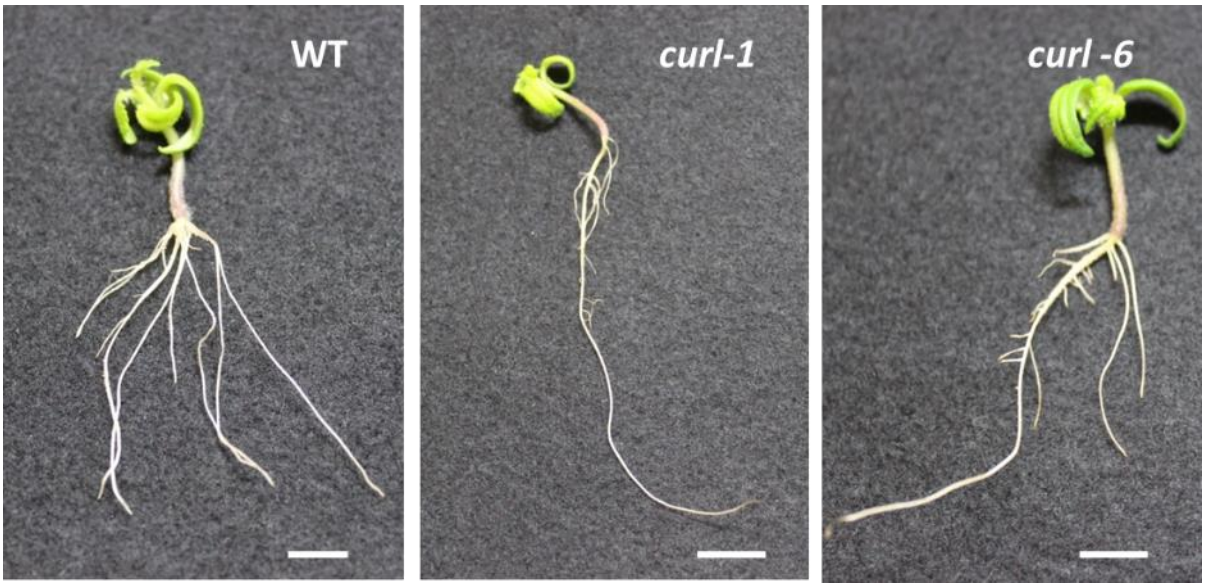

Fig. 3.1 The WT and the *curl* mutant seedlings grown in *in vitro* culture at 7 days old.

The *curl* mutants showed less and longer lateral root compared to that of the WT. Scale bar: 1 cm

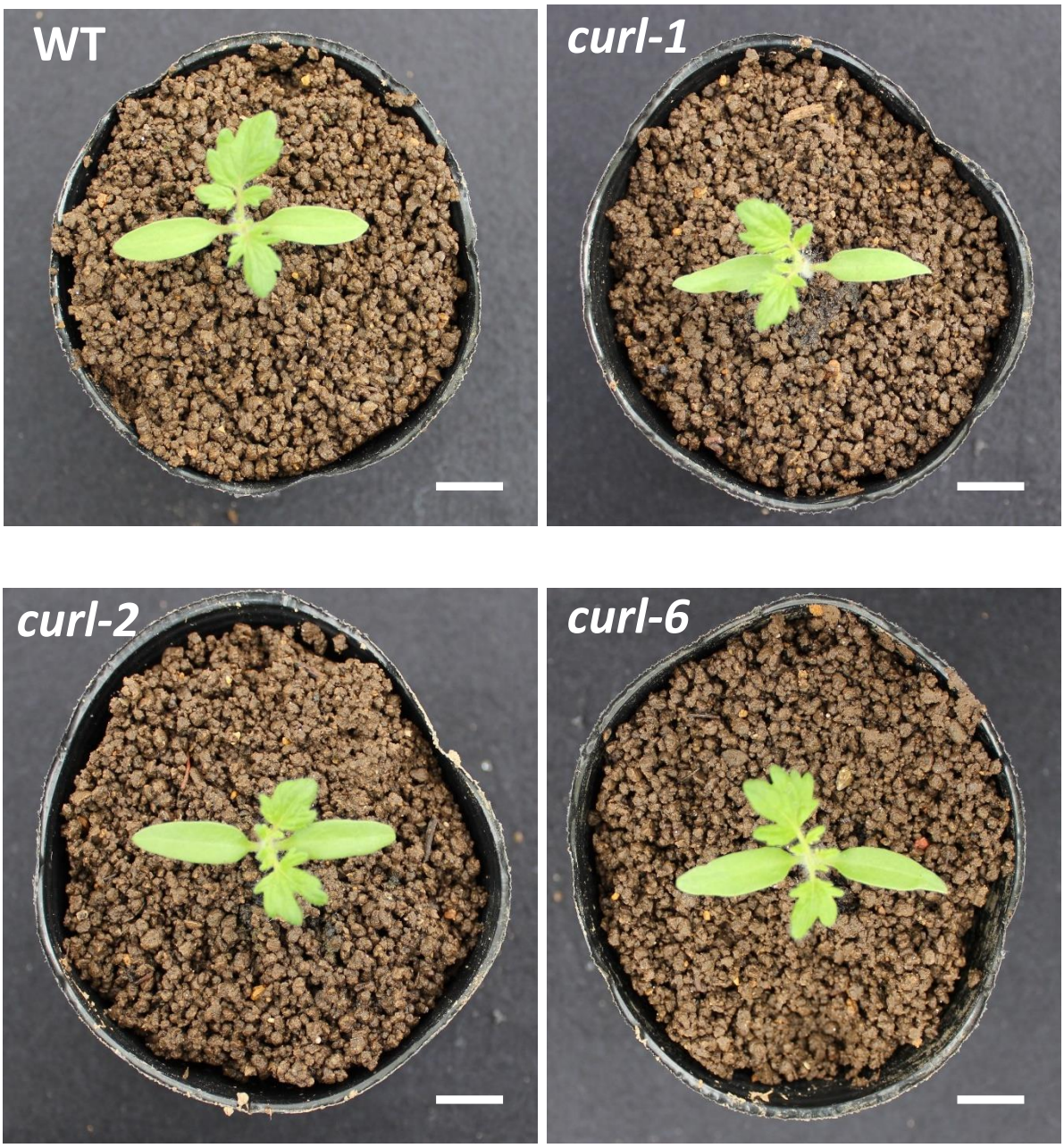

Fig. 3.2 The WT and the *curl* mutant seedlings at 10 days old.

The curly leaf phenotype was not evident at the seedling stage. The WT and *curl* mutants were similar at this stage. Scale bar: 1 cm

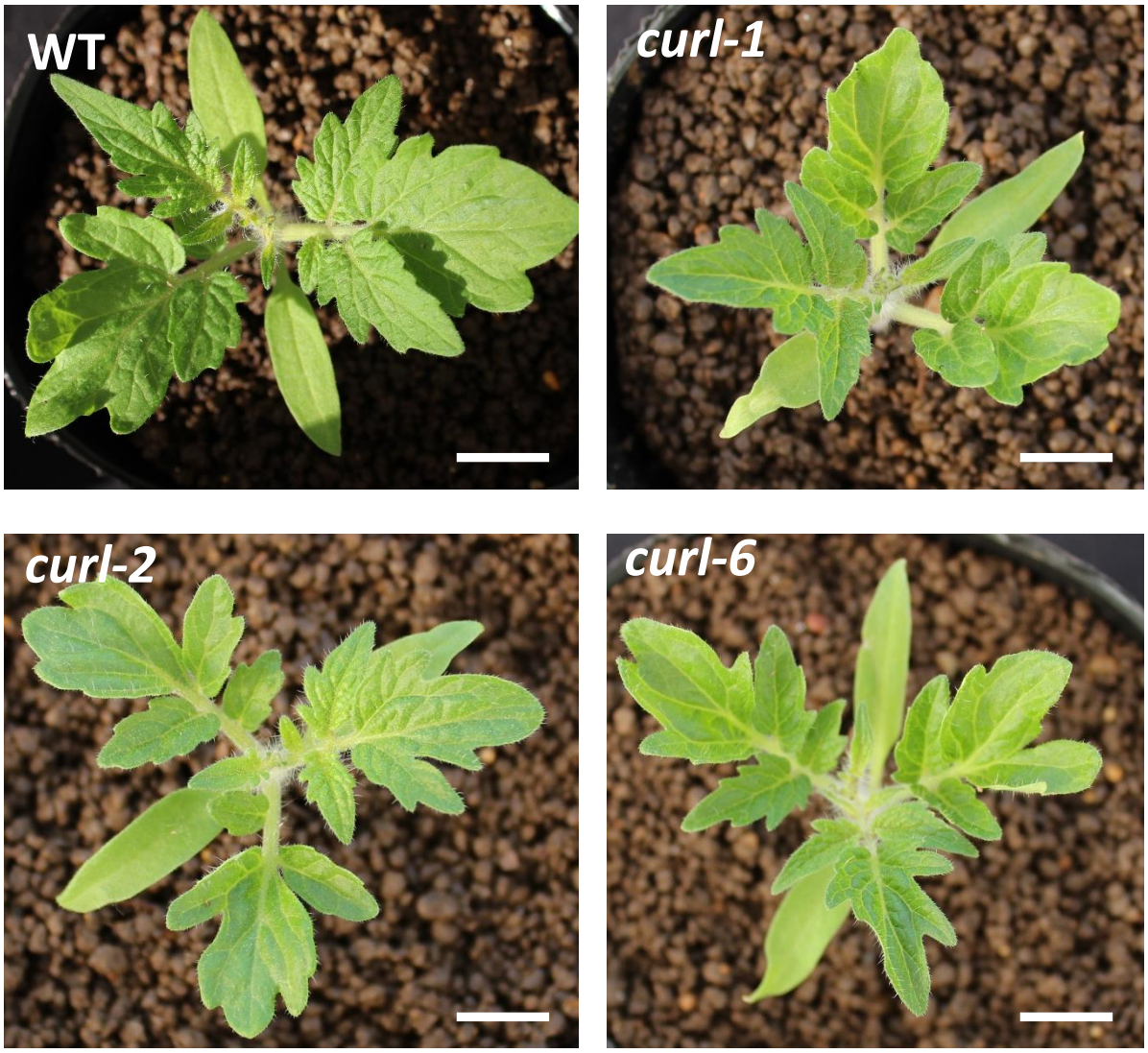

Fig. 3.3 The WT and the *curl* mutant seedlings at 3 weeks after sowing.

The *curl* mutant leaves slightly turn to curly at the lower part of stem at the 3 weeks after showing, however it was not so obvious. In this stage, the WT and mutant were distinguishable. Scale bar: 2 cm.

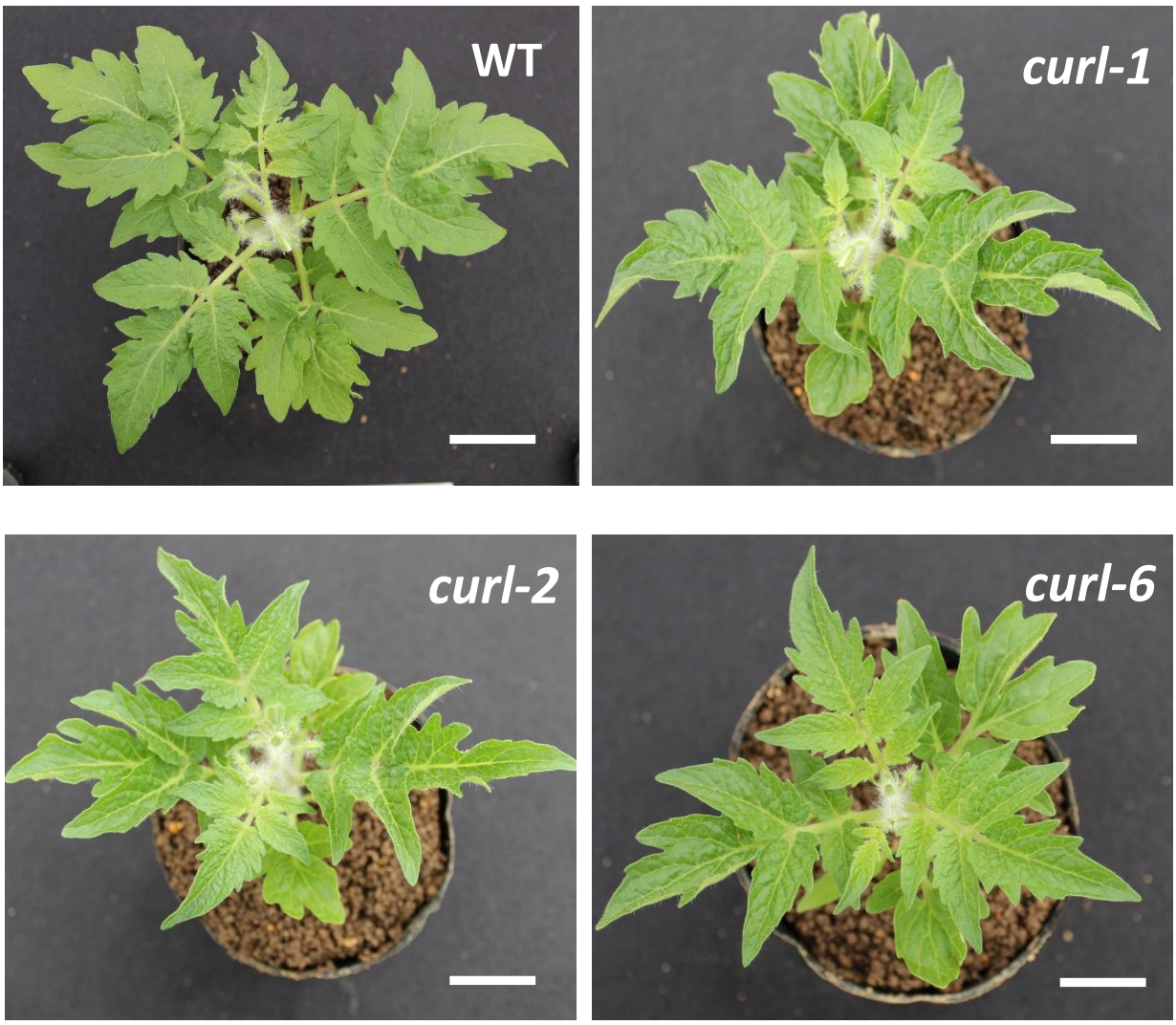

Fig. 3.4 The WT and the *curl* mutant seedlings at 5 weeks after sowing.

The *curl* mutant leaves gradually turned to curly at 5 weeks after showing. The leaves turned to curly for almost all leaflet (exclude newly developed leaf). Scale bar: 3 cm.

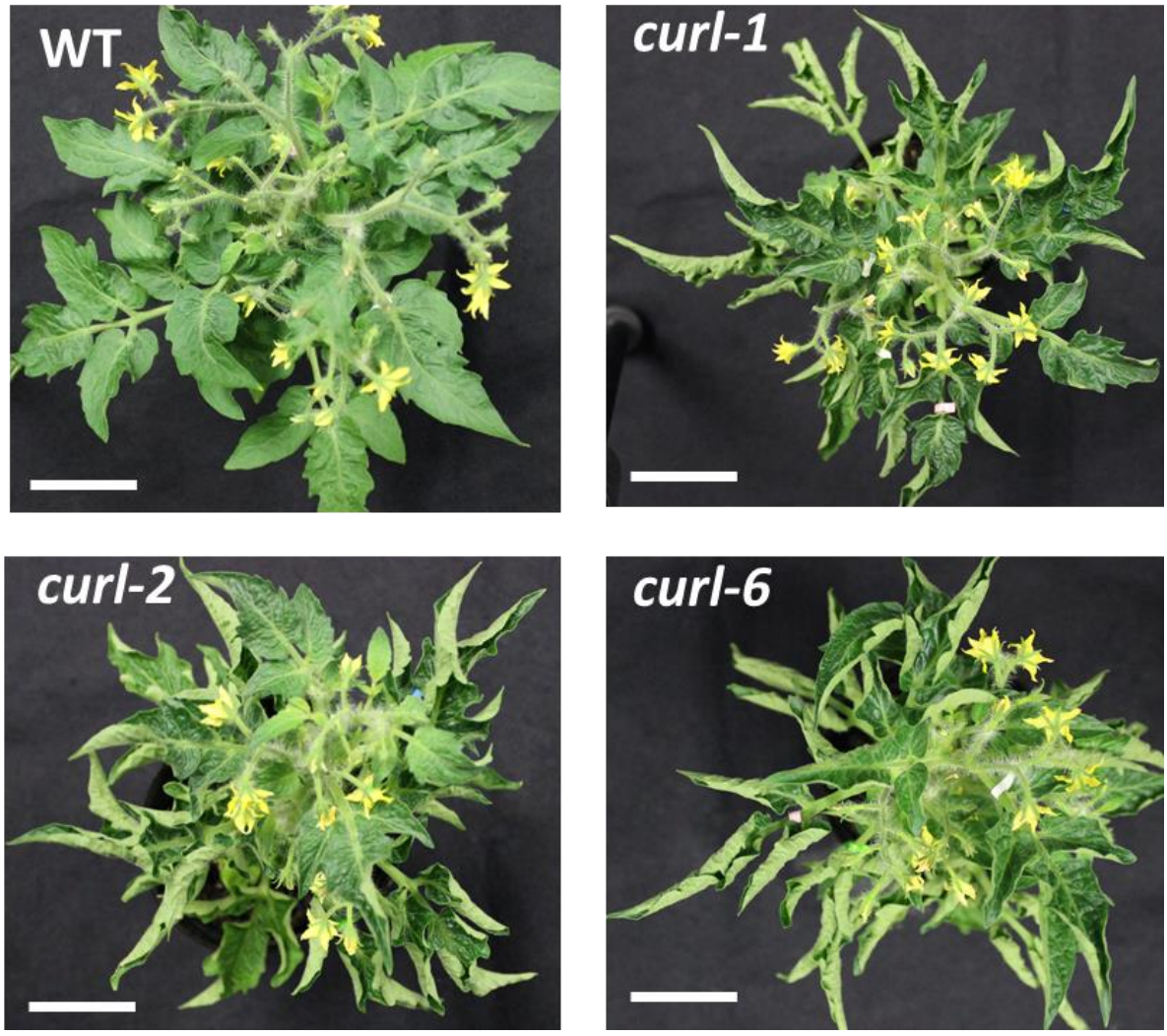

Fig. 3.5 The *curl* mutant images at two months after sowing.

At two months after showing, almost all leaves (exclude newly developed leaves) had turned to curly, and the curly leaf could not be restored once it was formed. Scala bar: 3 cm.

Fig. 3.6 Representative mutant leaf transition from normal to curly in *curl-2*.

(A) Newly developed leaf. (B) Early curly leaf (4 days after image (A)). (C) Fully curly leaf (7 days after (B)). Scale bar: 2 cm. The *curl* mutants formed normal flat leaf in the beginning. Leaf curly was initiated about four days after initiation.

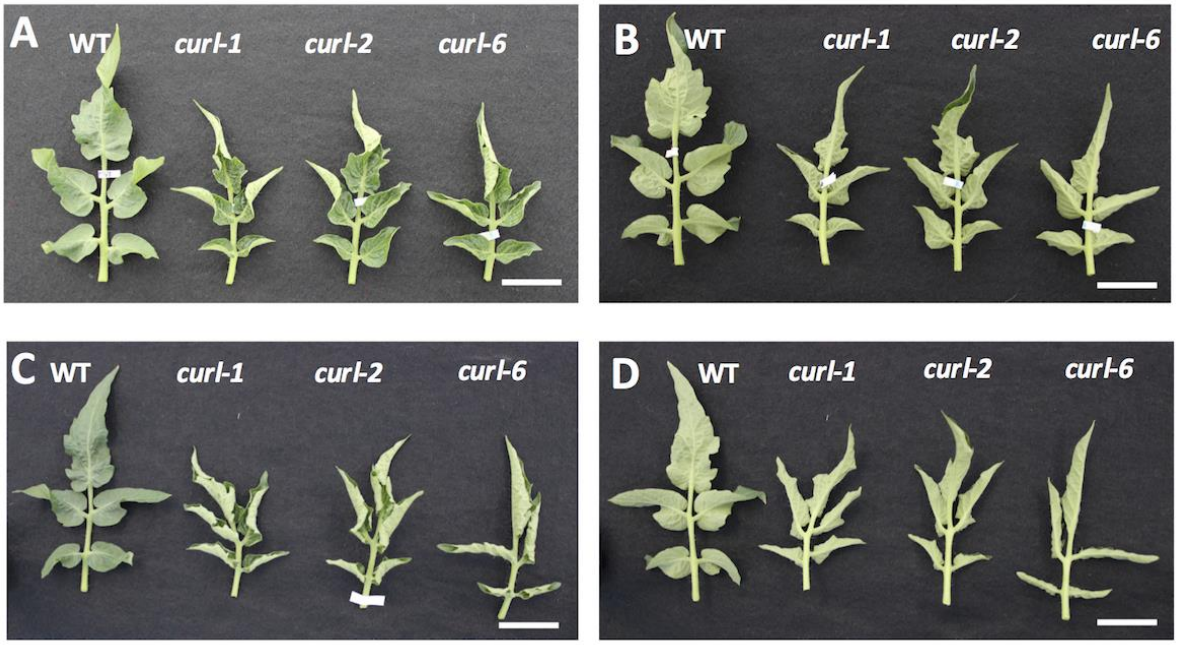

Fig. 3.7 Adaxial and abaxial surfaces of young (upper panel) and mature (bottom panel) tomato leaflets.

(A) Adaxial (upper) surface of young tomato leaflets. (B) Abaxial (bottom) surface of young tomato leaflets. Young leaflets were detached from 1.5-month-old plants. (C) Adaxial (upper) surface of mature tomato leaflets. (D) Abaxial (bottom) surface of mature tomato leaflet. Mature leaflets were detached from the 5th leaflet of 2.5-month-old plants. Scale bar: upper panel, 3 cm; bottom panel, 2 cm.

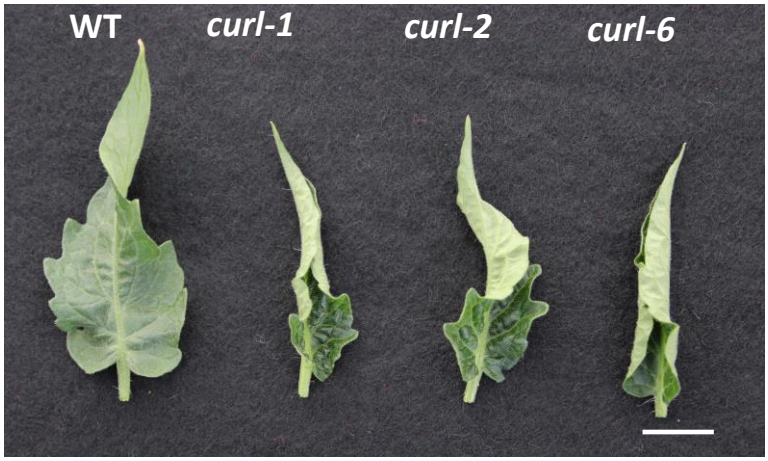

Fig. 3.8 The *curl* mutants showed shorter petiole and narrower leaf. Scale bar: 2 cm.

Chapter 4

Hormonal Content, Histological, and Gene Expression Analysis of the *curl* mutants

4.1 Introduction

Phytohormones play important role in leaf morphogenesis and development. One of important factors governing leaf adaxial-abaxial polarity is auxin. Auxin signal and environmental cues direct plant morphogenesis and development. It has been reported that auxin acts in a dose or concentration dependent manner. Auxin, which is controlled by its biosynthesis and transport, forms concentration gradient in developing plant organs that governing different cellular process, including cell division, expansion, and proliferation (Benjamins and Scheres, 2008; Vanneste and Friml, 2009).

Most leaves are dorsoventrally (upper to bottom) flattened and develop distinct upper (adaxial) and lower (abaxial) surfaces. Balanced coordination of polarity, auxin response, and cell division is essential for formation of normal and flat leaves development. Any imbalance of these coordination results in altered leaf shapes such as curly, crinkly, twisted, rolled, radial, or shrunken leaves (Yu et al., 2005; Liu et al., 2010; Liu et al., 2011; Serrano-Cartagene et al., 2000). The flat leave can be successfully formed by coordinated growth of epidermal, vascular, spongy cell in abaxial and palisade cell in adaxial surface (Horiguchi et al., 2006). The development of normal leaf requires cell expansion and division in precision manner. Although other phytohormones also control this polarity, auxin is reported to be a main player (reviewed in Enders et al., 2015). The increased growth in adaxial surface as compared to the abaxial surface cause epinastic (downward bending) curvature. Conversely, the increased growth of abaxial surface as compared to adaxial cause hyponastic (upward bending) curvature of leaf (reviewed in Sandalio et al., 2016). It has been reported that auxin plays role to control this mechanism. Any imbalance in auxin accumulation or gradient can lead this abnormality. Besides auxin, it has been well established that adaxial and abaxial fates are specified and regulated by the antagonistic interaction of several

transcription factors. Six families of TFs have been reported to control adaxial-abaxial polarity in the model plant *Arabidopsis thaliana*; class III homeodomain-leucine zipper (HD-ZIP), ASYMMETRIC LEAVES (AS), KANADI (KAN), AUXIN RESPONSE FACTOR (ARF), FILAMENTOUS FLOWER (FIL), and YABBY3 (YAB3) (reviewed in Nakata and Okada, 2013). Adaxial and abaxial fates are specified and regulated by the antagonistic interaction of these TFs.

In addition to these TFs, micro RNAs (miRNAs) are also known to regulate abaxial-adaxial leaf polarity through post-transcriptional gene expression (Han et al., 2004). In *Arabidopsis*, several genes involved in miRNAs pathways have been reported such as *ARGOUNATE1* (*AGO1*), *HYPONASTIC LEAVES* (*HYL1*), *Hasty, AUXIN RESPONSE FACTOR* (*ARF3* and *ARF4*), (reviewed in Nakata and Okada, 2013).

Numerous findings have indicated that *AtAUX1* plays an important role in root gravitropism and lateral root development (Bennet et al., 1996; Marchant et al., 1999). Root gravitropism response is also commonly used to check auxin response and distribution. In this chapter, I checked root gravitropism response of the *curl* mutant as well as endogenous content of auxin and cytokinins in three leave developmental stages, namely young leave, early curling leave, and mature leave when curly leave was fully developed. Also, I investigated the epidermal cell features of the *curl* mutants using a scanning electron microscope Furthermore, I also checked gene expression analyses of auxin-related leaf flatness, and an adaxial specification gene, *SlREV*, at mature leaf of the *curl* mutants.

4.2 Materials and Methods

4.2.1 Hormone analysis

Leaves were sampled at three stages from the same positions: young stage, early curling stage, and fully curled stage. Three biological replications were included at each stage. At least 100 mg of fresh leaves was immediately frozen in liquid nitrogen and crushed into a fine powder using a TissueLyser (Qiagen, Germany). Endogenous hormones were measured using a UHPLC-Q-Exactive (Thermo Fisher Scientific) system. Measurements were conducted as described by Kojima et al., 2009 and Shinozaki et al., 2015.

4.2.2 Root gravitropism response

For gravitropism response experiment, tomato seedlings were grown in *in vitro* culture for 4 days, and then the plant boxes were rotated 90° for one day.

4.2.3 Scanning electron microscope (SEM) experiment

The leaf epidermal surface was observed using a scanning electron microscope (Hitachi Tabletop Microscope TM3000, Japan) integrated with a monitor and Hitachi TM3000 software, set to Analy observation mode. The cell feature was measured at the mature leaf stage when the leaves were completely turned to curly, precisely in the same regions on adaxial and abaxial surfaces. Mature fresh leaves were sampled and flattened before being subjected to microscopic observation. Approximately 0.5 x 0.5 cm^2 of abaxial or adaxial surface was placed into a sample box, after which the epidermal pavement cell was imaged at 400x magnification for at least three biological replications. The cell size was quantified separately using CellSensStandard software. All measurements were obtained for at least three independently captured SEM images for each replication and three fields of view for each image.

For the number of pavement cell quantification, leaf samples were cut from midway precisely between the midrib to the margin of fully curly leaves. I used precisely the same position both in adaxial and in abaxial side, one side was used for adaxial pavement cell observation, and the other was used for abaxial. About 2-4 mm leaf sample in the tip area of transversal axis was cut irrespective the size from the midrib to the margin, and it was subjected to SEM experiment (Fig. 4.1). The cell number was counted thoroughly in that region. Measurements were obtained from three biological replications.

4.2.4 RNA extraction and cDNA synthesis, and qRT-PCR analysis

Total RNA was extracted from young and mature leaves (when the leaves were completely curly) using an RNeasy Mini Kit (QIAGEN) according to the manufacturer's protocol. To remove genomic DNA contamination, two steps were applied: an on-column RNase-free DNase Set (QIAGEN) and an RNA Clean & Concentrator™-5 (Zymo Research). Subsequently, cDNA was synthesized from 2000 ng of total RNA by a SuperScript VILO master mix (Invitrogen, Thermo Fisher Scientific, USA) according to the manufacturer's instructions.

The mRNA expression was quantified by qRT-PCR. A 10 ng/µl of cDNA template of three biological replicates was used for *SlLAX1* gene expression analysis. *SlActin* gene was used as an internal control (Lovdal and Lillo, 2009). The qRT-PCR reaction was carried out using CFX96 Real-Time System (Bio-Rad, http://www.bio-rad.com) with SYBR Premix ExTaq II (Ili RNase H Plus; TaKaRa Bio, Japan). The primers used in the qRT-PCR are listed in Table 4.1. Relative gene expression was quantified using $\Delta\Delta C_T$ method (Pfaffl, 2001). qRT-PCR mix reaction and thermal cycle condition are performed as described by Shinozaki et al., 2015. The primers for qRT-PCR were designed using the Primer3Plus website (http://primer3plus.com/), using joining two exons in either forward or reverse primer to exclude any possibility contamination of genomic DNA.

4.3 Result

4.3.1 Endogenous auxin and cytokinins contents of the *curl* mutants were normal

As described above, all *curl* mutants commonly have mutation in the *SlLAX1* gene, which encodes an auxin influx carrier. Functional characterization of this tomato gene has not been reported. To test the potential function of SlLAX1 as an auxin transporter in tomato, I measured the leaf endogenous level of auxin the *curl* mutants at three stages: in young leaves, before curly leaves formed; during early curly leaf formation; and in mature leaves, after leaves were fully curly. There was no significance different auxin between the WT and the *curl* mutants (Fig. 4.2). The IAA content significantly decreased from young leaves to mature leaves in both the WT and three *curl* mutants (Fig. 4.2 A). However, the auxin content at each leaf stage was comparable between the WT and *curl* mutants. Similarly, IAA conjugates and total IAA between the WT and the *curl* mutants were also comparable (Fig. 4.2B, C).

4.3.2 The *curl-6* showed gravitropism and lateral root formation defects

In *Arabidopsis*, numerous findings have indicated the role of LAX1/AUX1 family in root gravitropism and lateral root formation (Bennet et al., 1996; Marchant et al., 2002, reviewed in Swarup and Peret, 2012). Importantly, root agravitropism is the most prominent defect and well-characterized trait of the *Arabidopsis aux1* mutant. In addition, the *aux1* mutant also showed lateral root formation defects (Marchant et al., 2002). Thus, I further tested these traits in the *curl-6* mutant; as expected, the *curl-6* mutant showed agravitropism as well as reduced lateral root formation, in agreement with *Arabidopsis aux1* mutant phenotype (Fig. 4.3), suggesting the possibility of involvement of SlLAX1 as an auxin influx carrier in tomato similar to AtAUX1

4.3.3 Abaxial pavement cell size of the *curl* mutants was significantly larger

As the *curl* mutant phenotype is not related to water availability and relative humidity, and

the leaf was normal at the initiation which means not related to adaxial-abaxial polarity establishment, since the adaxial-abaxial polarity is established in the leaf primordia stage. I hypothesized that the curly leaf formation may related to differential cell growth on adaxial and abaxial surfaces. To observe histological features of the *curl* mutants, I measured pavement cell size and cell area using a scanning electron microscope (SEM) in the adaxial and abaxial surfaces at the mature leaf stage at the curly part (Table 4.2, Fig. 4.4). I noted that cell enlargement in the *curl* mutants was more prominent in the abaxial side. As a consequence, abaxial/adaxial pavement cell ratio was more prominent in the *curl* mutants. I also quantified the pavement cell number both in adaxial and abaxial surfaces. The number of pavement cells in both surfaces was comparable (Table 4.3). These data revealed that the leaf flatness impairment of the *curl* mutants is likely due to the differential cell growth between the adaxial and abaxial epidermal layers. Most likely, the curly leaf phenotype is related to cell enlargement in abaxial side.

4.3.4 Relative expression of auxin-related genes in the *curl* mutants

Recently, some studies have reported that impairment auxin biosynthesis, signaling, degradation, and conjugation result in leaf development defect such as wrinkled, curled leaf, and rounded leaf phenotype. I checked relative expression of some putative tomato auxin-related genes which were reported involved to control leaf flatness phenotype such as *AtDof5.1* (Kim et al. 2010) which is homologous to *SlDof25* and *SlDof28* in tomato (Cai et al. 2013), *LCR* (*LEAF CURLING RESPONSIVENESS*) (Song et al. 2012), *PNH* (*PINHEAD*) (Newman et al. 2012), *YUC1* (Cheng et al. 2007). At the young leaf stage, the expression level of LCR gene was slightly decreased in the *curl* mutants compared to that of WT but increased in the mature leaf (Fig. 4.5C, I). *YUC1* expression was also significantly decreased both in the young and mature leaves of the *curl* mutants (Fig. 4.5D, J) There was no significant different in *Sldof28,* and *PNH* at both stages (Fig.

4.5B, H, E, K). *SlDof25* expression level was increased in the *curl* mutants at the mature leaf stage (Fig. 4.5G), while there was no significant change at the young leaf stage (Fig. 4.5A). It has been reported that *Arabidopsis* activation tagging mutant *Dof5.1-D* exhibiting an upward-curling leaf phenotype by promoting *Revoluta* transcription (Kim et al. 2010). *Revoluta* (*Rev*) is an adaxial specification gene (Emery et al. 2003, Prigge et al. 2015). And most importantly, in tomato, it has also been reported that overexpression of a microRNA166-resistant version of *SLREV* (35S::REV^{Ris}) showed upward curly leaf phenotype (Hu et al. 2014). The gene expression of *SlDof 25* and *SlRev* was consistent with these findings (Fig. 4.5L).

4.4. Discussion

To test the potential function of SlLAX1 as an auxin transporter, I first measured leaf endogenous auxin content. However, IAA content was comparable between WT and the *curl* mutants at all stages (Fig. 4.2). Numerous findings have indicated that *AtAUX1* plays an important role in root gravitropism and lateral root development (Bennet et al., 1996; Marchant et al., 1999). Root gravitropism response is also commonly used to check auxin response and distribution. Therefore, I next tested these assays and found that the root gravitropism response of the *curl* mutant was affected by the *SlLAX1* mutation. In addition, lateral root emergence was also disrupted (Fig. 4.3). Although the functional characterization of SlLAX1 has not been conducted in tomato and I do not yet have direct evidence in this study, agravitropism and lateral root formation defects of the *curl* mutants indicated that SlLAX1 may have a potential function as an auxin transporter similar to *AtAUX1*, and SlLAX1 might participate in local auxin distribution without affecting total endogenous auxin content of the whole leaf. Functional analysis of *SlLAX1* gene remains to be determined. Alternatively, in this study, I subjected whole leaves to auxin measurement, which would make it difficult to see spatial auxin accumulation in leaves. The quantification of local measurements would help explain the effect of spatial auxin accumulation in the formation of curly leaf phenotype.

The curly leaf phenotype was not observed at the early stage of leaf development (Fig. 2.1C, D, Fig. 3.5), and does not related to relative humidity and water availability (Fig. 2.1E, G). Thus, I hypothesized that the curly leaf phenotype was caused by the alteration of adaxial/abaxial cell ratio rather than impairment adaxial-abaxial polarity since adaxial-abaxial polarity is established at the very early stage of leaf development, that is, at the primordium stage. To test this hypothesis, I measured pavement cell size in the epidermal adaxial and abaxial cell side at the mature leaves

when the leaf completely became curly. As I expected, pavement cell size in the abaxial in the *curl* mutants was significantly larger compared to that of WT, while there was no significant difference in the adaxial side. The number of pavement cell in adaxial and abaxial sides was comparable. The upward curling of the *curl* mutants might be explained by the differential growth of pavement cells in adaxial and abaxial cell surfaces, which is supported by similar observation of *incurvata6* (*icu6*), semi-dominant allele of the *AUXIN RESISTANT3* (*AXR3*), that showed an upward curly phenotype caused by a reduced adaxial/abaxial cell size ratio (Perez-Perez et al., 2010). The imbalance epidermal adaxial-abaxial cell growth which led to either epinastic (downward curvature) or hyponastic leaf is not new phenomenon. In previous finding, it was reported that auxin hyper accumulation plant produced leaf epinastic curvature that was formed due to an increased growth of the leaf adaxial side (Klee et al., 1987; Romano et al., 1993; Kim et al., 2007), that induced by reduced auxin export that may cause its hyper-accumulation on the adaxial side. Taken together, SlLAX1 might have a function not in the establishment of adaxial-abaxial polarity but rather in balancing adaxial/abaxial cell size ratio in later stages of leaf development. The evaluation of auxin distribution and/or analysis of *SlLAX1* gene expression on adaxial and abaxial leaf surfaces should allow for a better understanding of the *SlLAX1* function in this process.

According to the relative expression of some tomato putative auxin-related genes controlling leaf flatness, *SlYuc1* showed prominent changes in both young and mature leaves of the *curl* mutants. *YUC* is a family of genes that are orthologs to *ToTFZY* (Expo´sito-Rodrı´guez et al., 2007), which has a function in local auxin biosynthesis (Zhao et al., 2001). In the previous finding, it has been reported that *aux1* and *yuc* mutants in *Arabidopsis* have a synergistic effect to enhance each other to control leaf development. In *Arabidopsis*, activation tagging of *AtDof5.1* resulted in an upward curly leaf phenotype (Kim et al., 2010). Dof5.1 was demonstrated to promote the *Revoluta*

gene expression by binding to its promoter. Similarly to these finding (Kim at al., 2010), expression of *SlDof25,* an ortholog of Dof5.1*,* was increased in the all *curl* mutants (Fig. 4.5G). The *SlRev* expression level was also increased (Fig. 4.5L). Up regulation of *AtDof5.1* also repressed transcript levels of auxin biosynthesis genes, which is consistent with low expression level of *SlYuc1* in the *curl* mutants (Fig. 4.5D, J). In tomato, it has also been reported that overexpression of a microRNA166-resistant version of *SLREV* (35S::REV^{Ris}) showed upward curly leaf phenotype (Hu et al., 2014). Collectively, our findings are similar to previous findings which reinforce the partial disturbance of auxin homeostasis in the *SlLAX1* mutants.

Tables and Figures

Table 4.1 Primer pairs that used for qRT-PCR

Primer name	Forward sequence 5'- -3'	Reverse sequence 5'- -3'
SlDof25	TCCCAATTTGCATCAGTTACAACA	AACCTGGTCTGATTGAGCCC
SlDof28	CTGATCGAGCCCGGATGG	CCAGTACCTTTTAAAGCCTTGC
LCR	CCACTTGTACACCTACCAAGATGT	GGAGGCTTTCCTGGTTCCAA
Yuc1/ToFZY1	GGTGGTCAGAAATTCTGTGCA	AGTGCTACCTAAGGTTAAGTTAGCA
PNH	CGTTGGGCATGCATCAACTT	GGGTCCGGATTGAACTCCATT
SlREV	ACTCGACATGCTGGAGACAAC	AGATACCACCAGGCAAACACG

qRT-PCR primers were designed to span two exons either in forward or reverse sequence to remove possible contamination of genomic DNA.

Table 4.2 Adaxial and abaxial pavement cell size the *curl* mutants in the curly part measured by a scanning electron microscope

Line	Pavement cell size (μm)		Abaxial/adaxial pavement cell size ratio
	Adaxial	Abaxial	
WT	43.36 ± 2.1	42.11 ± 3.4	0.97
curl-1	36.04 ± 1.8	57.83 ± 6.4**	1.59**
curl-2	36.90 ± 1.2	58.69 ± 4.1**	1.61**
curl-6	38.07 ± 1.8	60.18 ± 1.3**	1.66**

Values are means ± SE (n=9). The asterisks represent statistically significant differences in means with equal variants based on Student's t-test (**P<0.01).
The cell feature was measured at the mature leaf stage when the leaves were completely turned to curly, precisely in the same regions on adaxial and abaxial surfaces.
The *curl* mutants showed a significantly larger abaxial/adaxial pavement cell size ratio compared to that of the wild-type (WT).

Table 4.3 Adaxial and abaxial pavement cell number of the *curl* mutants measured by a scanning electron microscope

Line	Pavement cell number (cells)		Abaxial/adaxial pavement cell number ratio
	Adaxial	Abaxial	
WT	1317.3 ± 49.5	1110.6 ± 70.8	0.84
curl-1	1207.5 ± 80.6	1073.5 ± 65.2	0.89
curl-2	1389.2 ± 105.2	1173.9 ± 26.9	0.85
curl-6	1304.3 ± 73.6	1156.8 ± 59.6	0.89

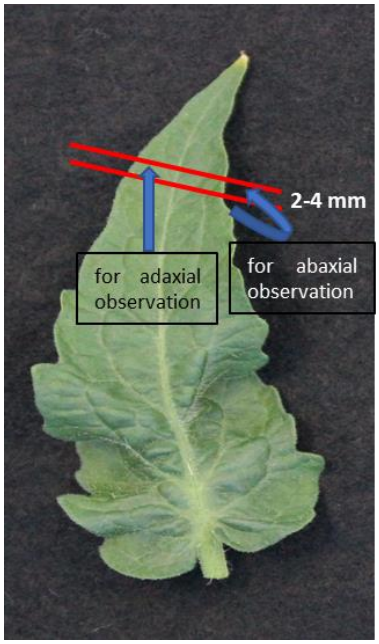

Fig. 4.1 Illustration of the method and leaf area that were used for adaxial-abaxial cell number quantification in the scanning electron microscope experiment.

Leaf samples were cut from midway precisely between the midrib to the margin of fully curly leaves. We used the same position both in adaxial and in abaxial side; one side was used for observation of adaxial pavement cell, and the other was used for observation of abaxial pavement cell. About 2-4 mm leaf sample in the tip area of transversal axis was cut irrespectively the size from the midrib to the margin. The cell number was counted thoroughly in that region. Measurements were carried out three biological replications.

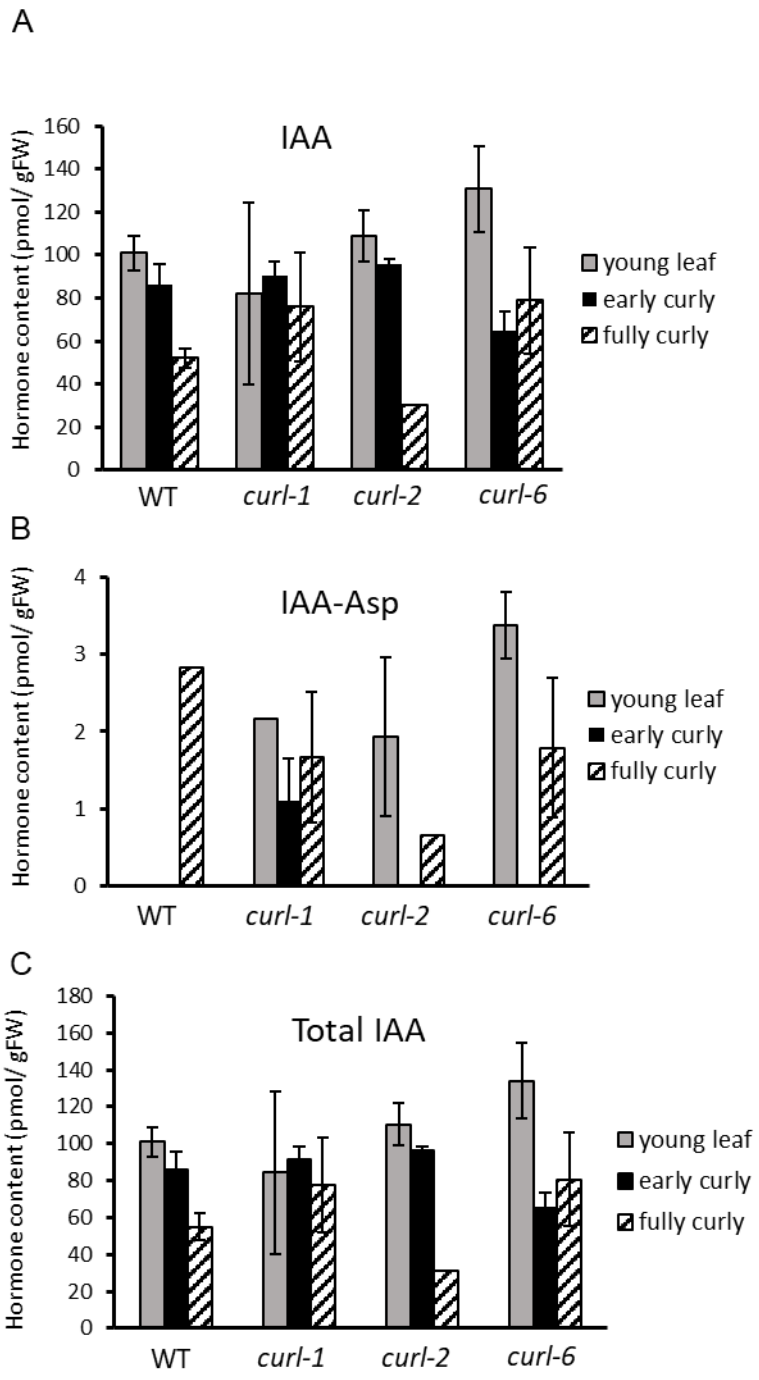

Fig. 4.2 Auxin content of the *curl* mutants measured at three stages. Young leaf (grey), early curly developed (black), and mature leaf (strip).

(A) Endogenous IAA (B) IAA in conjugate form (C) Total endogenous auxin content
IAA: indole-3-acetic acid, the active from of auxin, IAA-Asp: IAA conjugates with aspartate, inactive form of auxin

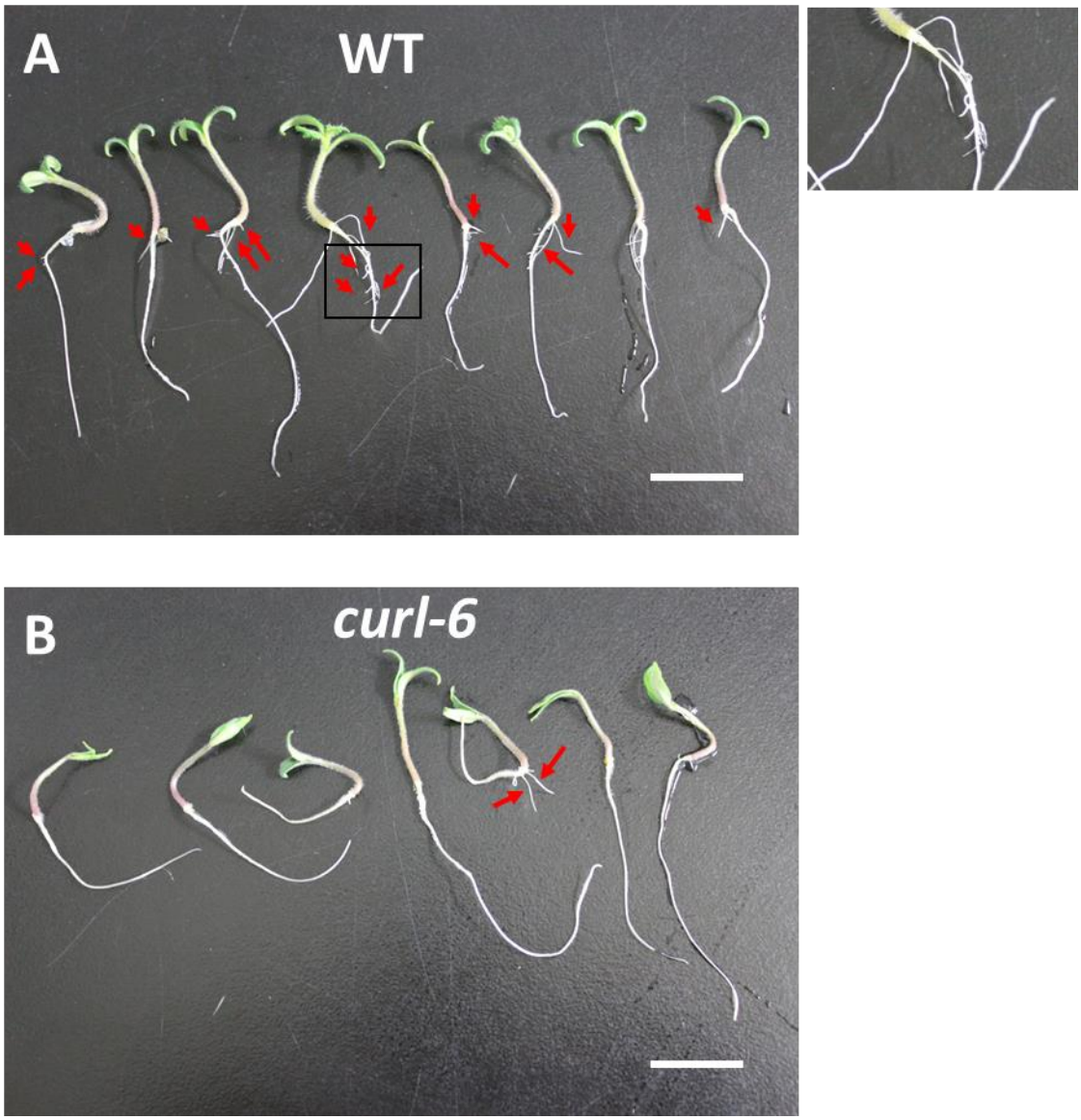

Fig. 4.3 Gravitropism response and lateral root formation of wild-type and a representative of *curl* mutants, *curl-6*.

(A) Wild-type (WT) seedlings showed a normal root gravitropism response and produced lateral roots. (B) The *curl-6* showed agravitropism and failed to form lateral roots at the early seedling stage. Scale bar: 2 cm.

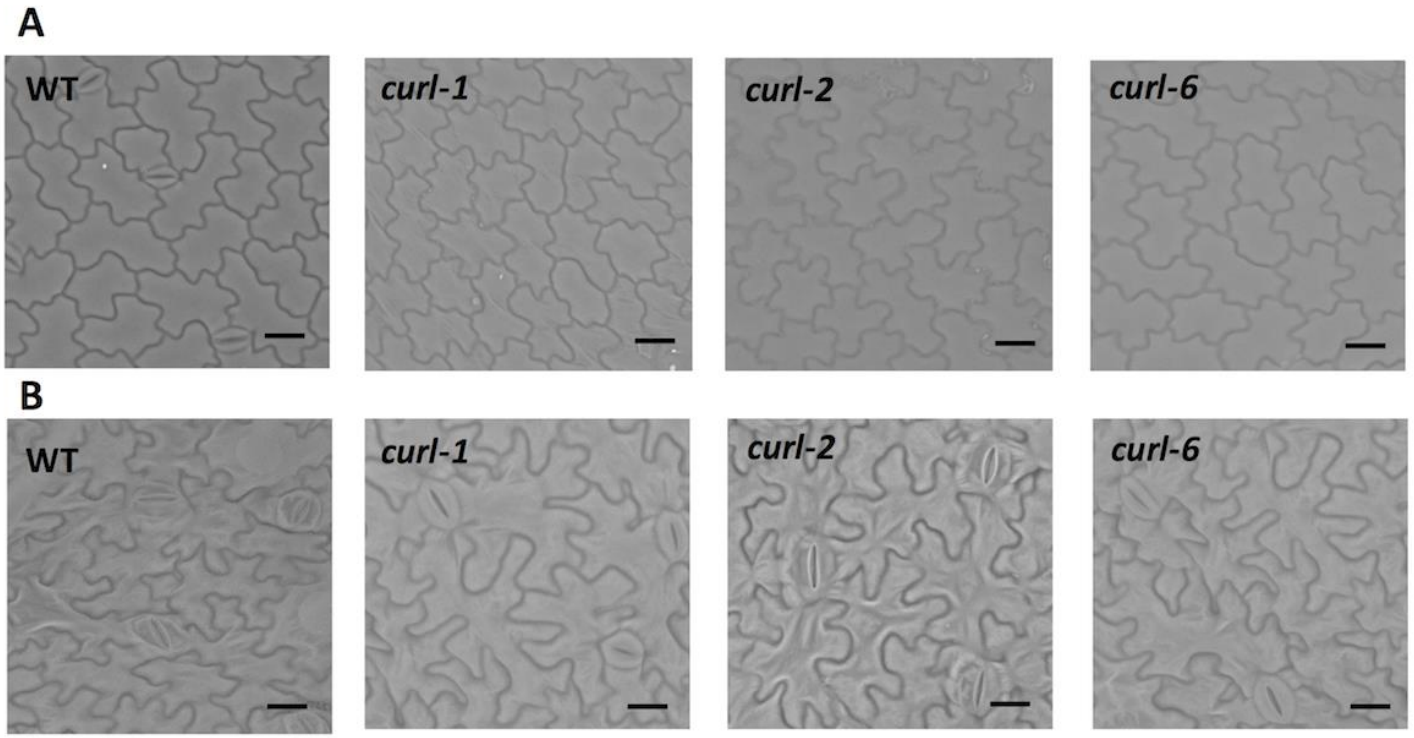

Fig. 4.4 Adaxial and abaxial pavement cell in the WT and the *curl* mutants at the curly part.

(A) The adaxial pavement cell size of WT and mutants was comparable Scale bar: 20 µm (B) The pavement cell size of all *curl* mutants in abaxial surface was significantly larger compared to that of wild-type. Scale bar: 10 µm.

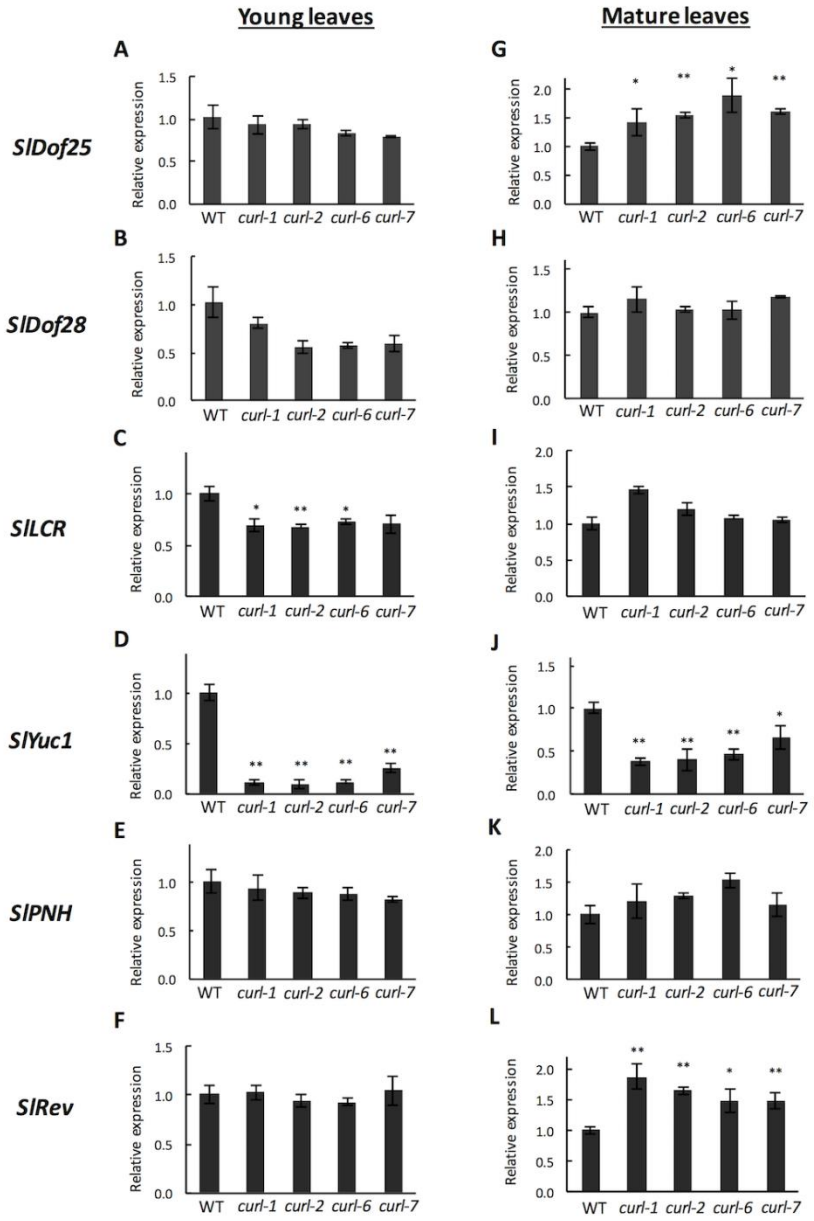

Fig. 4.5 Relative expression of auxin-related genes which were reported to control leaf flatness, observed by qRT-PCR at young and mature leaf stages.

(A-E) Relative expression of gene at young leaf stage (A) *SlDof25* (B) *SlDof28* (C) *SlLCR* (D) *SlYUC1* (E) *SlPNH* (F) Adaxial specification gene *SlRev* (G-L) Relative expression of gene at mature leaf stage, when leaf completely turned to curly (G) *SlDof25* (H) *SlDof28* (I) *SlLCR* (J) *SlYUC1* (K) *SlPNH* (L) Adaxial specification gene *SlRev.*

Values are means ± SE (n=3). The asterisks represent statistically significant differences in means with equal variants compared to the wild-type (WT) based on Student's t-test (*P<0.05, **P<0.01). *SlActin* gene was used as an internal control. The expression level of the *curl-1*, *curl-2*, and *curl-6* mutants was relative by the wild-type (WT) expression.

Chapter 5

General Discussion and Summary

5.1 General discussion

I characterized several alleles of tomato mutants exhibiting severe leaf upward-curling phenotypes at the mature leaf stage (Fig. 2.1). This mutant phenotype occurs irrespective of water content or relative humidity. Six lines were isolated using a forward genetic approach by visually selecting curly leaf phenotypes in a previously generated tomato mutant population (Saito et al., 2011; Shikata et al., 2016).

Map-based cloning combined with WES revealed that the mutation occurred in the *SlLAX1* gene (Fig. 2.6 and 2.7). Then, to validate the phenotype consistency, by utilizing TILLING as a reverse genetic approach, I screened another nonsense mutation allelic line, *curl-7*, which was generated by EMS. The *curl-7* mutant leaves were indistinguishable from those of the other previously selected lines (Fig. 2.7B, C). Furthermore, I confirmed the full-length coding sequence of *SlLAX1* (Fig. 2.8A, B), which supported the evidence that *SlLAX1* is the gene responsible for the curly leaf mutant phenotype. Taken together, the characterization of multiple alleles in this study that consistently showed indistinguishable phenotypes is strong evidence for the role of *SlLAX1* in controlling the curly leaf phenotype. To our knowledge, this study is the first example of the successful exome sequence application in tomato in the identification of causal gene preceded by a forward genetic approach.

SlLAX1 encodes a transmembrane amino acid transporter protein and belongs to the amino acid/auxin permease (AAAP) family. Homology searches indicated that the SlLAX1 protein sequence is homologous to *Arabidopsis thaliana AtAUX1* (AT2G38120). In *Arabidopsis*, AUX1 is one of four auxin influx carriers belonging to AUX1/LAX family that controls several developmental processes including gravitropism responses, venation patterns, and lateral roots (Vieten et al., 2007; Bennet et al., 1996). Although recent findings have indicated that the

AUX/LAX1 family also control aerial part development such as leaf serration (Kasprzewska et al., 2015), phyllotaxis patterning, vascular patterning, and xylem differentiation (Bainbridge et al., 2008; Fabregas et al., 2015), the role of AUX1/LAX gene family in leaf curling are poorly understood. In contrast, mutations in many auxin-related genes showed an impaired leaf flatness phenotype (Esteve-Bruna et al., 2013; Zgurski et al., 2005). In tomato, few studies have shown a relationship between auxin and leaf flatness; for instance, *SlARF4-RNAi* lines produce hyponastic leaves (Sagar et al., 2013) and *SlPIN4-RNAi* lines show leaf flatness defects as well as altered plant architecture (Pattison and Catala 2012). However, the role of *SlLAX1* in controlling leaf curly phenotype has not been reported in tomato or other major crops.

The tomato *AUX1/LAX* family consists of five genes (*SlLAX1-5*). They share high identity and similarity; the identity of *SlLAX2*, *SlLAX3*, *SlLAX4*, and *SlLAX5* with *SlLAX1* are 80.36%, 79.70%, 92.65%, and 80.87%, respectively (Sol Genomics Network). All *SlLAX* genes are expressed in the mature leave and root of tomato (Pattison and Catala, 2012). The single mutants depleting *SlLAX1* used in this study, *curl-1-7,* showed a severe phenotype effect in leaf flatness, suggesting that the importance of *SlLAX1* in controlling leaf flatness in mature leaves. Although the functional redundancy of the *AUX1/LAX* family, in addition to the function of *SlLAX1* itself, is poorly characterized in tomato, their function in *Arabidopsis* is well characterized especially in root development. Although four *AUX1/LAX* genes share high sequence identity and similarity, *AtAUX1* has the strongest auxin affinity and auxin influx activity (Peret et al., 2012, Rutschow et al., 2014). Peret et al. (2012) also reported that subfunctionalization of the AUX1/LAX family in root based on their distinct pattern of spatial expression and the subcellular localization. In contrast, the *AUX1/LAX* genes play redundantly in the context of phyllotaxy, vascular patterning, and xylem differentiation (Bainbridge et al., 2008; Fabregas et al. 2015). Therefore, the functional redundancy

of *SlLAXs* family in tomato leaf curling phenotype awaits further investigation.

Arabidopsis AUX1 protein has eleven transmembrane (TM) helixes and is located in the plasma membrane. Using publicly available server, I checked the prediction of transmembrane helices in the SlLAX1 protein. The *curl-2* and *curl-6* mutants (Fig.2.4B) carry a nonsense mutation at the 262nd a.a., which is located in the TM helix VII (http://www.cbs.dtu.dk/services/TMHMM/), which is equivalent to the central region of *AtAUX1* and has proven to be particularly important for protein function (Swarup et al. 2004). In addition, both *curl-1* and *curl-3* mutations (Fig. 2.4D) are located in the 145th a.a., which is located in TM helix IV, which is in the similar part of the N-terminal half of AtAUX1 and is essential for its correct localization (Peret et al., 2012). Furthermore, the *curl-1/curl-3*, *curl-2/curl-6*, and *curl-7* mutations caused nonsense mutations that can produce only 35, 63, and 45% of the WT protein, respectively (Fig. 2.4B, D, and 2.8A). Additionally, the relative expression of the *curl* mutant alleles (*curl-1*, *curl-2,* and *curl-6*) was less than 40% compared to that of WT (Fig. 2.5). These reasons presumably account for the loss-of-function mutations of the *SlLAX1* gene.

To test the potential function of SlLAX1 as an auxin transporter, I first measured leaf endogenous auxin content. However, IAA content was comparable between WT and the *curl* mutants at all stages (Fig. 4.2). Numerous findings have indicated that *AtAUX1* plays an important role in root gravitropism and lateral root development (Bennet et al., 1996; Marchant et al., 1999). Root gravitropism response is also commonly used to check auxin response and distribution. Therefore, I next tested these assays and found that the root gravitropism response of the *curl* mutants was affected by the *SlLAX1* mutation. In addition, lateral root emergence was also disrupted (Fig. 4.3). Although the functional characterization of SlLAX1 has not been conducted in tomato and I do not yet have direct evidence in this study, agravitropism and lateral root

formation defects of the *curl* mutants indicated that SlLAX1 may have a potential function as an auxin transporter similar to *AtAUX1*, and SlLAX1 might participate in local auxin distribution without affecting total endogenous auxin content of the whole leaf. Functional analysis of *SlLAX1* gene remains to be determined. Alternatively, in this study, I subjected whole leaves to auxin measurement, which would make it difficult to see spatial auxin accumulation in leaves. The quantification of local measurements would help explain the effect of spatial auxin accumulation in the formation and severity of leaf flatness.

The progression of curly in the mature leaf or later development stage presumably related to auxin distribution and gradient through *SlLAX1*. Auxin is synthesized in young tissue. The main sites of auxin biosynthesis are young leaf and shoot apex. In this study, the curly leaf initiated from leaf tip/distal area (Fig. 3.6). Probably due to defective auxin transport mediated by *SlLAX1* mutation, auxin depletion is occurred firstly at the tip. This idea is supported by Reindhardt et al. (2003) work. By observing auxin accumulation using PIN: GFP, they concluded that leaf primordial tip is an auxin sink. In the same analogy, as *PIN1* and *AUX/LAX* act sinegically as auxin transport carriers, presumably the impairment of auxin influx in the *curl* mutants make depletion of auxin in the tip area. Also, Ljung et al. (2001) experiment data could explain this phenomenon. They reported that auxin content in the tobacco single leaf varied, the highest auxin content was in the petiole, and auxin gradient was gradually decrease in proximo-distal (basal to tip) direction, supporting the evident the initiation of the curly leaf was first observed in the leaf tip region, followed by middle and basal.

The curly leaf phenotype was not observed at the early stage of leaf development (Fig. 2.1C, D, Fig. 3.5), and does not related to relative humidity and water availability (Fig. 2.1E, G). Thus, I hypothesized that the curly leaf phenotype was caused by the alteration of adaxial/abaxial cell

ratio rather than impairment adaxial-abaxial polarity since adaxial-abaxial polarity is established at the very early stage of leaf development, that is, at the primordium stage. To test this hypothesis, I measured pavement cell size in the epidermal adaxial and abaxial cell side at the mature leaves when the leaf completely became curly. As I expected, pavement cell size in the abaxial in the *curl* mutants was significantly larger compared to that of WT, while there was no significant difference in the adaxial side. The number of pavement cell in adaxial and abaxial sides was comparable. The upward curling of the *curl* mutants might be explained by the differential growth of pavement cells in adaxial and abaxial cell surfaces, which is supported by similar observation of *incurvata6* (*icu6*), semi-dominant allele of the *AUXIN RESISTANT3* (*AXR3*), that showed an upward curly phenotype caused by a reduced adaxial/abaxial cell size ratio (Perez-Perez et al., 2010). The imbalance epidermal adaxial-abaxial cell growth which led to either epinastic (downward curvature) or hyponastic leaf is not new phenomenon. In previous finding, it was reported that auxin hyper accumulation plant produced leaf epinastic curvature that was formed due to an increased growth of the leaf adaxial side (Klee et al., 1987; Romano et al., 1993; Kim et al., 2007), that induced by reduced auxin export that may cause its hyper-accumulation on the adaxial side. Taken together, SlLAX1 might have a function not in the establishment of adaxial-abaxial polarity but rather in balancing adaxial/abaxial cell size ratio in later stages of leaf development. The evaluation of auxin distribution and/or analysis of *SlLAX1* gene expression on adaxial and abaxial leaf surfaces should allow for a better understanding of the *SlLAX1* function in this process.

According to the relative expression of some tomato putative auxin-related genes controlling leaf flatness, *SlYuc1* showed prominent changes in both young and mature leaves of the *curl* mutants. *YUC* is a family of genes that are orthologs to *ToTFZY* (Expo´sito-Rodrı´guez et al., 2007), which has a function in local auxin biosynthesis (Zhao et al., 2001). In the previous finding, it has

been reported that *aux1* and *yuc* mutants in *Arabidopsis* have a synergistic effect to enhance each other to control leaf development. In *Arabidopsis*, activation tagging of *AtDof5.1* resulted in an upward curly leaf phenotype (Kim et al., 2010). Dof5.1 was demonstrated to promote the *Revoluta* gene expression by binding to its promoter. Similarly to these finding (Kim at al., 2010), expression of *SlDof25,* an ortholog of Dof5.1*,* was increased in the all *curl* mutants (Fig. 4.5G). The *SlRev* expression level was also increased (Fig. 4.5L). Up regulation of *AtDof5.1* also repressed transcript levels of auxin biosynthesis genes, which is consistent with low expression level of *SlYuc1* in the *curl* mutants (Fig. 4.5D, J). In tomato, it has also been reported that overexpression of a microRNA166-resistant version of *SLREV* (35S::REV^{Ris}) showed upward curly leaf phenotype (Hu et al., 2014). Collectively, our findings are similar to previous findings which reinforce the partial disturbance of auxin homeostasis in the *SlLAX1* mutants.

The fact that lower auxin content triggers cell expansion is well established (Ishida et al., 2012, reviewed in Velasquez et al., 2016). I hypothesize that the loss-of-function of *SlLAX1* in the *curl* mutants results in imbalance adaxial/abaxial pavement cell growth leading to curly leaf phenotype. Depletion of SlLAX1 in the *curl* mutants disrupts auxin transport in either adaxial or abaxial leaf surface. Given that there was no significant different in the adaxial pavement cell size (Table 4.2, Fig. 4.4), SlLAX1 action appears to be restricted to the abaxial side. SlLAX1 belongs to the SlLAXs family and other members are known to be expressed in leaves (Pattison and Catala, 2012). It is possible that other influx transporters compensate for the loss-of-function of SlLAX1 in the adaxial side. In contrast, the data suggest that SlLAX1 is a major determinant of auxin transportation dominant in the abaxial side. In adaxial side, where SlLAX1 is not a major auxin influx carrier, presumably auxin content of the *curl* mutants was similar or higher than that of the WT, while decreased auxin content in abaxial side due to low influx carrier activity. Auxin which

is not uptake by abaxial cell, may be accumulated in the adaxial side, or alternatively accumulated in the extracellular space (most likely the latter because the cell number in the adaxial and abaxial was comparable, means there was no increasing of cell division in adaxial). Therefore, the auxin content in the *curl* mutants could be maintained at the similar level with the WT, although local auxin content in the local region was disturbed (Fig. 4.2). Imbalance adaxial/abaxial cell growth due to differential auxin accumulation is also well established (Perez-Perez et al., 2010, reviewed in Sandalio et al., 2016). I speculate that the lower auxin content in abaxial cell surface triggers cell expansion and imbalance cell growth in both surface leading to curly leaf emergence. This hypothesis awaits further investigation. Locally depletion auxin content in the leaf causes different gene expression compared to the WT (Fig. 4.5). Differential of the expression level is determined by which type of cells corresponding gene mainly expressed (whether SlLAX1 is a major auxin transport in that cell) and the gene respond to auxin. Lower expression of *SlYuc1* does not change leaf auxin content presumably because *SlYuc* is family genes (Expósito-Rodríguez et al., 2007). Other *SlYuc* genes may compensate total auxin biosynthesis, resulting in comparable amounts of auxin content in entire leaf.

The mutation in the *curl* mutants had also effects in the whole plant growth (Table 3.4-3.7). The mutants leaf diameter and leaf area were also markedly narrower and reduced compared to that of WT (Table 3.12, 3.13 Fig. 3.8). It is also possible controlled by the mutation in *SlLAX1*. Alternatively, the severe curly leaf may also affect photosynthesis that led the reducing the overall growth of leaf. These two possibilities could not be distinguished in the current experimental data.

In brief, this study contributes to the newly characterized role of *SlLAX1* in controlling leaf development in tomato by balancing the adaxial-abaxial pavement cell enlargement potentially mediated by auxin. The evaluation of auxin distribution and/or analysis of *SlLAX1* gene expression

on adaxial and abaxial leaf surfaces should allow for a better understanding of the *SlLAX1* function in this process. Additionally, analysis of double mutants with other *LAX* or *PIN* family members and other adaxial-abaxial-specification genes would be helpful to dissect the precise mechanism of *SlLAX1* in normal leaf development in plants.

5.2 Summary

Tomato (*Solanum lycopersicum* L.) is an economically important crop in both tropical and in temperate regions. It is widely cultivated in almost all countries and it is used for both as fresh consumption and as raw material for processing industries. It is considered as one of the main sources of nutrition to support our health. Furthermore, tomato has been selected as an excellent model plant for genomic studies in the Solanaceae family, particularly as the most important model system for fleshy fruit development, vegetative development as well as a model for climacteric fruit. Additionally, in 2012, the tomato genome sequence has also been published. This effort can be valued as a significant achievement for accelerating tomato research both in basic and in applied research as well as for breeding program.

Leaves are the major plant organs whose primary function involves photosynthesis. It has been known that auxin controls various aspects of plant growth and development, including leaf initiation, expansion, and differentiation. Unique and intriguing auxin features include its polar transport, which is mainly controlled by the *AUX1/LAX* and *PIN* gene families as influx and efflux carriers, respectively. The role of *AUX1/ LAX* genes in root development is well documented, but the role of these genes in leaf morphogenesis remains unclear. In this study, I isolated six lines of the curly leaf phenotype '*curl*' mutants from a γ-ray and ethyl methanesulfonate (EMS) mutagenized population.

The objectives of this study are (1) to investigate the responsible gene controlling the mutant phenotype (2) to characterize the morphology and genetic features of the *curl* mutants (3) to characterize the role of the responsible gene in leaf morphogenesis.

Allelism test revealed that all mutants were allelic. Using a forward genetic approach and a map-based cloning strategy combined with whole-exome sequencing, I observed that a mutation

likely occurred in the *SlLAX1* (*Solyc09g014380*) gene, which is homologous to *Arabidopsis AUX1* (*AtAUX1*), which encodes an auxin influx carrier. *SlLAX1* encodes a transmembrane amino acid transporter protein and belongs to the amino acid/auxin permease (AAAP) family. In *Arabidopsis*, several studies have reported that AUX1 is an auxin influx carrier that controls several developmental processes including gravitropism responses, venation patterns and lateral leaf development. The function of *SlLAX1* in controlling leaf flatness has not been reported in tomato or other major crops. Then, to validate the candidate gene by utilizing TILLING as a reverse genetic approach, I screened another nonsense mutation allelic line, *curl-7*, which was generated by EMS. The *curl-7* mutant leaves were indistinguishable from those of the other previously selected lines. Taken together, the characterization of multiple alleles in this study that consistently showed indistinguishable phenotypes is strong evidence for the role of *SlLAX1* in controlling the curly leaf phenotype. To our knowledge, this study is the first example of the successful exome sequence application in tomato in the identification of causal gene preceded by a forward genetic approach.

SlLAX1 encodes a transmembrane amino acid transporter protein and belongs to the amino acid/auxin permease (AAAP) family. The tomato *AUX1/LAX* family consists of five genes (*SlLAX1-5*). They share high identity and similarity; the identity of *SlLAX2*, *SlLAX3*, *SlLAX4*, and *SlLAX5* with *SlLAX1* are 80.36%, 79.70%, 92.65%, and 80.87%, respectively. All *SlLAX* genes are expressed in the mature leave and root of tomato. The single mutants which has loss-of-function of *SlLAX1* used in this study, *curl-1-7,* showed a severe phenotype effect in leaf flatness, suggesting that the importance of *SlLAX1* in controlling leaf flatness in mature leaves.

Numerous findings have indicated that *AtAUX1* plays an important role in root gravitropism and lateral root development. Root gravitropism response is also commonly used to check auxin response and distribution. The root gravitropism response of the *curl* mutants was affected by the *SlLAX1* mutation. In addition, lateral root emergence was also disrupted, indicated that SlLAX1 may have a potential function as an auxin transporter similar to *AtAUX1*, and SlLAX1 might participate in local auxin distribution without affecting total endogenous auxin content of the whole leaf.

The curly leaf phenotype was not observed at the early stage of leaf development and does not related to relative humidity and water availability. I hypothesized that the curly leaf phenotype was caused by the alteration of adaxial/abaxial cell ratio rather than impairment adaxial-abaxial polarity since adaxial-abaxial polarity is established at the very early stage of leaf development, that is, at the primordium stage. As I expected, pavement cell size in the abaxial in the *curl* mutants was significantly larger compared to that of WT, while there was no significant difference in the adaxial side. The number of pavement cell in adaxial and abaxial sides was comparable. The upward curling of the *curl* mutants might be explained by the differential growth of pavement cells in abaxial cell surfaces.

Briefly, through map-based cloning combined with WES, I characterized several alleles of the curly leaf mutants, which have nonsense mutation in the *SlLAX1* gene. I reported that the *SlLAX1* gene controls curly leaf phenotype in the tomato *curl* mutants. This feature has never been characterized. The characterization of several alleles of single *curl* mutants in this study sheds light on the pivotal role of *SlLAX1* in controlling leaf flatness mediated by normal adaxial-abaxial pavement cell growth. I also combined forward and reverse genetic approaches to validate the candidate gene. Using TILLING technology, I screened another nonsense mutant allele that

consistently shows a similar curly leaf phenotype with that of the *curl* mutants obtained by a forward genetic approach. This finding contributes to the newly characterized role of *SlLAX1* in controlling or maintaining leaf adaxial-abaxial polarity in tomato by balancing the adaxial-abaxial cell expansion that potentially mediated by auxin. The evaluation of auxin distribution on the adaxial and abaxial leaf surfaces remains to be determined. Additionally, analysis of double mutants with other *LAX* or *PIN* family members and other adaxial-abaxial-specification genes would be helpful to dissect the precise mechanism of *SlLAX1* in normal leaf development in plants.

Acknowledgements

In this chapter, let me express my deepest gratitude to all the people who supported me during my doctoral course at the University of Tsukuba. First of all, I would like to express my sincere gratitude to my respected academic supervisor, Prof. Hiroshi EZURA, Professor, Faculty of Life and Environmental Sciences, University of Tsukuba. Thank you very much for allowing me to join such an innovative research group, also for your warm guidance, beneficial idea and advice, unlimited support as well as enlightening discussion.

Furthermore, I would like to express great thanks to my closest teacher, Dr. Tohru ARIIZUMI, Associate Professor, Faculty of Life and Environmental Sciences, University of Tsukuba. Please allow me to express my sincere thanks for your guidance since the time I started to plan my research, for continuous support and unlimited help during research, for every beneficial idea and advise, as well as great discussion during my doctoral course. Next, I would like to thank Dr. Ryoichi YANO, Assistant Professor, Faculty of Life and Environmental Sciences, University of Tsukuba for continuous support in my research.

Furthermore, I would like to thank my doctoral thesis committee, Prof. Sumiko SUGAYA, Professor, Faculty of Life and Environmental Sciences, University of Tsukuba, and Prof. Michiyuki ONO, Professor, Faculty of Life and Environmental Sciences, University of Tsukuba. I really appreciate your help in revising my doctoral thesis, also for many great ideas and comments, as well as critical questions in the completion of this master thesis.

Besides that, I also wish to express my sincere thanks to all the teachers in our research group, Dr. Chiaki MATSUKURA, Dr. Naoya FUKUDA, Dr. Satoko NONAKA, Dr. Seung Won KANG, Dr. Yoshihiro OKABE, as well as the post-doctoral fellows in Sosaikaki`s lab. Thank you very much for all attention, suggestions, discussion and assistance during my master course.

I would also like to express my sincere thanks to all Sosaikaki lab`s members for technical support, suggestion and comments during seminar and lab meeting as well as laughter and friendship during my study. Thank you for your sincere smile and help as well as convenient working atmosphere that feels like home.

Furthermore, allow me to express my deepest gratitute to the Tokyo Marine Kagami Memorial Foundation for full financial support during my doctoral course and also thanks to all the foundation’s staff for your support.

Last but not least, I would like to express my endless and sincere thanks to my family; my parents, Imron Pulungan and Zahraini Lubis, my sister and brother, Ade and Imzar, and my grandmother, Makrifah, for your unlimited and endless support, love, and pray. You are my steadfast supporters during this PhD. course even throughout my life.

And overall, I owe to the God, Allah SWT, the Almighty for always giving me continuous blessing, health and strength throughout my life

References

Abe A, Kosugi S, Yoshida K, Natsume S, Takagi H, Kanzaki H, Matsumura H, Yoshida K, Mitsuoka C, Tamiru M, Innan H, Cano L, Kamoun S, Terauchi R (2012) Genome sequencing reveals agronomically important loci in rice using MutMap. Nat Biotechnol **30:** 174–178

Aloni R, Aloni E, Langhans M, Ullrich CI (2006). Role of cytokinin and auxin in shaping root architecture: regulating vascular differentiation, lateral root initiation, root apical dominance and root gravitropism. Ann Bot **97:** 883–893

Ariizumi T, Kishimoto S, Kakami R, Maoka T, Hirakawa H, Suzuki Y, Ozeki Y, Shirasawa K, Bernillon S, Okabe Y, Moing A, Asamizu E, Rothan C, Ohmiya A, Ezura H (2014) Identification of the carotenoid modifying gene *PALE YELLOW PETAL 1* as an essential factor in xanthophyll esterification and yellow flower pigmentation in tomato (*Solanum lycopersicum*). Plant J **79:** 453–465

Austin RS, Vidaurre D, Stamatiou G, Breit R, Provart NJ, Bonetta D, Zhang J, Fung P, Gong Y, Wang PW, McCourt P, Guttman DS (2011) Next-generation mapping of *Arabidopsis* genes. Plant Journal **67:** 715–725

Bainbridge K, Guyomarc'h S, Bayer E, Swarup R, Bennett M, Mandel T, Kuhlemeier C (2008) Auxin influx carriers stabilize phyllotactic patterning. Genes Dev **22:** 810–823

Bar M, Ori N (2014) Leaf development and morphogenesis. Development **141:** 4219–4230

Barkoulas M, Hay A, Kougioumoutzi E, Tsiantis M (2008) A developmental framework for dissected leaf formation in the *Arabidopsis* relative *Cardamine hirsuta*. Nat Genet **40**: 1136–1141

Benjamins R, Scheres B (2008) Auxin: the looping star in plant development. Annu Rev Plant Biol **59:** 443-465

Benková E, Michniewicz M, Sauer M, Teichmann T, Seifertová D, Jürgens G, Friml J (2003) Local, efflux-dependent auxin gradients as a common module for plant organ formation. Cell **115:** 591–602

Bennett MJ, Marchant A, Green HG, May ST, Ward SP, Millner PA, Walker AR, Schulz B, Feldmann KA (1996) *Arabidopsis AUX1* gene: a permease-like regulator of root gravitropism. Science **273:** 948–950

Bennett MJ, Marchant A, May ST, Swarup R (1998) Going the distance with auxin: unravelling the molecular basis of auxin transport. Philos Trans R Soc Lond B Biol Sci **353:** 1511–1515

Blakeslee JJ, Peer WA, Murphy AS (2005) Auxin transport. Curr Opin Plant Biol **8:** 494–500

Blein T, Pautot V, Laufs P (2013) Combinations of mutations sufficient to alter *Arabidopsis* leaf dissection. Plants **2:** 230–247

Boutté Y, Ikeda Y, Grebe M (2007) Mechanisms of auxin-dependent cell and tissue polarity. Curr Opin Plant Biol **10:** 616–623

Braybrook SA, Kuhlemeier C (2010) How a plant builds leaves. Plant Cell **22:** 1006–1018

Cai X, Zhang Y, Zhang C, Zhang T, Hu T, Ye J, Zhang J, Wang T, Li H, Ye Z (2013) Genome-wide analysis of plant-specific Dof transcription factor family in tomato. J Integr Plant Biol **55:** 552–566

Cheng Y, Dai X, Zhao Y (2007) Auxin synthesized by the yucca flavin monooxygenases is essential for embryogenesis and leaf formation in *Arabidopsis*. Plant Cell **19:** 2430–2439

Chusreeaeom K, Ariizumi T, Asamizu E, Okabe Y, Shirasawa K, Ezura H (2014) A novel tomato mutant, *Solanum lycopersicum elongated fruit1* (*Slelf1*), exhibits an elongated fruit shape caused by increased cell layers in the proximal region of the ovary. Mol Genet Genomics **289:** 399–409

Davies JN, Hobson GE (1981) The constituents of tomato fruit: the influence of environment, nutrition and genotype. Crit Rev Food Sci Nutr **15:** 205–280

Delbarre A, Muller P, Imhoff V, Guern J (1996) Comparison of mechanisms controlling uptake and accumulation of 2,4-dichlorophenoxy acetic acid, naphthalene-1-acetic acid, and indole-3-acetic acid in suspension-cultured tobacco cells. Planta **198:** 532–541

Emery JF, Floyd SK, Alvarez J, Eshed Y, Hawker NP, Izhaki A, Baum SF, Bowman JL (2003) Radial Patterning of *Arabidopsis* shoots by class III HD-ZIP and KANADI genes. Curr Biol **13**: 1768–1774

Emmanuel E, Levy AA (2002) Tomato mutants as tools for functional genomics. Curr Opin Plant Biol **5:** 112–117

Enders TA, Strader LC (2015) Auxin activity: past, present, and future. Am J Bot **102:** 180–196

Eshed Y (2004) Asymmetric leaf development and blade expansion in Arabidopsis are mediated by KANADI and YABBY activities. Development **131:** 2997–3006

Esteve-Bruna D, Perez-Perez JM, Ponce MR, Micol JL (2013) *incurvata13*, a novel allele of *AUXIN RESISTANT6*, reveals a specific role for auxin and the SCF complex in *Arabidopsis* embryogenesis, vascular specification, and leaf flatness. Plant Physiol **161:** 1303–1320

Expósito-Rodríguez M, Borges AA, Borges-Pérez A, Hernández M, Pérez JA (2007) Cloning and biochemical characterization of *ToFZY*, a tomato gene encoding a flavin monooxygenase involved in a tryptophan-dependent auxin biosynthesis pathway. J Plant Growth Regul **26:** 329–340

Fàbregas N, Formosa-Jordan P, Confraria A, Siligato R, Alonso JM, Swarup R, Bennett MJ, Mähönen AP, Caño-Delgado AI, Ibañes M (2015) Auxin influx carriers control vascular patterning and xylem differentiation in *Arabidopsis thaliana*. PLoS Genet **11:** 1–26

Fernandez-Pozo N, Menda N, Edwards JD, Saha S, Tecle IY, Strickler SR, Bombarely A, Fisher-York T, Pujar A, Foerster H, Yan A, Mueller LA (2015) The Sol Genomics Network (SGN)-from genotype to phenotype to breeding. Nucleic Acids Res **43:** D1036–D1041

Floyd SK, Bowman JL (2010) Gene expression patterns in seed plant shoot meristems and leaves: homoplasy or homology? J Plant Res **123:** 43–55

Friml J (2003) Auxin transport - shaping the plant. Curr Opin Plant Biol **6:** 7–12

Gady ALF, Hermans FWK, Wal MHBJ Van De, Loo EN Van, Visser RGF, Bachem CWB (2009) Implementation of two high throughput techniques in a novel application: detecting point mutations in large EMS mutated plant populations. Plant Methods **5:** 13

Garcia V, Bres C, Just D, Fernandez L, Tai FWJ, Mauxion J-P, Le Paslier M-C, Bérard A, Brunel D, Aoki K, Alseekh S, Fernie AR, Fraser PD, Rothan C (2016) Rapid identification of causal mutations in tomato EMS populations via mapping-by-sequencing. Nat Protoc **11:** 2401–2418

Giovannoni JJ (2004) Genetic regulation of fruit development and ripening. Plant Cell **16:** 170–181

Gisbert C, Bishop GJ, Dixon MS, Martı E (2006) Genetic and physiological characterization of tomato cv. Micro-Tom. J Exp Bot **57:** 2037–2047

Guenot B, Bayer E, Kierzkowski D, Smith RS, Mandel T, Zádníková P, Benková E, Kuhlemeier C (2012) PIN1-independent leaf initiation in *Arabidopsis*. Plant Physiol **159:** 1501–1510

Han M-H, Goud S, Song L, Fedoroff N (2004) The *Arabidopsis* double-stranded RNA-binding protein HYL1 plays a role in microRNA-mediated gene regulation. Proc Natl Acad Sci U S A **101:** 1093–1098

Hao S, Ariizumi T, Ezura H (2017) *SEXUAL STERILITY* is essential for both male and female gametogenesis in tomato. Plant Cell Physiol **58**: 22–34

Hashmi U, Shafqat S, Khan F, Majid M, Hussain H, Kazi AG, John R, Ahmad P (2015) Plant exomics: concepts, applications and methodologies in crop improvement. Plant Signal Behav **10:** e976152

Horiguchi G, Ferjani A, Fujikura U (2006) Coordination of cell proliferation and cell expansion in the control of leaf size in *Arabidopsis thaliana*. J Plant Res **119:** 37–42

Hu G, Fan J, Xian Z, Huang W, Lin D, Li Z (2014) Overexpression of *SlREV* alters the development of the flower pedicel abscission zone and fruit formation in tomato. Plant Sci **229**: 86–95

Ishida T, Adachi S, Yoshimura M, Shimizu K, Umeda M, Sugimoto K (2010) Auxin modulates the transition from the mitotic cycle to the endocycle in *Arabidopsis*. Development **137**: 63–71

Kalve S, De Vos D, Beemster GTS (2014) Leaf development: a cellular perspective. Front Plant Sci **5:** 1–25

Kasprzewska A, Carter R, Swarup R, Bennett M, Monk N, Hobbs JK, Fleming A (2015) Auxin influx importers modulate serration along the leaf margin. Plant J **83:** 705–718

Kim HS, Kim SJ, Abbasi N, Bressan RA, Yun DJ, Yoo SD, Kwon SY, Choi SB (2010) The DOF transcription factor Dof5.1 influences leaf axial patterning by promoting *Revoluta* transcription in Arabidopsis. Plant J **64:** 524–535

Kim JI, Sharkhuu A, Jin JB, Li P, Jeong JC, Baek D, Lee SY, Blakeslee JJ, Murphy AS, Bohnert HJ, Hasegawa PM, Yun D, Bressan RA (2007) *yucca6*, a dominant mutation in Arabidopsis, affects auxin accumulation and auxin-related phenotypes. Plant Physiol **145:** 722–735

King R, Bird N, Ramirez-Gonzalez R, Coghill JA, Patil A, Hassani-Pak K, Uauy C, Phillips AL (2015) Mutation scanning in wheat by exon capture and next-generation sequencing. PLoS One **10:** 1–18

Klee HJ, Horsch RB, Hinchee MA, Hein MB, Hoffmann NL (1987) The effects of overproduction of two *Agrobacterium tumefaciens* T-DNA auxin biosynthetic gene products in transgenic petunia plants. Genes & Dev **1:** 86–96

Kobayashi M, Nagasaki H, Garcia V, Just D, Bres C, Mauxion LP, Le Paslier M, Brunel D, Suda K, Minakuchi Y, Toyoda A, Fujiyama A, Toyoshima H, Suzuki T, Igarashi K, Rothan C, Kaminuma E, Nakamura Y, Yano K, Aoki K (2014) Genome-wide analysis of intraspecific DNA polymorphism in 'Micro-Tom', a model cultivar of tomato (*Solanum lycopersicum*). Plant Cell Physiol **55:** 445–454

Kojima M, Kamada-nobusada T, Komatsu H, Takei K, Kuroha T, Mizutani M, Ashikari M, Ueguchi-tanaka M, Matsuoka M, Suzuki K, Sakakibara H (2009) Highly sensitive and high-throughput analysis of plant hormones using MS-probe modification and liquid chromatography – tandem mass spectrometry: an application for hormone Profilling in *Oryza sativa*. Plant Cell Physiol **50:** 1201–1214

Kramer EM (2004) PIN and AUX/LAX proteins: their role in auxin accumulation. Trends Plant Sci **9:** 578–582

Kramer EM, Bennett MJ (2006) Auxin transport: a field in flux. Trends Plant Sci **11:** 382–386

Lee C, Chronis D, Kenning C, Peret B, Hewezi T, Davis EL, Baum TJ, Hussey R, Bennett M, Mitchum MG (2011) The novel cyst nematode effector protein 19C07 Interacts with the *Arabidopsis* auxin influx transporter LAX3 to control feeding site development. Plant Physiol **155:** 866–880

Lincoln C, Britton JH, Estelle M (1990) Growth and development of the *axrl* mutants of *Arabidopsis*. Plant Cell **2**: 1071–1080

Liu Z, Jia L, Mao Y, He Y (2010) Classification and quantification of leaf curvature. J Exp Bot **61:** 2757–2767

Liu Z, Jia L, Wang H, He Y (2011) HYL1 regulates the balance between adaxial and abaxial identity for leaf flattening via miRNA-mediated pathways. J Exp Bot **62:** 4367–4381

Ljung K, Bhalerao RP, Sandberg G (2001) Sites and homeostatic control of auxin biosynthesis in *Arabidopsis* during vegetative growth. Plant J **28:** 465–474

Løvdal T, Lillo C (2009) Reference gene selection for quantitative real-time PCR normalization in tomato subjected to nitrogen, cold, and light stress. Anal Biochem **387:** 238–242

Marchant A (1999) AUX1 regulates root gravitropism in *Arabidopsis* by facilitating auxin uptake within root apical tissues. EMBO J **18:** 2066–2073

Marchant A (2002) AUX1 promotes lateral root formation by facilitating indole-3-acetic acid distribution between sink and source tissues in the *Arabidopsis* seedling. Plant Cell **14:** 589–597

Marchler-Bauer A, Bo Y, Han L, He J, Lanczycki CJ, Lu S, Chitsaz F, Derbyshire MK, Geer RC, Gonzales NR, Gwadz M, Hurwitz DI, Lu F, Marchler GH, Song JS, Thanki N, Wang Z, Yamashita RA, Zhang D, Zheng C, Geer LY, Bryant SH (2017) CDD/SPARCLE: functional classification of proteins via subfamily domain architectures. Nucleic Acids Res **45:** D200–D203

Marchler-Bauer A, Derbyshire MK, Gonzales NR, Lu S, Chitsaz F, Geer LY, Geer RC, He J, Gwadz M, Hurwitz DI, Marchler GH, Song JS, Thanki N, Wang Z, Yamashita RA, Zhang D, Zheng C, Bryant SH (2015) CDD: NCBI's conserved domain database. Nucleic Acids Res **43:** D222–D226

Mascher M, Jost M, Kuon J-E, Himmelbach A, Aßfalg A, Beier S, Scholz U, Graner A, Stein N (2014) Mapping-by-sequencing accelerates forward genetics in barley. Genome Biol **15:** R78

Mathews H, Clendennen SK, Caldwell CG, Liu XL, Connors K, Matheis N, Schuster DK, Menasco DJ, Wagoner W, Lightner J, Wagner DR (2003) Activation tagging in tomato identifies a transcriptional regulator of anthocyanin biosynthesis, modification, and transport. Plant Cell **15:** 1689–1703

Matsukura C, Aoki K, Fukuda N, Mizoguchi T, Asamizu E, Saito T, Shibata D, Ezura H (2008) Comprehensive resources for tomato functional genomics based on the miniature model tomato Micro-Tom. Curr Genomics **9:** 436–443

McCallum CM, Comai L, Greene EA, Henikoff S (2000a) Targeted screening for induced mutations. Nat Biotechnol **18:** 455–457

McCallum CM, Comai L, Greene EA, Henikoff S (2000b) Targeting induced local lesions in genomes (TILLING) for plant functional genomics. Plant Physiol **123:** 439–442

McConnell JR, Barton MK (1998) Leaf polarity and meristem formation in *Arabidopsis*. Development **125:** 2935–2942

McConnell JR, Emery J, Eshed Y, Bao N, Bowman J, Barton MK (2001) Role of PHABULOSA and PHAVOLUTA in determining radial patterning in shoots. Nature **411:** 709–713

Meissner R, Chague V, Zhu Q, Emmanuel E, Elkind Y, Levy AA (2000) A high throughput system for transposon tagging and promoter trapping in tomato. Plant J **22(3):** 265-274

Meissner R, Jacobson Y, Melmed S, Levyatuv S, Shalev G, Ashri A, Elkind Y, Levy A (1997) A new model system for tomato genetics. Plant J **12:** 1465–1472

Menda N, Semel Y, Peled D, Eshed Y, Zamir D (2004) *In silico* screening of a saturated mutation library of tomato. Plant J **38:** 861–872

Minoia S, Petrozza A, Onofrio OD, Piron F, Mosca G, Sozio G, Cellini F, Bendahmane A, Carriero F (2010) A new mutant genetic resource for tomato crop improvement by TILLING technology. BMC Res Notes **3:** 69

Nakata M, Okada K (2013) The leaf adaxial-abaxial boundary and lamina growth. Plants **2:** 174–202

Neff MM, Turk E, Kalishman M (2002) Web-based primer design for single nucleotide polymorphism analysis. Trends Genet **18:** 613–615

Newman KL, Fernandez AG, Barton MK (2002) Regulation of axis determinacy by the Arabidopsis *PINHEAD* gene. Plant Cell **14:** 3029–3042

Okabe Y, Ariizumi T, Ezura H (2013) Updating the Micro-Tom TILLING platform. Breed Sci **63:** 42–48

Okabe Y, Asamizu E, Ariizumi T, Shirasawa K, Tabata S, Ezura H (2012) Availability of Micro-Tom mutant library combined with TILLING in molecular breeding of tomato fruit shelf-life. Breed Sci **62:** 202–208

Okabe Y, Asamizu E, Saito T, Matsukura C, Ariizumi T, Brs C, Rothan C, Mizoguchi T, Ezura H (2011) Tomato TILLING technology: development of a reverse genetics tool for the efficient isolation of mutants from Micro-Tom mutant libraries. Plant Cell Physiol **52:** 1994–2005

Okada K (1991) Requirement of the auxin polar transport system in early stages of *Arabidopsis* floral bud formation. Plant Cell **3:** 677–684

Paciorek T, Zažímalová E, Ruthardt N, Petrášek J, Stierhof Y-D, Kleine-Vehn J, Morris DA, Emans N, Jürgens G, Geldner N, Friml J (2005) Auxin inhibits endocytosis and promotes its own efflux from cells. Nature **435:** 1251–1256

Passam HC, Ioannis CK, Penelope JB, Dimitrios S (2007) A review of recent research on tomato nutrition, breeding and post-harvest technology with reference to fruit quality. Eur J Plant Sci Biotechnol **1:** 1-21

Pattison RJ, Catalá C (2012) Evaluating auxin distribution in tomato (*Solanum lycopersicum*) through an analysis of the *PIN* and *AUX/LAX* gene families. Plant J **70:** 585–598

Peret B, Rybel B De, Casimiro I, Benkova E, Swarup R, Laplaze L, Beeckman T, Bennett MJ (2009) *Arabidopsis* lateral root development: an emerging story. Trends Plant Sci 1360-1385

Peret B, Swarup K, Ferguson A, Seth M, Yang Y, Dhondt S, James N, Casimiro I, Perry P, Syed A, Yang H, Reemmer J, Venison E, Howells C, Perez-Amador MA, Yun J, Alonso J, Beemster JTS, Laurent L, Murphy A, Bennett MJ, Nielsen E, Swarup R (2012) *AUX/LAX* genes encode a family of auxin influx transporters that perform distinct functions during *Arabidopsis* development. Plant Cell **24:** 2874–2885

Pérez-Pérez JM, Candela H, Robles P, López-Torrejón G, Del Pozo JC, Micol JL (2010) A role for *AUXIN RESISTANT3* in the coordination of leaf growth. Plant Cell Physiol **51:** 1661–1673

Pfaffl MW (2001) A new mathematical model for relative quantification in real-time RT–PCR. Nucleic Acids Res **29:** 16–21

Prigge MJ, Otsuga D, Alonso JM, Ecker JR, Drews GN, Clark SE (2005) Class III homeodomain-leucine zipper gene family members have overlapping, antagonistic, and distinct roles in Arabidopsis development. Plant Cell **17**: 61–76

Qi J, Wang Y, Yu T, Cunha A, Wu B, Vernoux T, Meyerowitz E, Jiao Y (2014) Auxin depletion from leaf primordia contributes to organ patterning. Proc Natl Acad Sci **111:** 18769–18774

Reinhardt D, Pesce E-R, Stieger P, Mandel T, Baltensperger K, Bennett M, Traas J, Friml J, Kuhlemeier C (2003) Regulation of phyllotaxis by polar auxin transport. Nature **426:** 255–260

Robert HS, Grunewald W, Sauer M, Cannoot B, Soriano M, Swarup R, Weijers D, Bennett M, Boutilier K, Friml J (2015) Plant embryogenesis requires AUX/LAX-mediated auxin influx. Development **142:** 702–711

Romano CP, Cooper ML, Klee HJ (1993) Uncoupling auxin and ethylene effects in transgenic tobacco and *Arabidopsis* plants. Plant Cell **5:** 181–189

Rutschow HL, Baskin TI, Kramer EM (2014) The carrier AUXIN RESISTANT (AUX1) dominates auxin flux into *Arabidopsis* protoplasts. New Phytol **204:** 536–544

Sagar M, Chervin C, Mila I, Hao Y, Roustan J-P, Benichou M, Gibon Y, Biais B, Maury P, Latche A, Pech J-C, Bouzayen M, Zouine M (2013) *SlARF4*, an auxin response factor involved in the control of sugar metabolism during tomato fruit development. Plant Physiol **161:** 1362–1374

Saito T, Ariizumi T, Okabe Y, Asamizu E, Hiwasa-Tanase K, Fukuda N, Mizoguchi T, Yamazaki Y, Aoki K, Ezura H (2011) TOMATOMA: a novel tomato mutant database distributing Micro-Tom mutant collections. Plant Cell Physiol **52:** 283–296

Sandalio LM, Rodríguez-Serrano M, Romero-Puertas MC (2016) Leaf epinasty and auxin: a biochemical and molecular overview. Plant Sci **253:** 187–193

Schneeberger K (2014) Using next-generation sequencing to isolate mutant genes from forward genetic screens. Nat Rev Genet **15:** 662–676

Shikata M, Hoshikawa K, Ariizumi T, Fukuda N, Yamazaki Y, Ezura H (2016) TOMATOMA update: phenotypic and metabolite information in the Micro-Tom mutant resource. Plant Cell Physiol **57:** e11

Shinozaki Y, Hao S, Kojima M, Sakakibara H, Ozeki-Iida Y, Zheng Y, Fei Z, Zhong S, Giovannoni JJ, Rose JKC, Okabe Y, Heta Y, Ezura H, Ariizumi T (2015) Ethylene suppresses tomato (*Solanum lycopersicum*) fruit set through modification of gibberellin metabolism. Plant J **83:** 237–251

Shirasawa K, Isobe S, Hirakawa H, Asamizu E, Fukuoka H, Just D, Rothan C, Sasamoto S, Fujishiro T, Kishida Y, Kohara M, Tsuruoka H, Wada T, Nakamura Y, Sato S, Tabata S (2010) SNP discovery and linkage map construction in cultivated tomato. DNA Res **17:** 381–391

Sieburth LE, Deyholos MK (2006) Vascular development: the long and winding road. Curr Opin Plant Biol **9:** 48–54

Song JB, Huang SQ, Dalmay T, Yang ZM (2012) Regulation of leaf morphology by MicroRNA394 and its target *LEAF CURLING RESPONSIVENESS*. Plant Cell Physiol **53:** 1283–1294

Steinmann T, Geldner N, Grebe M, Mangold S, Jackson CL, Paris S, Gälweiler L, Palme K, Jürgens G (1999) Coordinated polar localization of auxin efflux carrier PIN1 by GNOM ARF GEF. Science **286:** 316–318

Stemple D (2004) TILLING- a high throughput harvest for functional genomics. Nat Rev Genet **5:** 1–7

Swarup K, Benková E, Swarup R, Casimiro I, Péret B, Yang Y, Parry G, Nielsen E, Smet I De, Vanneste S, Levesque MP, Carrier D, James N, Calvo V, Ljung K, Kramer E, Roberts R, Graham N, Marillonnet S, Patel K, Jones JDG, Taylor CG, Schachtman DP, May S, Sandberg G, Benfey P, Friml J, Kerr I, Beeckman T, Laplaze L, Bennett MJ (2008) The auxin influx carrier LAX3 promotes lateral root emergence. Nat Cell Biol **10:** 946-954

Swarup R (2004) Structure-function analysis of the presumptive *Arabidopsis* auxin permease *aux1*. Plant Cell **16:** 3069–3083

Swarup R, Marchant A, Ljung K, Sandberg G, Palme K, Bennett M (2001) Localization of the auxin permease AUX1 suggests two functionally distinct hormone transport pathways operate in the *Arabidopsis* root apex. **15:** 2648–2653

Swarup R, Péret B (2012) AUX/LAX family of auxin influx carriers - an overview. Front Plant Sci **3:** 1–11

Tomato Genome Consortium (2012) The tomato genome sequence provides insights into fleshy fruit evolution. Nature **485:** 635–641

Tromas A, Perrot-Rechenmann C (2010) Recent progress in auxin biology. Comptes Rendus - Biol **333:** 297–306

Untergasser A, Cutcutache I, Koressaar T, Ye J, Faircloth BC, Remm M, Rozen SG (2012) Primer3-new capabilities and interfaces. Nucleic Acids Res **40:** 1–12

Untergasser A, Nijveen H, Rao X, Bisseling T, Geurts R, Leunissen JAM (2007) Primer3Plus, an enhanced web interface to Primer3. Nucleic Acids Res **35:** 71–74

Vanneste S, Friml J (2009) Auxin: a trigger for change in plant development. Cell **136:** 1005–1016

Veit B (2004) Determination of cell fate in apical meristems. Curr Opin Plant Biol **7:** 57–64

Velasquez SM, Barbez E, Kleine-Vehn J, Estevez J (2016) Auxin and cellular elongation. Plant Physiol **170**: 1206-1215

Vieten A, Sauer M, Brewer PB, Friml J (2007) Molecular and cellular aspects of auxin-transport-mediated development. Trends Plant Sci **12:** 160–168

Warr A, Robert C, Hume D, Archibald A, Deeb N, Watson M (2015) Exome sequencing: current and future

perspectives. Genes Genome Genetics **5:** 1543–1550

Watanabe S, Mizoguchi T, Aoki K, Kubo Y, Mori H, Imanishi S, Yamazaki Y, Shibata D, Ezura H (2007) Ethylmethanesulfonate (EMS) mutagenesis of *Solanum lycopersicum* cv. Micro-Tom for large-scale mutant screens. Plant Biotechnol **24:** 33–38

Wolters H, Anders N, Geldner N, Gavidia R, Jürgens G (2011) Coordination of apical and basal embryo development revealed by tissue-specific GNOM functions. Development **138:** 117–126

Yang H, Murphy AS (2009) Functional expression and characterization of Arabidopsis ABCB, AUX 1 and PIN auxin transporters in *Schizosaccharomyces pombe*. Plant J **59:** 179–191

Yu L, Yu X, Shen R, He Y (2005) *HYL1* gene maintains venation and polarity of leaves. Planta **221:** 231–242

Zgurski JM, Sharma R, Bolokoski DA, Schultz EA (2005) Asymmetric auxin response precedes asymmetric growth and differentiation of asymmetric leaf and asymmetric leaf. Plant Cell **17:** 77–91

Zhao Y (2001) A role for flavin monooxygenase-like enzymes in auxin biosynthesis. Science **291:** 306–309

Zouine M, Fu Y, Chateigner-Boutin AL, Mila I, Frasse P, Wang H, Audran C, Roustan JP, Bouzayen M (2014) Characterization of the tomato *ARF* gene family uncovers a multi-levels post-transcriptional regulation including alternative splicing. PLoS One **9:** 1–12